ERS-2 OPR Product Validation Report

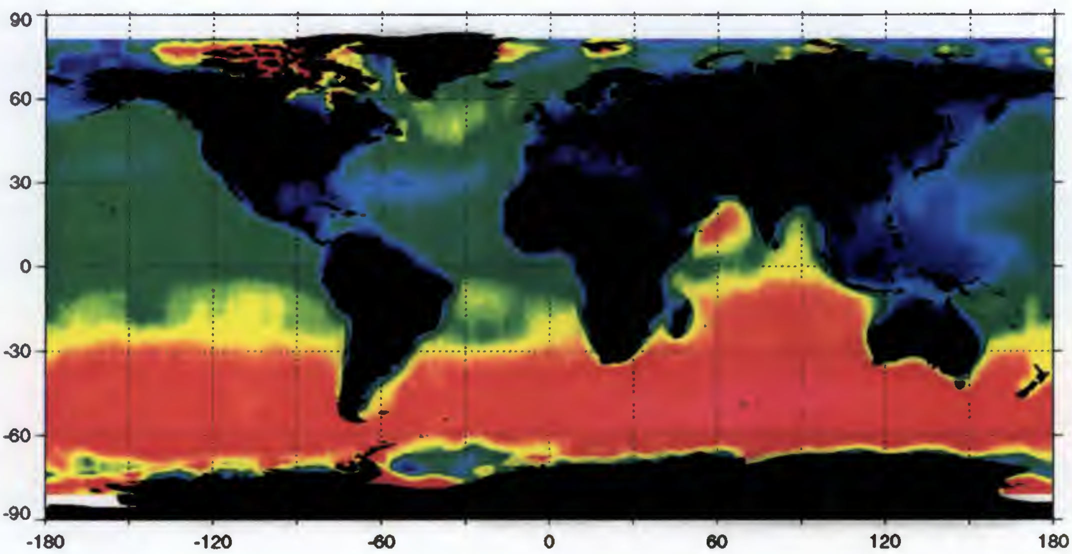

Editors: J. Benveniste and B. Greco – ESA/ESRIN

Document ID: ER-RP-ESA-GS-0484
Issue: 1.1
Date: April 1997

European Space Agency
Agence spatiale européenne

ESRIN

Via Galileo Galilei - Casella Postale 64 - 00044 Frascati (Italy)
Tel. (39) 6 941801 - Fax (39) 6 94180 280

Editing Authors: J. Benveniste and B. Greco — ESA/ESRIN

Contributing Authors:

P.D. Cotton
P.G. Challenor

R. Scharroo
R. Floberghagen

T. Engelis

C. Guérin
S.-A. Boukabara
L. Eymard

J. Stum
J.-P. Dumont
J. Durandeu
F. Ogor
P.-Y. Letraon
O.-Z. Zanifé
P. Gaspar

P. Queffeulou

Document title:	ERS-2 OPR Product Validation Report
Document ID:	ER-RP-ESA-GS-0484
Issue:	1.1
Date:	April 1997

Table of content

1. Introduction

The ERS-2 Radar Altimeter Ocean Product (OPR) validation exercise is mandatory prior to releasing the product to the users. The validation of the OPR product itself is the last step of the OPR processing chain formal acceptance test, obeying severe standards. These acceptance tests were performed as part and parcel of the F-PAF refurbishing for ERS-2 and are not related here. This report focuses on the inspection of the OPR products and the associated user documentation.

The validation of the altimetric range parameters and the Wind and Wave parameters require different expertise, thus the related validation work should be performed by different groups. The primary and most complex altimetric parameters are the ones related to the Range and consequently have been double-checked by two independent groups. Even though the OPR from ERS-2 is built with the same algorithms as ERS-1, it is derived from a different instrument and laid out on a different format (including additional parameters).

2. ERS-2 OPR Validation Plan Summary

The ESA strategy for conducting this exercise was to contract Scientific Institutes with well established expertise in Altimetry. Furthermore, it was deemed highly desirable that the Institutes performing the work be independent from the Processing and Archiving Facility development and operation.

For the reasons above, the range-related validation would be more thoroughly done by one group with extensive experience in using the ERS-1 OPR and a second group with extensive experience in Altimetric missions but not particularly in ERS-1, providing a 'fresh' view, free from any *a priori*, on the OPR Product. As we did not expect difficulty with the Wind & Wave parameters the validation work would be conducted by only one group. The validation of the wet tropospheric altimeter path delay correction, the integrated water vapor and the integrated water content, from the Microwave Radiometer (MWR), within the OPR product would be performed by the group already involved in the MWR calibration.

These institutional groups were identified at the time of organising the ERS2 RA and MWR Commissioning Working Group, based on their expertise and expressed interest to support ESA for the Commissioning of ERS-2. Thus a subgroup to the above mentioned Working Group was created as follows :

Institute	**Task**	**Project manager**
Southampton Oceanography Centre (UK)	Wind & Wave Validation	D. Cotton
Delft University of Technology (NL)	Range Validation 1	R. Scharroo
SpaceTec (Greece)	Range Validation 2	T. Engelis
Centre d'Études des Environnements Terestre et Planétaires (F)	MWR data Validation	L. Eymard

3. ERS-2 OPR Validation Results

The validation exercise was performed on the first four repeat cycles of ERS-2 OPR data produced with the version 5 of the F-PAF processing chain. The data covers the period from 3 May 1995 to 28 August 1995 data was distributed on specially-made CD-ROM.

This report collates the final report from each of the tasks listed in the table above. During the actual work several reports corresponding to sub-tasks were issued and reviewed by the validation sub-group. After several review iterations the final reports were produced and the OPR user manual was up-issued with significant improvement generated from the validation exercise to clarify descriptions and definitions. The OPR processing Chain was also upgraded to version 6, incorporating the latest models and algorithms. The last two sections in this report covers the validation of the version 6 changes with respect to the deltas with version 5 and a verification against Topex wind and wave data. The body of this report is constituted with the following reports:

ERS-2 Radar Altimeter OPR Product Verification: Wind and Wave Parameters, P.D. Cotton and P.G. Challenor, SOC, June 1996

Geophysical Validation of the F-PAF ERS-2 OPR Radar Altimeter Ocean Product, R. Scharroo and R. Floberghagen, DUT, April 1996.

Geophysical Validation of the F-PAF ERS-2 Altimeter OPR Product, T. Engelis, SpaceTec Ltd, April 1996.

CETP Contribution to the validation of the ERS-2 OPR Products, C. Guérin, S.-A. Boukabara and L. Eymard, CETP, March 1996.

A comparison of ERS-2 OPR issued from software versions number 5 and software version 6, J. Stum, J.-P. Dumont, J. Durandeu, F. Ogor, P.-Y. Letraon, O.-Z. Zanifé, and P. Gaspar, CLS, October 1996.

ERS-2 OPR version 6.3 validation: Comparison of ERS-2 and Topex SWH and $Sigma_0$ measurements, P. Queffeulou, IFREMER, October 1996.

Specific conclusions can found within each report. A summary conclusion is drawn is section 4.

3.1 ERS-2 Radar Altimeter OPR Product Verification: Wind and Wave Parameters

P.D. Cotton and P.G. Challenor

SOC

ERS-2 Radar Altimeter OPR Product Verification: Wind and Wave

P.D. Cotton and P.G. Challenor

June 1996

James Rennell Division
Southampton Oceanography Centre
European Way
Southampton
SO14 3ZH
UK

Southampton Oceanography Centre

ERS-2 Radar Altimeter OPR Product Verification: Wind and Wave Parameters

P.D. Cotton and P.G. Challenor - Southampton Oceanography Centre (James Rennell Division)

Introduction

This report presents results from a verification analysis of the wind/wave parameters on the ERS-2 radar altimeter OPR product. The analysis has been carried out on the first four repeat cycles of ERS-2 OPR data, covering the period 3rd May to 28th August 1995 and produced by version 5 of the CERSAT software. A parallel analysis was carried out on the equivalent ERS-1 OPR data, cycles 145-148 - also produced by version 5 of the software.

The product verification consisted of three parts: the verification of the product format; the analysis of the setting of data flags, of the presence of default and extreme values; and analysis of the distribution functions of the wind wave parameters and their standard deviations. Analysis of the ERS-2 FD product, and a report on calibration of the ERS-2 OPR wind/wave parameters is provided elsewhere [*ESA*, 1996a and 1996b].

It has been established that the $\sigma 0$ values in this release of the ERS-2 OPR data are approximately 3.9 dB too high [Dumont, 1996], resulting in the provided wind speed being too low. Where appropriate in our analyses (e.g. for the occurrence of extreme values, and comparison of ERS-1 and ERS-2 OPR $\sigma 0$ and wind speed distributions) we have adjusted ERS-2 $\sigma 0$ by subtracting 3.9 dB and recalculating the wind speed with the Witter and Chelton [1991] algorithm.

OPR Format and Product Documentation

The format specification was taken to be that given in the ERS-2 RA OPR Product User Manual[*CERSAT*, 1996]. Product checking was primarily restricted to the wind/wave parameters in the OPR pass files.

Data extraction software was written at SOC based on [*CERSAT*, 1996]. The data format of all of the records in each of the pass files was checked on each of the 4 ERS-2 CDroms (and also the ERS-1 OPR data) and no format errors were found. We welcome the more detailed information provided in the document [*CERSAT*, 1996], and recognise this as a major improvement on the documentation provided with the original release of ERS-1 data. It is our recommendation that the user should have the fullest information available about the product (s)he is given, they are then able to make informed decisions about the subsequent use of the data. The data provider may not always appreciate the full range of analyses and uses the data are subject to, and so are not necessarily in the best position to decide which information is necessary for the user.

Summary

The data format was found to be consistent and reliable, and correctly documented. No formatting errors have been found in any of the first four cycles of ERS-2 version 5 OPR data.

Data Flags

The occurrence of the first 24 data flags in the measurement confidence data (MCD), which provide general validity and quality assessment information, was summed over each of the four ERS-2 cycles. These occurrences are provided for each cycle in Table 1 as a percentage of the total number of 1 Hz data records. The equivalent ERS-1 occurrence percentages over the same periods are given for comparison. Due to processing problems at SOC, data for ERS-1 cycle 146 are unavailable.

Before concentrating on the wind/wave flags, we can make a few initial observations. Firstly we see that a consistent and significant fraction (37-42%) of the data records are labelled as being invalid in some way (flag bit 0). The cause is indicated by bits 1, 2 and 3, with 2 and 3 being raised more often than bit 1. Overall, we see consistent occurrence of flags in ERS-1 and ERS-2 data, and indeed we can also see similar trends between cycles in both data sets. The main exception is an unusually high (54%) occurrence of bit 10 (quality of internal calibration correction to $\sigma 0$) in ERS-2 cycle 4. This high percentage of flagged $\sigma 0$ data is of concern, and we are not aware of the cause of this problem. Flag bits 12 (type of internal calibration for range correction), 13 (single point target response used to derive $\sigma 0$), 17 (simultaneous radiometer data present), 18 and 19 (two radiometer channel values nominal) were never found to be set. Flag bits 4, 5, and 6 (quality indicators relevant to range measurements); 14 (ocean tracking nominal); and 22 and 23 (presence of DPAF mean sea surface, and quality affected by manoeuvre) were only rarely set (0.01% or less).

Other analyses [Engelis ,1996] seem to be consistent with these findings - in their analysis they found that flag bits 5,6,10,12, and 23 were never set, and that bit 4 was only once non-zero.

Flag Bit	ERS-2 001	ERS-1 145	ERS-2 002	ERS-1 146	ERS-2 003	ERS-1 147	ERS-2 004	ERS-1 148
0	37.59	39.95	39.67	-	42.65	42.24	41.91	41.20
1	0.03	4.24	0.72	-	3.95	3.82	3.97	3.82
2	30.35	31.79	31.79	-	34.75	34.34	33.92	33.28
3	17.35	11.96	18.50	-	15.15	14.92	14.28	14.02
4	0.00	<0.01	0.00	-	<0.01	<0.01	<0.01	<0.01
5	0.00	0.00	0.00	-	<0.01	<0.01	<0.01	0.00
6	0.00	0.02	0.00	-	0.00	0.00	0.00	<0.01
7	0.67	0.47	0.59	-	0.30	0.42	0.33	0.43
8	1.16	0.77	1.16	-	1.00	0.61	0.93	0.56
9	0.53	0.40	0.59	-	0.60	0.32	0.53	0.27
10	0.00	0.00	0.00	-	0.25	0.00	54.27	0.00
11	0.11	0.15	0.11	-	0.04	0.17	0.04	0.20
12	0.00	0.00	0.00	-	0.00	0.00	0.00	0.00
13	0.00	0.00	0.00	-	0.00	0.00	0.00	0.00
14	0.00	0.00	0.00	-	0.00	<0.01	0.00	0.00
15	2.54	1.20	2.61	-	2.36	0.71	2.32	0.67
16	0.31	0.21	0.32	-	0.16	0.08	0.15	0.08
17	0.00	0.00	0.00	-	0.00	0.00	0.00	0.00
18	0.00	0.00	0.00	-	0.00	0.00	0.00	0.00
19	0.00	0.00	0.00	-	0.00	0.00	0.00	0.00
20	0.09	0.08	0.09	-	0.03	0.09	0.03	0.10
21	0.00	0.00	0.00	-	0.01	0.00	0.57	0.00
22	0.01	<0.01	0.01	-	<0.01	<0.01	0.00	0.00
23	<0.01	<0.01	0.00	-	0.00	0.00	0.00	0.00

Table 1. Occurrence of data flags by cycle, as a percentage of total data records. In this and all subsequent tables, a value of <0.01 indicates that the flag has been set at least once (but in a percentage of less than 0.01% of the total number of records).

Looking specifically at the occurrence of the significant wave flag bit (7), we see that this is set on less than 0.7% of the records of all data cycles, indicating good coverage of valid data for this parameter. The $\sigma 0$ flag bits are raised in 0.6-1.2 % of data records for bit 8 (quality of backscatter estimate), and 0.3-0.6 % of records for bit 9 (quality of $\sigma 0$ telemetry parameters), whilst bit 10 (quality of internal $\sigma 0$ calibration correction) is raised in ERS-2 data only on cycle 4 but then on 54.27% of data records (see earlier comments). We also note that the flag bit used to indicate $\sigma 0$ is out of range for wind speed calculation (bit 15) is set on just over 2% of data records for ERS-2 but only on 0.7-1.2% of records for ERS-1.This difference may be due to the known bias of +3.9 dB in the ERS-2 data.

The occurrence of flags was also analysed by region to establish whether any unexpected geographic pattern was present, the ten regions were : North Atlantic (20°-60°N, 280°-80°E), Equatorial Atlantic (20°S-20°N, 280°-30°E), South Atlantic (20°-40°S, 290°-30°E), North Pacific (20°-60°N, 110°-280°E), Equatorial Pacific (20°S-20°N, 110°-280°E), South Pacific (20°-640°S, 110°-290°E), North Indian (0°-30°N, 30°-110°E), South Indian (0°-40°S, 30°-110°E), Southern Ocean (40°-60°S), and the Antarctic (60°-80°S). Here we only consider results for ERS-2 data from cycle 1, summarised in Table 2.

Flag Bit	N Atl	E Atl	S Atl	N Pac	E Pac	S Pac	N Ind	S Ind	S Oc	AA'tc	Globe
0	34.68	47.10	27.39	34.15	5.89	14.38	71.35	9.41	1.60	62.52	37.59
1	0.04	0.01	<0.01	0.03	0.01	0.01	0.07	0.01	<0.01	0.04	0.03
2	26.94	37.20	20.69	25.04	4.34	11.70	51.04	6.67	1.12	55.46	30.35
3	13.56	11.86	7.88	15.41	3.04	3.47	23.93	3.73	0.90	25.71	17.35
4	0.00	0.00	0.00	0.00	0.00	0.00	0.00	0.00	0.00	0.00	0.00
5	0.00	0.00	0.00	0.00	0.00	0.00	0.00	0.00	0.00	0.00	0.00
6	0.00	0.00	0.00	0.00	0.00	0.00	0.00	0.00	0.00	0.00	0.00
7	0.49	0.26	0.19	0.32	0.29	0.16	0.38	0.18	0.06	1.31	0.67
8	1.73	1.08	1.14	0.83	2.02	0.94	1.17	1.69	0.14	0.77	1.16
9	1.15	0.75	0.67	0.44	1.47	0.63	0.84	1.32	0.04	0.00	0.53
10	0.00	0.00	0.00	0.00	0.00	0.00	0.00	0.00	0.00	0.00	0.00
11	0.09	0.02	0.09	0.03	0.02	0.13	0.06	0.02	0.08	0.37	0.11
12	0.00	0.00	0.00	0.00	0.00	0.00	0.00	0.00	0.00	0.00	0.00
13	0.00	0.00	0.00	0.00	0.00	0.00	0.00	0.00	0.00	0.00	0.00
14	0.00	0.00	0.00	0.00	0.00	0.00	0.00	0.00	0.00	0.00	0.00
15	3.71	2.18	2.38	3.15	3.61	1.90	3.05	2.80	0.47	1.94	2.54
16	0.31	0.23	0.03	0.51	0.21	0.04	0.69	0.02	0.02	0.11	0.31
17	0.00	0.00	0.00	0.00	0.00	0.00	0.00	0.00	0.00	0.00	0.00
18	0.00	0.00	0.00	0.00	0.00	0.00	0.00	0.00	0.00	0.00	0.00
19	0.00	0.00	0.00	0.00	0.00	0.00	0.00	0.00	0.00	0.00	0.00
20	0.07	0.01	0.05	0.03	0.02	0.05	0.04	0.02	0.02	0.32	0.09
21	0.00	0.00	0.00	0.00	0.00	0.00	0.00	0.00	0.00	0.00	0.00
22	0.00	0.00	0.00	0.01	0.00	<0.01	0.08	0.00	0.00	0.00	0.01
23	0.00	0.00	0.00	0.00	0.03	0.00	0.00	0.00	0.00	0.00	<0.01

Table 2. Percentage Occurrence of flags by region, ERS-2 OPR Cycle 001

We see that the largest proportions of data labelled invalid occur in the North Indian (71.35%), and Antarctic regions (62.52%), the predominance of setting of bits 2 and 3 suggest that the cause is either land or other "non-ocean" measurement. In the three Atlantic regions and the North Pacific, between 27% and 47% of the data are labelled invalid, compared to 14% in the South Pacific, 9% in the South Indian Ocean, 6% in the Equatorial Pacific, and less than 2% in the Southern Oceans - where the highest data return is achieved.

It is otherwise difficult to pick out any significant geographical dependencies. The only clear tendency is the preferential raising of Bit 7 (significant wave height) in the Antarctic (1.3% of data records compared to the global average of 0.65%), but this is to be expected and is likely due to the presence of ice contaminating the waveform. It is surprising that there is no apparent similar tendency in backscatter, which should in theory be at least as sensitive to the presence of ice. The value of $\sigma 0$ is indicated as being out of range for calculation of wind speed (bit 15) in approximately 3%, and above, of the records in the North Atlantic, the Equatorial Pacific, and the North and South Indian Oceans, whereas this flag is raised for only 0.5% of data records in the Southern Ocean. As the value of $\sigma 0$ is 3.9 dB too high we may have expected most data to be rejected in low wind speed (i.e. high $\sigma 0$) regions, but there is no clear indication that this is the case.

Summary

The Product User Manual [*CERSAT*, 1996] indicates that the processes which are responsible for the setting of data flags and the creation of default values are uncorrelated. Whereas default values indicate no data are available, flags may either indicate the reason for this lack of data, or that the data in the product may be of less reliable quality. So long as the grounds for setting flags are clearly explained, we think that this philosophy is acceptable. However, we would recommend that the thresholds used in determining whether a flag is set for various parameters are made available to the user - perhaps they could be released with the cycle information provided with each CD.

The use of the flags on the whole seems consistent with the document description, though we were not able to test this exhaustively. There is an outstanding query about the description of flags 23 and 24 to be resolved. We would also like to note the high occurrence of flag 10 in cycle 4 data, and emphasise that this proportion of invalid $\sigma 0$ data is not acceptable.

Default and Out of Range Values of Significant Wave Height

The significant wave height parameters in cycle 1 of ERS-2 OPR data were then analysed for rejected data, on the basis of quality flags, or occurrence of out of range or default values (as defined in *CERSAT* [1996]). 10 checks were made, given in Table 3.

Note that all values of SWH_LUT were found to be set to zero, and consequently SWH data are identical to SWH_raw data. (for brevity we have replaced SWH by Hs)

Cause	N Atl	E Atl	S Atl	N Pac	E Pac	S Pac	N Ind	S Ind	S Oc	AA'tc	Globe
bit 0 or bit 7	35.18	47.37	27.58	34.46	6.18	14.54	71.73	9.59	1.66	63.83	38.26
σ Hs= 0	0.00	<0.01	0.00	0.00	0.00	0.00	0.00	0.00	0.00	<0.01	<0.01
σHs= 32767	35.21	47.30	27.46	34.57	6.04	14.45	71.64	9.49	1.65	64.01	38.58
Hs_raw = 0	1.85	0.28	0.07	1.10	1.36	0.13	1.98	0.39	0.02	2.39	1.91
Hs_raw = 32767	34.68	47.10	27.39	34.15	5.89	14.38	71.35	9.41	1.60	62.52	37.59
Hs= 0	1.85	0.28	0.07	1.10	1.36	0.13	1.98	0.39	0.02	2.39	1.91
Hs= 32767	34.68	47.10	27.39	34.15	5.89	14.38	71.35	9.41	1.60	62.52	37.59
Hs> 5	35.63	47.56	27.62	34.85	6.43	14.62	72.03	9.70	1.71	65.43	39.34
Hs> 30	34.71	47.12	27.40	34.17	5.90	14.39	71.37	9.41	1.60	62.53	37.61
σHs>2.0 & > 2.0*Hs	0.74	0.27	0.08	0.58	0.35	0.10	0.52	0.15	0.06	2.44	1.55

Table 3. Occurrence of default or out of range values in parameters effecting significant wave height, given as a percentage of total data records, separated according to region. For ERS-2 cycle 1.

Flag bit 0 (the general record validity flag) and flag bit 7 (the wave height flag) may be used to identify doubtful significant wave height data, by selecting records where either or both flags are set. Considering row 1 in Table 3 and rows 0 and 7 in Table 1 together, it seems as though the setting of bits 0 and 7 is mutually exclusive (i.e. the percentages in Table 3 row 1 are equal to the sum of the percentages in Rows 0 and 7 in Table 1). One would expect that some otherwise valid data would have doubtful quality wave height values and the small increase in percentage (e.g. in ERS-2 cycle 1, 37.59% records with bit 0 set to 38.26% with either bit 0 or bit 7) is consistent with this.

Very few zero values of standard deviation in significant wave height are found - Table 3 row 2 (< 0.01% globally), but a significant proportion, 1.91% globally, of SWH_raw, (and hence also SWH) are set to zero. The Product User Manual indicates that if negative values for SWH are calculated, these are set to zero. Looking at row 1 in Table 1 and rows 5 and 7 in Table 3 we see perfect correspondence between the setting of SWH and SWH_raw to their default values and the setting of bit 0 (37.59%). Standard deviation SWH is set to its default value in a slightly higher proportion (38.58%) of the data. This higher occurrence is probably because this parameter cannot be calculated if Nval is equal to 1, when the default value is set, but when a non zero value of SWH can be returned.

The occurrence of significant wave height parameter values out of expected range, rows 8 and 9, are almost all due to default values, but it is evident that small percentages of non-default higher values do occur (0.8% for STD SWH, 2% for SWH).

Finally, on the basis of distributions of standard deviation in significant wave height, a trial range of acceptable STD SWH was selected (STD SWH greater than 2.0 AND greater than 2.0 times the significant wave height). Applying this test would reject 1.55% of the data.

As we saw in the previous section, the largest proportion of data are rejected in the North Indian and Antarctic Oceans, and this mostly on the grounds of flag bit 0 being raised, and hence default values of SWH and SWH_raw being set (causes 5 and 8). As may have been expected, occurrences of zero SWH (and SWH_raw, causes 4 and 6) are lowest in the South Atlantic, South Pacific and Southern Oceans (<0.13%), and highest in the Antarctic (2.39%). A similar pattern emerges in data rejected for the test of standard deviation in wave height in row 10, with the largest percentage of data being rejected in the Antarctic (2.44%) and the lowest percentage rejected in the South Atlantic Ocean (0.06%).

Summary

Most non-valid significant wave height data occurs due to the setting of flag bit 0 (the general data validity flag. The specific SWH data flag (bit 7) occurs in an extra 0.06% to 0.7% of the data, depending on data cycle and region. Occurrence of default values in SWH, SWH_raw and STD SWH appears to almost entirely coincide with the setting of flag bit 0, but there are a small number of other occasions when the default values are set in STD SWH. Practically no zero values of STD SWH occur, but a measurable proportion do occur in SWH (1.91%). A validity test based on the value of STD SWH would reject 1.5% of data records.

We conclude that the identification of invalid SWH parameters by flags or default values is consistent with our expectations.

Default and Flagged Values of Sigma0

An equivalent analysis was applied to the $\sigma0$ related parameters in cycle 1 of ERS-2 OPR data. 15 checks were made, defined in Table 4. Because the raw sigma0 values are 3.9 dB too high, we have not investigated the occurrence of sigma0 parameters out of expected range. As the calibration of the microwave radiometer is still underway, we have also excluded $\sigma0$ parameters which rely on radiometer data from our analysis.

As was found for the SWH data, we see that including the specific parameter flags in our cause for rejection (8 and 9, or 8, 9 and 10) slightly increases the proportion of rejected records (from 37.59% to 38.75%). Bit 0 still accounts for the vast majority of the rejected data. Flag bit 10 is never set in ERS-2 cycle 1. The inclusion of the radiometer flags rejects a further 0.7% of the data (but note only the radiometer land flag is ever used). We also see that $\sigma0$_raw, $\sigma0$, STD $\sigma0$ and the calibration and look up table corrections all are set to default when flag bit 0 is raised, and very rarely otherwise (check with Table 2 row 1). STD $\sigma0$ is an exception to this, and shows a slightly higher occurrence of default values, as did STD_SWH in the last section. Of all the parameters, only STD $\sigma0$ (very rarely) and $\sigma0$_lut_cor (on every occasion when it is not default) are ever set to zero.

Data rejected by a test based on the value of STD $\sigma0$, (STD $\sigma0$ > 0.3 dB) mostly consist of those set to default values, but a further 0.04% of data records (globally) were found to exceed this limit.

We can identify the same geographical dependencies that were found in previous sections, i.e. the lowest percentage of rejected or default data records are to be found in the Southern Oceans and Equatorial Pacific, and the largest percentage in the Antarctic Ocean.

Cause	N Atl	E Atl	S Atl	N Pac	E Pac	S Pac	N Ind	S Ind	S Oc	AA'tc	Globe
bits 0, 8 or 9	36.41	48.18	28.53	34.99	7.91	15.33	72.57	11.09	1.73	63.29	38.75
bits 0, 8, 9, 10	36.41	48.18	28.53	34.99	7.91	15.33	72.57	11.09	1.73	63.29	38.75
0, 8, 9, 10, 17, 18, 19, 20	36.46	48.19	28.56	35.01	7.92	15.38	72.61	11.11	1.75	63.56	38.82
$\sigma 0$_raw= 0	0.00	0.00	0.00	0.00	0.00	0.00	0.00	0.00	0.00	0.00	0.00
$\sigma 0$_raw= 32767	34.69	47.10	27.39	34.15	5.90	14.39	71.36	9.42	1.60	62.55	37.60
sd $\sigma 0$= 0	0.00	0.00	0.00	0.00	0.00	0.00	0.00	0.00	0.00	0.01	0.01
sd $\sigma 0$ = 32767	35.22	47.30	27.46	34.57	6.04	14.45	71.64	9.50	1.65	64.02	38.58
$\sigma 0$= 0	0.00	0.00	0.00	0.00	0.00	0.00	0.00	0.00	0.00	0.00	0.00
$\sigma 0$= 32767	34.69	47.10	27.39	34.15	5.90	14.39	71.36	9.42	1.60	62.55	37.60
$\sigma 0$_lut_cor= 0	64.35	52.47	72.36	65.00	93.68	85.30	27.98	90.32	96.45	32.72	60.40
$\sigma 0$_lut_cor= 32767	34.68	47.10	27.39	34.15	5.89	14.38	71.35	9.41	1.60	62.52	37.59
$\sigma 0$_cal_cor= 0	0.00	0.00	0.00	0.00	0.00	0.00	0.00	0.00	0.00	0.00	0.00
$\sigma 0$_cal_cor= 32767	34.68	47.10	27.39	34.15	5.89	14.38	71.35	9.41	1.60	62.52	37.59
sd$\sigma 0$ > 0.3	35.26	47.32	27.48	34.60	6.06	14.48	71.68	9.51	1.66	64.07	38.62

Table 4. Occurrence of flagged or default values in parameters effecting sigma0 , given regionally as a percentage of total data records in area. ERS-2 OPR data, cycle 1

Summary

The occurrence of flags and default values seems in accordance with expectations, and an acceptable proportion of unflagged data show physical values. Again most invalid data are identified by flag bit 0, with the sigma0 specific flags set in a further 1.3% of data records. A data test to identify data records with STD$\sigma 0$ > 0.3 would only reject a further 0.04% of data, perhaps indicating a lower threshold may be required. However, final, and more comprehensive, conclusions should be reserved until data are released with the appropriate 3.9 dB correction applied.

Data Flags and Default Values in Wind Speed

The occurrence of flags relating to wind speed in cycle 1 of ERS-2 OPR data was analysed, Table 5. Because all the wind speeds in the OPR product are derived from $\sigma 0$ data containing a known bias, ws and ws_lw have been recalculated using Witter and Chelton [1991], after the subtraction of 3.9 dB from $\sigma 0$ and $\sigma 0$ _lw.

Cause	N Atl	E Atl	S Atl	N Pac	E Pac	S Pac	N Ind	S Ind	S Oc	AA'tc	Globe
bits 0, 15	38.39	49.28	29.77	37.29	9.50	16.28	74.40	12.23	2.06	64.45	40.13
bits 0, 15, 17, 18, 19, 20	38.44	49.28	29.80	37.31	9.51	16.32	74.42	12.24	2.08	64.75	40.20
ws= 0	0.00	0.00	0.00	0.00	0.00	0.00	0.00	0.00	0.00	0.00	0.00
ws = 32767	34.69	47.10	27.39	34.15	5.90	14.39	71.36	9.44	1.60	62.55	37.60
ws_lw = 0	0.00	0.00	0.00	0.00	0.00	0.00	0.00	0.00	0.00	0.00	0.00
ws_lw= 32767	36.64	49.13	29.64	35.47	7.27	15.66	72.05	10.86	3.19	63.07	38.85
ws (adj)> 20.15	34.69	47.10	27.39	34.15	5.90	14.39	71.36	9.44	1.60	62.55	37.60
ws_lw (adj)> 20.15	36.64	49.13	29.64	35.47	7.27	15.66	72.05	10.86	3.19	63.07	38.85

Table 5. Regional occurrence of default or out of range values in parameters effecting wind speed, given as a percentage of total data records. ERS-1 OPR data, cycle 1.

We can see that testing for flag bit 0 or flag bit 15 ($\sigma 0$ out of range for wind speed calculation) identifies a further 2.5% of data records than are found if only bit 0 is tested (see Table 2). This flag also identifies more data records than the $\sigma 0$ test of rows 1, 2 and 3 in Table 4. The testing of the radiometer flag further increases the percentage data rejected, though only slightly.

All of the occurrence of out of range wind speeds (> 20.15 ms^{-1}) appears to be due to default values. No zero values of wind speed were identified. It was noticed in *CERSAT* [1995] that the maxima for the expected ranges for uncorrected wind speed and wind speed correct for liquid water content are different (20.15 $ms^{-1}$and 30.00 ms^{-1} respectively). It is mentioned in *CERSAT* [1995] that the wind speed algorithm only holds for ws < 20.15 ms^{-1}, and so the higher limit seems unjustified.

The same geographical tendencies identified in the previous sections are again evident.

Summary

Until corrected $\sigma 0$ measurements are used to generate wind speed values within the OPR product it is not possible to thoroughly test the wind speed measurements for occurrences of data out of range.. Different expected range maxima are specified in the Product User Manual for ws and ws_lw.

Suggested Tests for Valid Ocean data

Based on the definition of flags in the Product User Manual, and on the occurrence distribution functions of wind and wave related parameters (see below), we defined three preliminary data quality tests (one for significant wave height and two for $\sigma 0$), set to reject data as follows:

swh: flags bits 0 or 7 set;

STD_H_Alt > 0.3 m;

STD_SWH> 2.0 m *and* STD_SWH > 2.0* SWH;

SWH≤ 0 m *or* SWH > 30.0 m;

$\sigma 0$ (1) Not testing for radiometer liquid water correction

flag bits 0, 8, 9, or 10 set;

STD_H_Alt > 0.3 m;

STD_sigma0 > 0.3 dB;

Sigma0 (adjusted) ≤ 0 dB *or* Sigma0 (adjusted) > 20.0 dB

$\sigma 0$ (2) Testing for radiometer liquid water correction

as for $\sigma 0$ (1) but also test for flag bits 17, 18, 19 or 20.

We have not had the opportunity to thoroughly analyse whether these quality test reliably exclude all doubtful data, but they are based on experience with other altimeter data sets, and so should provide a reasonably thorough indication of the proportion of valid ocean data. We applied these tests to all data records in ERS-2 OPR cycle 1,Table 6.

Test	N Atl	E Atl	S Atl	N Pac	E Pac	S Pac	N Ind	S Ind	S Oc	AA'tc	Globe
swh	37.53	47.84	27.70	35.94	7.80	14.75	74.09	10.11	1.73	67.55	41.12
$\sigma 0$ (1)	39.97	50.41	30.74	37.59	11.31	17.51	74.89	13.51	2.66	71.97	44.07
$\sigma 0$ (2)	39.98	50.41	30.75	37.59	11.31	17.51	74.90	13.51	2.66	72.05	44.08

Table 6. Regional occurrence of data rejected according to defined SWH and *s0* quality tests, given as a percentage of total data records in each region.

Considering test 1(SWH) by comparing the right hand column of Table 6 with that of Table 3, we can see that about a further 3% of data records are identified with this test than are given purely by considering flags bits 0 and 7, with the new test rejecting 41.12% of data records in ERS-2 cycle 1.

Both of the $\sigma 0$ tests reject a slightly larger proportion of the data than the SWH tests (about 3% more), and these also identify 5% more data records than would be found if only the $\sigma 0$ data flags were relied upon.

We can identify the same regional dependencies in the data rejected by all three tests. Most data are rejected in the North Indian Ocean and the Antarctic regions (67-75%), least in the Southern Ocean, the South Indian Ocean and the Equatorial Pacific (1.7-11%). This matches the previous characteristics observed in the regional analysis of the setting of data flags.

Summary

Tests for valid SWH and $\sigma 0$ are suggested which including checking data flags, parameters out of expected ranges, and standard deviations within specified bounds. Roughly 60% of data records pass these tests, representing an acceptable proportion of validated data records.

Significant Wave Height Distribution Functions

Although this report is not intended to present a calibration of ERS-2 wave heights (or other parameters), it is nonetheless important to check the occurrence distribution functions of these parameters, to ensure that these data contain physically realistic distributions. Occurrence distribution functions were generated by summing occurrence of data records with SWH in 0.02 m wide bins. SWH distribution functions for ERS-2 (cycle 2) and ERS-1 (cycle 146) are presented in Figure 1.

Data with significant wave heights equal to 0.0 m were not included (2% of ERS-2 data).

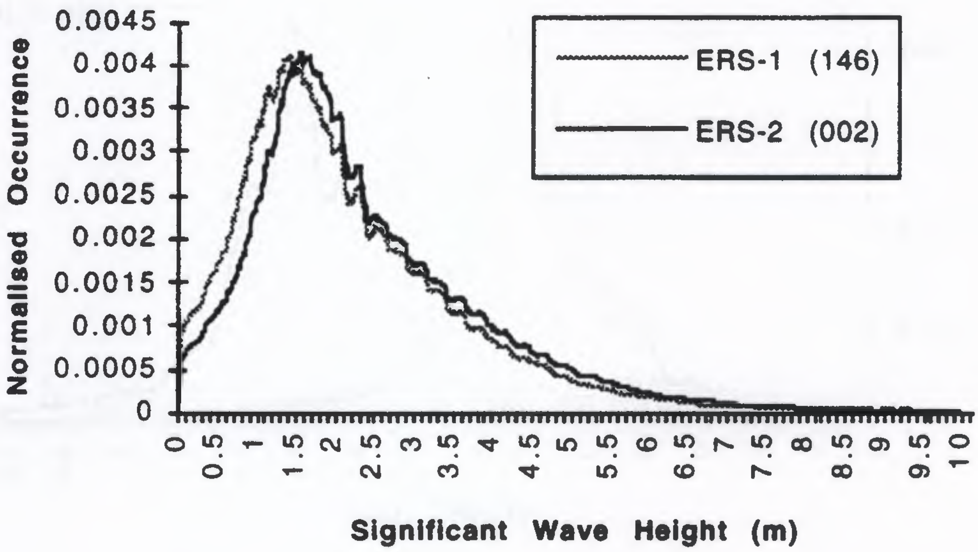

Figure 1. Probability Distribution Function for ERS-1 (grey and dashed line) and ERS-2 (solid line) significant wave heights

We can see that the ERS-2 and ERS-1 data have very similar shapes, both displaying the skewed distribution expected of ocean wave height measurements. There is a degree of offset between the two SWH data sets, in the form of an apparent bias of 0.2 m. We believe that the ERS-2 data provide a distribution function which is more physically realistic at very low wave heights, giving a lower occurrence in the lowest (< 0.02 m) bin. It is also encouraging that there is no low wave height cut-off, as is found in the ERS-2 Fast Delivery data set [ESA, 1996a].

Summary

The ERS-2 OPR data display a physically realistic, and continuous, significant wave height distribution function. This occurrence distribution function appears to be more satisfactory than that shown by the ERS-1 OPR data, and represents a clear improvement on the currently released ERS-2 FD product.

Sigma0 Distribution Functions

Occurrence distributions of ERS-2 OPR sigma0 were similarly compiled from cycle 2 data, from uncorrected and adjusted (i.e. after subtracting 3.9 dB) sigma0. These two distribution functions are compared to that for ERS-1 cycle 146 in Figure 2.

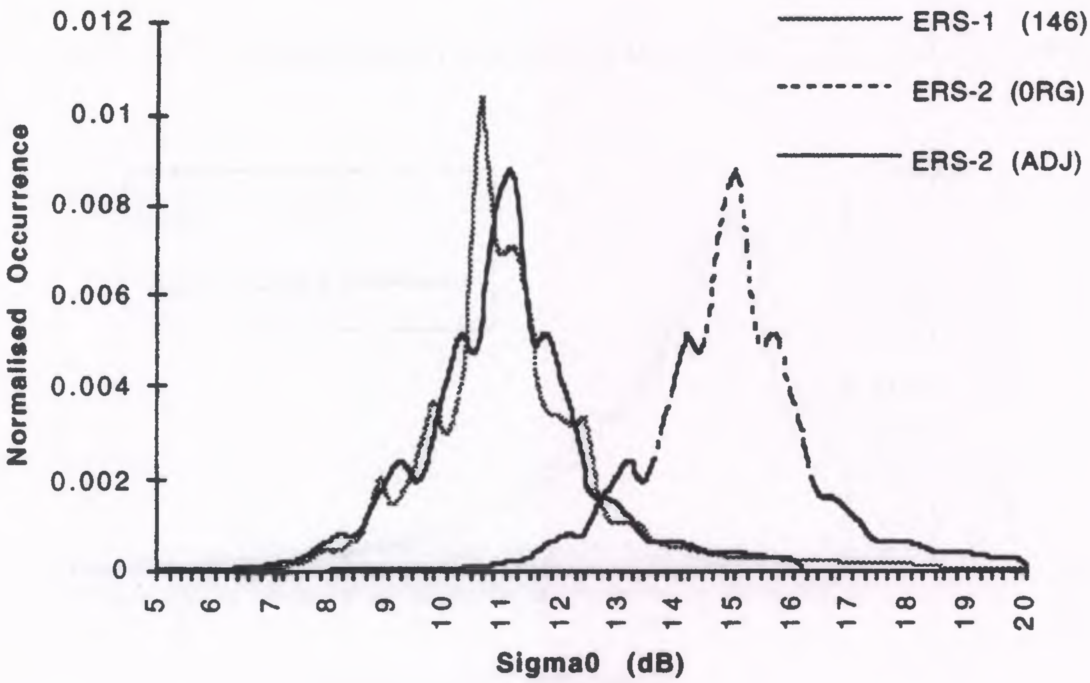

Figure 2. Sigma0 Probability Distribution Function for ERS-1 (grey and dashed line) and original (dashed line) and adjusted ERS-2 (solid line) OPR data.

There is evident improvement in agreement with ERS-1 data after the-3.9 dB adjustment has been applied to the ERS-2 data. There are some subsidiary peaks in the ERS-2 distribution functions which are unlikely to represent true variations in the actual sea surface sigma0 distribution functions, and probably result from instrumental discontinuities. Apart from these small irregularities , the resultant distribution shape is satisfyingly smooth and symmetrical, and indeed again appears to show an improvement on that of ERS-1.

Summary

After applying the -3.9 dB correction to ERS-2 OPR sigma0, the resulting distribution agrees reasonably well, on broad terms, with that of ERS-1. There are some unphysical peaks in the distribution function, which are probably a instrumental characteristic, and these will result in irregularities in the derived wind speed distribution functions.

Wind Speed Distribution Functions

Two sets of occurrence distributions of ERS-2 OPR wind speed were compiled from cycle 2 data, from the provided wind speed data and for wind speeds calculated from the Witter and Chelton [1991] algorithm after 3.9 dB had been subtracted from sigma0. These two distribution functions are compared to one for ERS-1 cycle 146 in Figure 3.

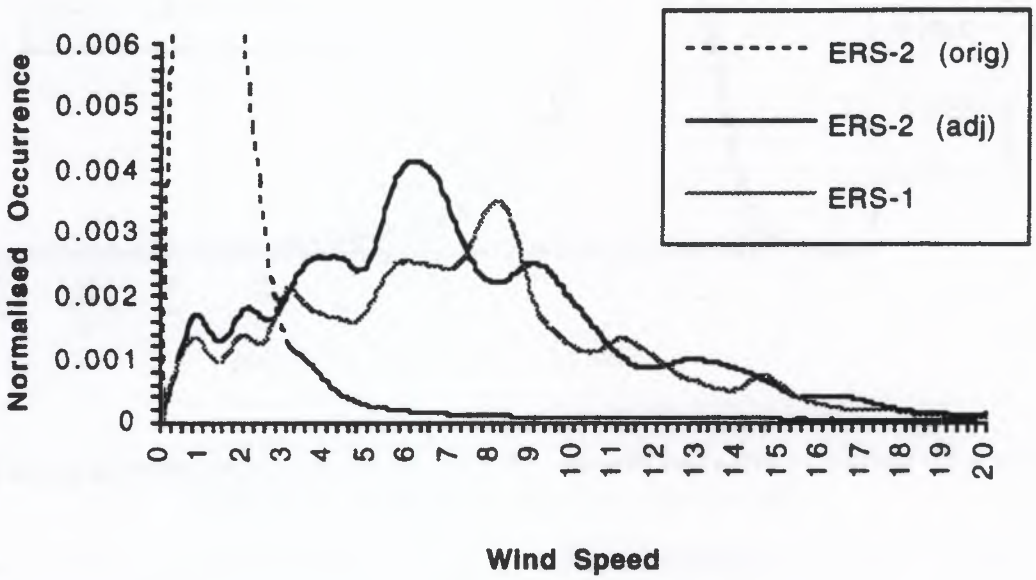

Figure 3. Wind Speed Probability Distribution Function for ERS-1 (dashed grey line) and original (dashed line) and adjusted (solid line) ERS-2 OPR data.

It is clear that the original data (dashed line, mode at ~1 ms^{-1}) gave much too low wind speeds. After the data were corrected, however, there is again reasonable, general agreement between the ERS-2 and ERS-1 distribution functions, although there is some indication that ERS-2 wind speeds may still be biased slightly low with respect to ERS-1. There are small scale differences between these two distribution functions which may partly relate to different wind speeds in the ocean areas sampled, but are probably mainly due to differences in instrument characteristics.

Summary

After applying the correction to the ERS-2 OPR data, the resulting wind speed distribution function agrees well, on broad terms, with that of ERS-1. There are some residual, small scale peaks in the distribution function, which result from irregularities in the sigma0 distribution function.

Distribution Functions of Standard Deviations of OPR Parameters

Data records with high standard deviations may indicate high variability in the surface illuminated by the altimeter, and so should be regarded with suspicion. The 20 Hz standard deviations can therefore be used as a possible indicator for non-ocean signals, and users may choose to set tests to identify appropriate records. Data from different satellite altimeter data sets characteristically have different normal ranges of standard deviations, and so it is important to establish these ranges. Here we have generated probability distribution functions of the 20Hz standard deviations for altimeter range, Figure 4, significant wave height, Figure 5 and radar backscatter, Figure 6. The standard deviations have not been normalised by Nval.

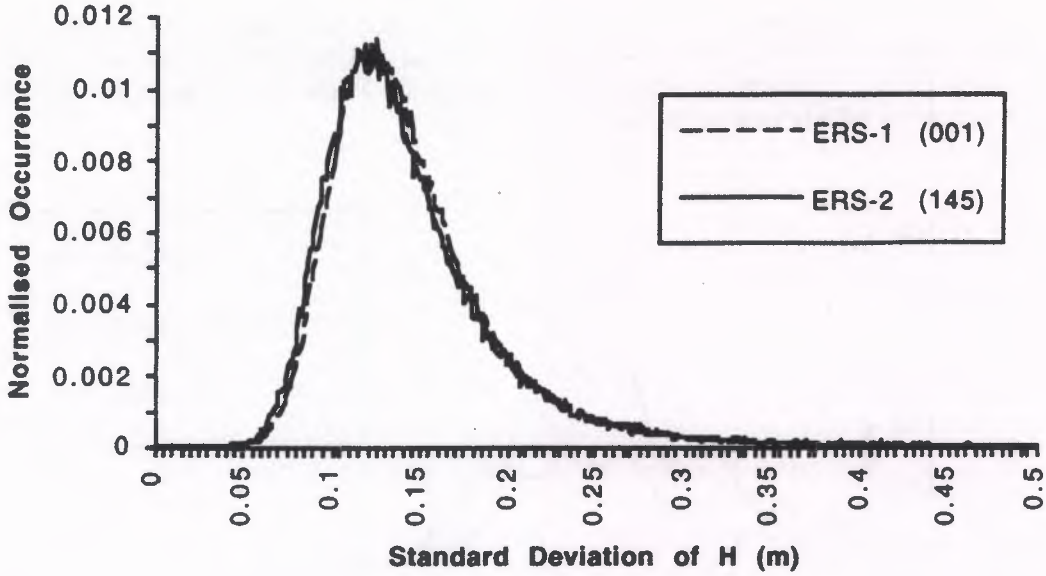

Figure 4. Probability Distribution Function of standard deviation in altimeter range, for ERS-1 (dashed line) and ERS-2 (solid line) OPR data.

The probability distribution functions of altimeter range are almost identical for ERS-1 and ERS-2, with a distribution mode at about 0.13 m (the ERS-1 mode is possibly slightly higher). The functions generated are smooth and continuous and agree with expected behaviour. We can see from this figure that our SOC STD H_alt threshold of 0.3 m would remove a small proportion of data from the tail of the distribution.

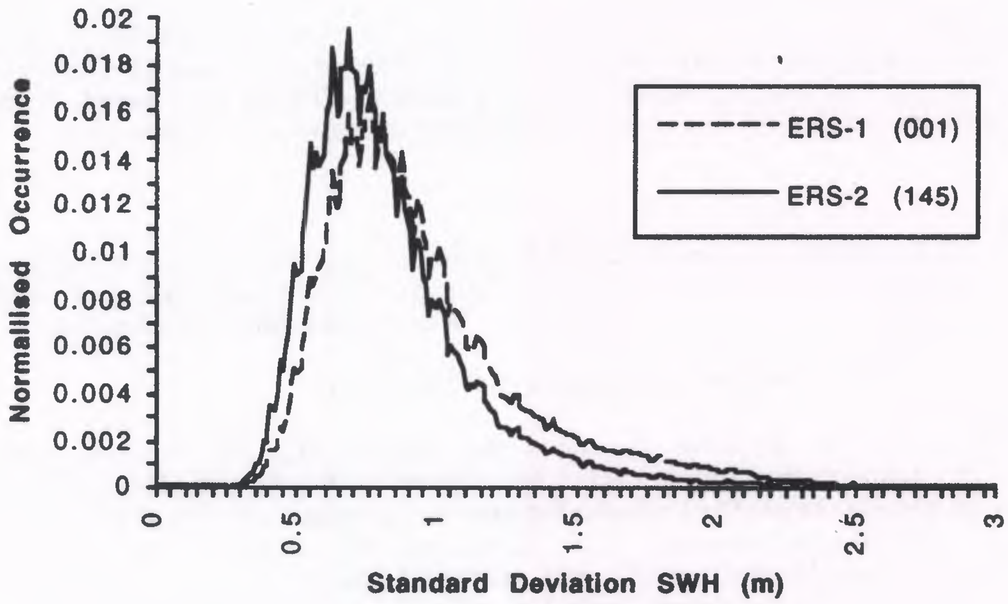

Figure 5. Probability Distribution Function of standard deviation in significant wave height, for ERS-1 (dashed line) and ERS-2 (solid line) OPR data.

The STD_SWH distribution in displayed in Figure 5 exhibits some small scale irregularities, and has a mode at approximately 0.7 m. A data test based purely on STD_SWH > 2.0m would again exclude a small proportion of data from the tail of the distribution. The mode of the ERS-1 distribution is slightly higher than that of ERS-2.

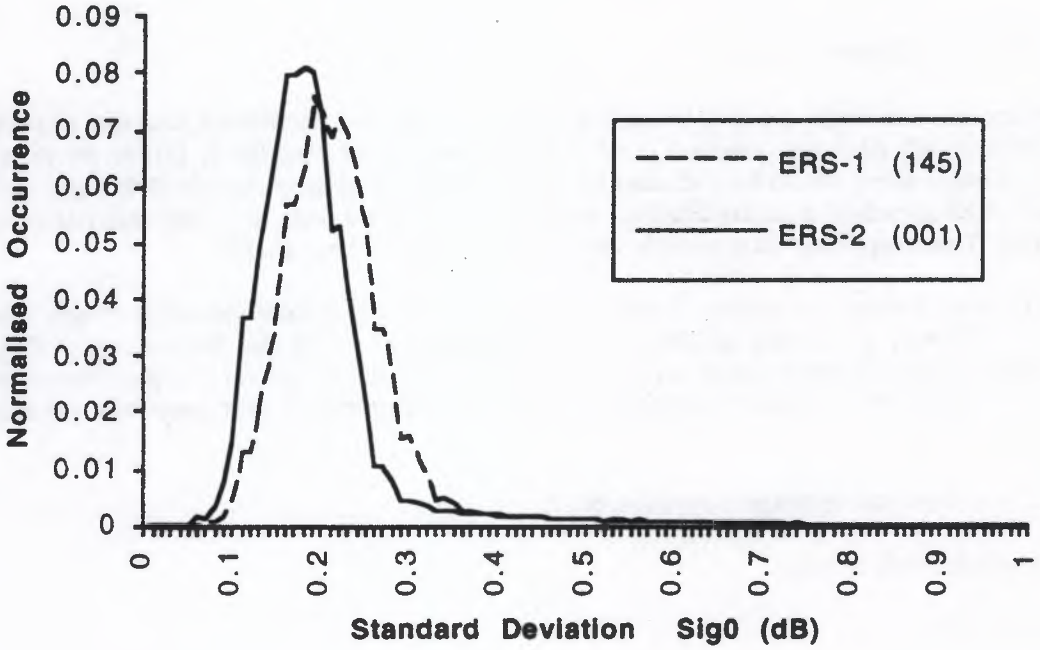

Figure 6. Probability Distribution Function of standard deviation in sigma0, for ERS-1 (dashed line) and ERS-2 (solid line) OPR data.

From figure 6 we can see that the standard deviation in $\sigma0$ has a mode of 0.2 dB, and that there appears to be some limitations in the resolution of these data. The test rejecting data records with STD $\sigma0$ ($\sigma0$ > 0.3 dB) would again affect a small fraction of the data in the tail of the distribution.

Summary

The distribution functions of standard deviations (as given in the OPR product) show physically realistic functions, and suggest the data tests based on thresholds in STD H_alt, STD_SWH, and STD $\sigma0$ would exclude a small proportion of the data. *CERSAT* [1995] gives no suggestions as to expected ranges in these parameters.

Conclusions

In general terms we found the ERS-2 OPR (version 5) product correctly formatted and well documented. However, this product contains an incorrectly calibrated $\sigma0$, which results in wind speeds which are completely unrealistic. If a 3.9 dB correction is applied [Dumont, 1996] physically realistic $\sigma0$ and wind speed distributions result. The significant wave heights do not show any similar large biases and have distributions which are physically realistic. ERS-2 cycle 4 contains an unacceptable number of data records containing invalid $\sigma0$ data. Further specific points are given below.

Product Format and Documentation

The product format has been found to be consistent, and reliable. No formatting errors were found in the first four cycles of ERS-2 OPR version 5 data. There is an inconsistency in the Product User

Manual [*CERSAT*, 1996], in that different maxima in expected wind speed ranges are given for wind_sp (20.15 ms^{-1}) and wind_sp_LW (30.0 ms^{-1}) - the latter limit is beyond the applicability of Witter and Chelton [1991].

We would recommend that the limits used to set the altimeter quality flag bits 4-11 are made available to the users, perhaps in the product information distributed with each OPR CD data cycle.

Flag setting, and Default Values

The setting of data flags appears broadly consistent with documentation and our expectations. About 40% of all data are labelled invalid by the setting of flag bit 0, larger proportions of individual parameters would be excluded by the examination of their specific data flags. Over 54% of data in ERS-2 cycle 4 data are labelled as having invalid $\sigma 0$, due to faulty internal calibration corrections. This proportion data records with invalid $\sigma 0$ is not acceptable.

The philosophy behind the setting of data flags, and the use of default values, is clearly described in *CERSAT* [1996]. Note that all data records labelled as invalid (by the setting of flag bit 0) subsequently have all their fields set to their default value (except for number, time, latitude, longitude and MCD). *CERSAT* [1996] also document recommends that users use the following hierarchy of tests:

1) Validity of the 1-Hz measurement (flag bit 0)

2) Non-default value of field

then, optionally,

3) Specific parameter flags

4) Parameter out of 'normal' range.

Distribution Functions

Analysis of distribution functions for significant wave height, adjusted $\sigma 0$ and adjusted wind speed found that these distributions were physically realistic and consistent with our previous experience with other altimeter data sets. However, final conclusions for $\sigma 0$ and wind speed cannot be provided until a data set with properly calibrated $\sigma 0$ (and hence wind speed) is released.

Standard Deviations

Analysis of the standard deviations of altimeter range, significant wave height, and $\sigma 0$ concluded that these parameters were realistically represented. The resolution in the data limits the ability to create smooth distribution functions for $\sigma 0$. We found the description of the algorithms used to generate these parameters [*CERSAT* , 1995] a little confusing.

References

CERSAT,1996, ERS-2 RA/ATSR products, User Manual, Ref. C2-MUT-A-01-IF, Vsn. 2.0, IFREMER, January 1996.
Dumont, J.P., 1996, Tuning of the ERS-2 OIP software, CLS.OC/NT/96.002, Toulouse, January 1996.
ESA, 1996a, Report of ERS-2 Radar Altimeter Commissioning Working Team, Ed. Benveniste, ESRIN. May 1996.
ESA, 1996b, Calibration of ERS-2 Radar Altimeter OPR data, Ed. Benveniste, ESRIN. May 1996.
Engelis, T.,1996, Geophysical Validation of F-PAF ERS-2 OPR, ESA report, February, 1996
Witter, D.L., and D.B. Chelton, 1991, A Geosat altimeter wind speed algorithm and a method for altimeter wind speed algorithm development, J. Geophys. Res., 96, 8853-8860.

3.2 Geophysical Validation of the F-PAF ERS-2 OPR Radar Altimeter Ocean Product

R. Scharroo and R. Floberghagen

DUT

Geophysical Validation of the F-PAF ERS–2 OPR Radar Altimeter Ocean Product

Remko Scharroo and Rune Floberghagen

Final Report of ESA/ESRIN contract P4500543/PDEX/E

15 April 1996

Delft Institute for Earth-Oriented Space Research
Delft University of Technology
Kluyverweg 1, 2629 HS Delft
The Netherlands

DEOS
Delft Institute for Earth-Oriented Space Research

CHAPTER 1

Introduction

Any useful application of the altimeter range measurements requires an extensive amount of auxiliary data and corrections. These data are therefore supplied on the OPR product together with the 1-Hz altimeter measurements of range, wave height, and wind speed. Validation of the OPR product is therefore implicitly also a validation of all auxiliary data: the precision at which the sea level can be derived from the altimeter range measurement is limited by the precision of each of the corrections.

1.1 Validation process

Validation of the range data on the OPR product was divided into three phases:

Phase 1. Assessment of the Product User Manual (PUM) [*CERSAT*, 1996], data format, and content.

Phase 2. Generation of statistics of range related measurements and corrections which form the basis for edit criteria.

Phase 3. Qualification of the derived product of sea level height based on the selected measurements and corrections.

In Phase 1 we have identified the shortcomings in the PUM, the data format, and data content, as specified in two interim reports [*Floberghagen*, 1995; *Scharroo and Floberghagen*, 1996]. Key points in these reports are:

- Textual corrections to the PUM. These are currently incorporated in Version 2.0 of the PUM.
- Physically improper derivation of the Doppler correction from the range rate rather than the altitude rate. (Section 2.6.1.)
- Confusion about the data flagging and the correspondence of flag bits with data fields set to their default values. This lead to additional recommendations to the user described in Section 2.2.1.
- Ambiguous flagging of overland and ice measurements

The intention of Phase 2 is to provide a set of selection criteria that could be recommended to the user. It would guide the user in selecting those measurements that are directly applicable to the user's need, and would not corrupt results. Here we must distinguish several applications of altimeter data. For example, tidal research does not require a tide model to be available on the data records, whereas the studies of ocean currents explicitly demand the exclusion of data over lakes and inland waters, data that are so valuable to others. This report will mainly focus on the ocean applications, avoiding coastal regions and inland data (Chapter 2).

Phase 3 of the validation determines the quality of the OPR measurements and corrections in comparison to alternative data. In particular, we focus here on the important atmospheric delay corrections. Furthermore, we try to assess the internal quality of the derived sea level height by means of crossover height differences and collinear tracks analyses. Where possible, we examine whether alternative corrections would decrease the crossover height difference, and therefore improve the quality of the sea level determination (Chapters 2 and 3).

1.2 Definition of sea level

Before we can discuss the derivation of sea level heights from the altimeter range measurement and corrections, we have to define what we mean by sea level. Depending on the application, definitions may differ, and some corrections may be included or not. Here, we try to establish a nomenclature that is tractable for each field of altimetry.

Altimeter range is the distance between the centre-of-mass of the satellite and the sea surface as measured by the radar altimeter, corrected for instrumental effects but not for propagation delays: H_Alt on the OPR.

Orbital altitude is the height of the satellite centre-of-mass above a well-defined reference ellipsoid as determined from (precise) orbit computations: H_Sat

Atmospheric delays are the sum of the (one-way) path delay of the radar pulse through the atmosphere with respect to the velocity in vacuum. There are three components to the path delay, caused by ions, neutral particles and water vapour: Iono_Cor + Dry_Cor + Wet_Cor. As an alternative to the wet tropospheric correction from meteorological models, there is the path delay provided by the ATSR/M radiometer: Wet_H_Rad.

Sea state bias is the effect that the radar pulse is better reflected by the wave troughs than the wave crests, which implies that the altimeter always measures a sea level below the level obtained by averaging the true air-sea interface level over the entire footprint. The correction for this effect is (to first order) proportional to the wave height and is given on the OPR as SSB_Cor.

Sea level is the term used for the height of the sea-air interface averaged over the footprint and referenced to the reference ellipsoid. It is computed from

$$H_{sea} = \mathrm{H\_Sat} - \mathrm{H\_Alt} - \mathrm{Iono\_Cor} - \mathrm{Dry\_Cor} - \left\{ \begin{array}{c} \mathrm{Wet\_Cor} \\ \mathrm{Wet\_H\_Rad} \end{array} \right\} - \mathrm{SSB\_Cor}$$

Solid earth tide is the vertical displacement of the earth's crust due to gravitational attraction of Sun and Moon, not counting the constant term. This is represented by H_Set on the OPR.

Ocean tide comprises the elastic ocean tide H_Eot and the tidal loading H_Lt. The latter is the effect of the tidal waves on the earth's crust.

Inverse barometer effect Inv_Bar is the "tidal effect" on the sea surface that is due to changes in atmospheric pressure and can be computed from the dry tropospheric correction using the equations given in Section 6.2.3 of the PUM.

Geoid is a level at which the sum of gravitation and rotation is constant. This is the hypothetical level of the sea at absence of tides, currents, *etc.*: H_Geo

Dynamic topography is the sea surface elevation due to global and regional ocean currents. It can be computed from

$$H_{dyn} = H_{sea} - \text{H\_Set} - \text{H\_Eot} - \text{H\_Lt} - \text{Inv\_Bar} - \text{H\_Geo}$$

(assuming all measurements and corrections to be perfect).

Mean sea surface is the sum of the time averaged dynamic topography and the geoid height. The OPR provides two mean sea surface models: H_MSS_DPAF and H_MSS_OSU

Therefore, the derivation of the ocean currents from the dynamic topography or the assembling of a mean sea surface model requires a lot of corrections to be given and to be correct. Here, one is for instance faced with the fact that the ocean tide is not given for some shallow and enclosed seas, and these derived quantities can not be determined.

When, however, one uses altimeter data to compute ocean tides in these coastal areas, one would not first subtract the ocean tidal elevation. This also requires a careful selection of the measurements to eliminate those that are possibly contaminated by land in the foot print, or those taken over inland waters like lakes. One can not use the land flag for the radiometer measurement for this (Bit 20 of MCD) because it has a much larger "footprint" than the altimeter.

But even the exclusion of data for which the ocean tide is not given does not guarantee that data the remaining data will not be contaminated by land in the footprint, since (1) the ocean tide model does not exclude small islands because of the comparatively course grid spacing of $0.5° \times 0.5°$and (2) ocean tides are also provided for areas permanently covered by floating shelf ice. Therefore, we have used an external $5' \times 5'$ land mask to exclude coastal measurements.

CHAPTER 2

Measurement Elements and Corrections

Applications like oceanography and geodesy require an extensive amount of corrections to transform the altimeter range measurements to estimates of the local sea level height. Both the measurements and corrections have to be quality-checked based on the available information on the OPR, like the Measurement Confidence Data MCD and the standard deviations of the measurements.

In this Chapter we will discuss the most important data elements of the OPR for computing sea level heights from the altimeter range measurements. Criteria are devised to eliminate rogue measurements.

Statistics are given for ERS–2 Cycle 2, but are equally applicable to other "ocean mode" cycles of ERS–2 or ERS–1. The "ice mode" cycles have more altimeter data invalidated because of non-ocean tracking. The selection criteria, however, equally apply to "ice mode" cycles.

2.1 General considerations

2.1.1 Measurement concept

As described in the PUM, three quantities are determined from the shape of the waveform: range, wave height, and wind speed.

- The delay time between transmission and reception of the radar pulse is a measure for the altimeter range: the height of the altimeter above the surface.
- The total received power is a measure for the backscatter from the surface, hence of the rippling of the surface, which relates to the wind speed.
- The rate at which the power increases to its maximum is a measure for the difference in height between the wave peeks and wave troughs, or the Significant Wave Height.

This means that if the waveform does not comply to an expected shape (the Brown Model), at least one of the measurement parameters will be out of an expected range, or is poorly estimated, in which case the measurement should be rejected. Wave height and wind speed are therefore also used as selection criteria for the range measurements.

2.1.2 20-Hz and 1-Hz measurements

The altimeter produces 1000 chirps per second. Upon return, 50 chirps are averaged into one waveform and processed individually. This produces each second 20 *independent* estimates of range, wave height, and backscatter. If one of these estimates is outside a predefined range (*not* mentioned in the PUM), corresponding flag bits of the Measurement Confidence Data **MCD** are set to "bad".

To reduce the data stream to manageable proportions, the 20-Hz measurements of backscatter and wave height are averaged into the 1-Hz values **Sigma0_Raw** and **SWH** and their respective standard deviations **Std_Sigma0** and **Std_SWH**. It must be stressed that the standard deviations are those of the *20-Hz* measurements, and will therefore be much larger than the standard deviations of 1-Hz measurements provided on some other altimeter products. Because of the virtual independence of the 20-Hz measurements, the recorded standard deviations may be divided by $\sqrt{\text{Nval}}$, where **Nval** is the number of valid 20-Hz measurements used for computing the 1-Hz measurement.

The 20-Hz measurements of range are first fitted with a linear function. The 1-Hz value **H_Alt_Raw** is the range indicated by the linear fit half-way the tenth and eleventh 20-Hz measurement. The standard deviation **Std_H_Alt** is determined from the scatter of the 20-Hz measurements around the linear fit. Again, we may divide this value by $\sqrt{\text{Nval}}$ to get a value comparable with the 1-Hz standard deviations of the range measurement provided on other altimeter products.

The 1-Hz measurements may be set to their respective default values 32767 or 2147483647 to indicate that the computation of the 1-Hz value was not possible or out of a specified range. These are *not* the ranges given in the PUM for each element, which are merely provided as typical values.

There is *no explicit correspondence* between the flag bits of the **MCD** and the default values for the measurements and corrections. This leads to following procedure to quality check the primary elements related to the altimeter range measurement (Table 2.1):

- An element is invalid when the value is set to the default.
- An element is invalid when at least one of the corresponding bits of the **MCD** is set to 1.
- A valid element can be further checked against a predefined range.

2.1.3 Operating modes

The altimeter has two principal operating modes: ice tracking mode, and ocean tracking mode. These terms do refer to the type of surface that is most efficiently tracked in either mode, although it is not essential that the altimeter is actually operating in ice tracking mode to measure over ice. The difference between the two modes is the width of the tracking window. Ice tracking mode has a wide range window with a course resolution, allowing for rapid changes in range along the flight path. In ocean tracking mode the window is smaller, has a significantly higher resolution, but can only follow shallow slopes.

A third mode, acquisition mode, provides no proper measurements, but is needed when the altimeter fails to lock onto the surface because the waveform has shifted out of the range window.

To complicate things, terms "ocean mode cycle" and "ice mode cycle" are used to indicated which tracking modes are used during a cycle. "Ocean mode" here means the satellite is always operating in ocean tracking mode, also over land and

Field	Description	Unit	Flags	Minimum	Maximum
H_Alt	Altimeter range	mm	4 5 6	779 500 000	820 500 000
H_Sat	Orbital altitude	mm	23	779 500 000	820 500 000
Std_H_Alt	Sigma range	mm		1	500
SWH	Significant Wave Height	cm	7	0	800
Std_SWH	Sigma SWH	cm		1	200
Wind_Sp	Wind speed[a]	cm/s	15	0	800
Sigma0	Backscatter coefficient	10^{-2} dB	8 9 10	700	2300
Dry_Cor	Dry tropo correction	mm		–2400	–2100
Wet_Cor	Wet meteo correction	mm	21	–600	–1
Wet_H_Rad	Wet radio correction[b]	mm	17 18 19 20	–600	–1
Iono_Cor	Ionospheric correction	mm		–150	–1
H_Eot	Elastic ocean tide	mm	16	–2500	2500
Nval	Number of 20-Hz obs	mm		17	20

[a] Wind speed is not used as edit criterion, but is supplied here for reference only

[b] When the wet radiometer correction is absent, the wet meteorological correction is used instead

Table 2.1 Edit criteria and histogram ranges used to validated the various data fields supplied on the OPR

ice surfaces. Cycle 1, 2, and all consecutive *even* Cycles of ERS–2 are "ocean mode cycles". Cycle 3 and consecutive *odd* Cycles are "ice mode", indicating that the altimeter is switched to its course ice tracking mode over land and permanently ice covered surfaces and remains in ocean tracking mode over (open) ocean surfaces.

Because (on the OPR) data acquired in non-ocean tracking mode are invalidated in "ice mode" cycles, these cycles do not supply any data over lakes, ponds, and marshes, as in the "ocean mode" cycles.

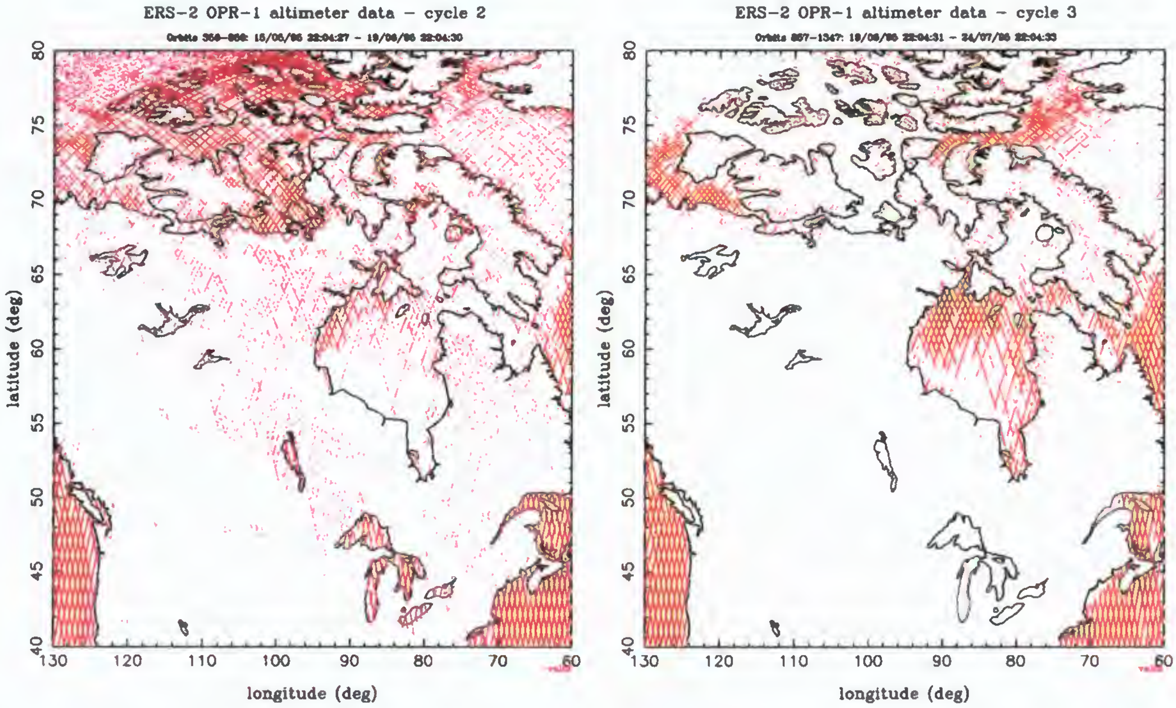

Figure 2.1 "Valid ocean returns" over Canada. **Left:** Ocean-mode Cycle 02. **Right:** Ice-mode Cycle 03.

2.2 Characterisation data

2.2.1 Measurement Confidence Data

Quality flags are provided to indicate the validity of the altimeter measurements and corrections. The PUM provides information on which data elements refer to which bits of MCD (See also Table 2.1). However, when one of the corresponding bits is set to 1 ("bad") the data field may not be set to its default. Also, a default value in one of the data fields does not require any of the corresponding bits of MCD to be set. Therefore, checks on the flag bits as well as default values have to be applied to eliminate rogue measurements. Refer to Section 6.3 of the PUM for more information on flag bits and defaults.

The most important bit of the MCD is bit 0. It indicates the validity of the altimeter measurement. When set to 1 ("invalid"), all elements but the time, latitude, and longitude are set to their defaults. This is actually a very impractical use of disk space, because these data records tell you virtually nothing, not even the orbital altitude that *could* be helpful for interpolation purposes.

Only "valid" measurements with bit 0 set to 0 are discussed in the following.

Causes of invalidation are explained in Section 4.2.1 of the PUM. In short, a measurement is flagged "invalid" when either of the following is true.

- The instrument is not in ocean tracking mode. This means that for "ice mode" cycles all measurements over the land are rejected (See Section 2.1.3).
- Invalid telemetry.
- Measurement is over a 100% land-covered area.
- The measurement is not over 100% ocean-covered area and the waveform is not "ocean-like".
- The measurement is over a 100% ocean-covered area beyond 45° latitude and

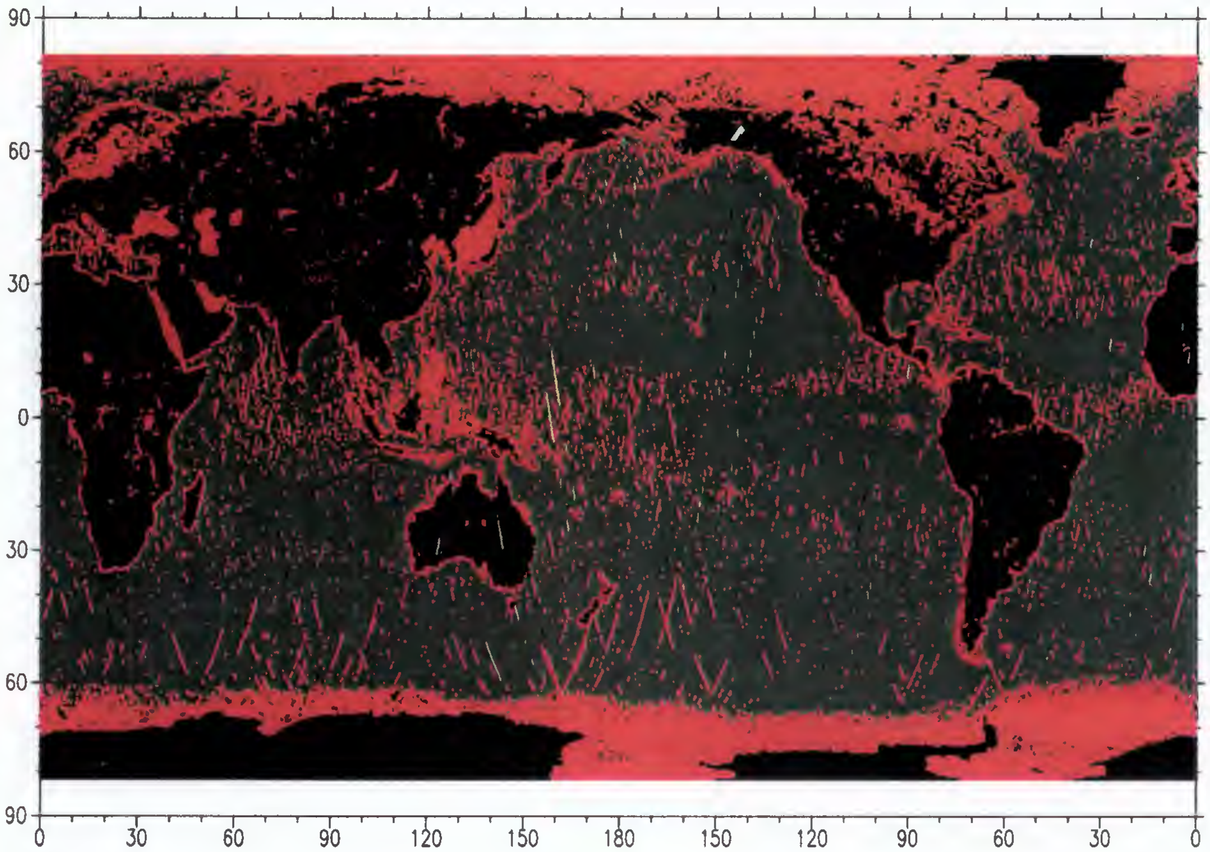

Figure 2.2 Distribution of OPR altimeter measurements. **Black:** data flagged "invalid" by bit 0 of MCD. **Red:** data rejected by any of the criteria mentioned in this Chapter. **Green:** remaining data.

the waveform is not "ocean-like".

This means that data over lakes, marshes, and ponds are retained in the data product as *valid ocean returns* when the land mask indicates 100% water, or when the waveform is "ocean-like". Figure 2.1 shows that this encompasses a lot of measurements that have to be rejected when the altimeter data are used for oceanographic purposes. The OPR product contains no straightforward means to separate lakes from ocean, but to check various other elements.

In Figure 2.2 the location of all records flagged "invalid" (bit 0 is 1) are plotted as black dots; red and green dots represent "valid" data (bit 0 is 0), where red dots indicate rejection by at least one of the criteria mentioned in the following. Note that the checks used for the MCD bit 0 that are intended to exclude returns from (sea-)ice is clearly not exhaustive, *e.g.*, permanent floating ice masses like the Antarctic ice shelfs (areas one would rather call "land" than "ocean") are flagged 100% ocean and many of the measurements pass the "ocean-like" return criterion as well as various other criteria including the presence of ocean tides.

For "ice mode" cycles like Cycle 3, the majority of the lake data is removed because the altimeter is in ice mode over the continents. Still, a conspicuously large number of non-ocean data is retained as *valid ocean returns* (Figure 2.1).

2.2 Characterisation data

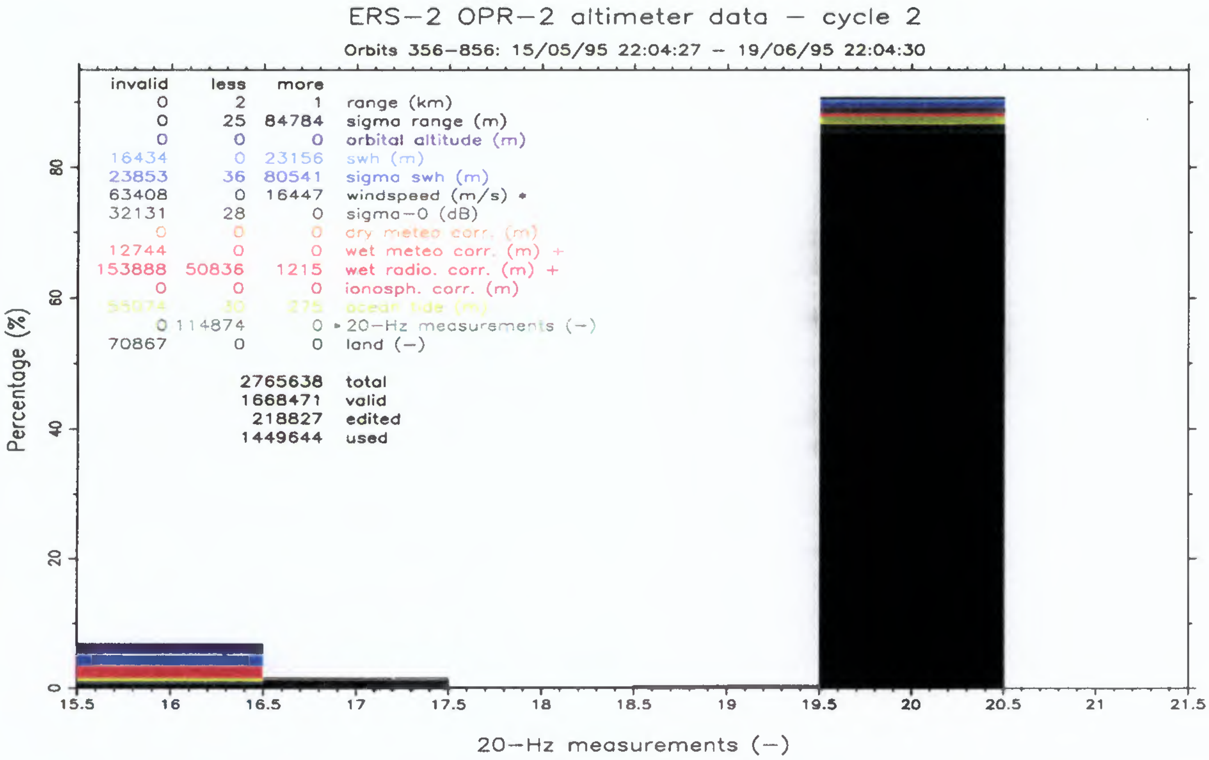

Figure 2.3 Histogram of the number of 20-Hz measurements Nval.

2.2.2 Number of 20-Hz measurements

Figure 2.3 shows the histogram of the number of valid 20-Hz measurements per 1-Hz observation Nval. The black part of the histogram (as in all following this one) indicates the histogram of the selected records, records that pass all selection criteria mentioned in Table 2.1. The coloured part of the histogram indicates which part of the *valid* measurements is removed because of one of the other fields is out of range, set to its default, or is flagged "bad" by a corresponding bit of MCD.

In the leftmost bar all 1-Hz observations consisting of less than 17 20-Hz measurements are gathered. The majority of these observations are also rejected by other criteria, so the lower criterion Nval > 16 is not over-selective. The observations that are rejected on the basis of the criterion are plotted in Figure 2.4 and clearly coincide with the presence of sea ice.

The fact that the bar at 17 20-Hz measurements is larger than 18 and 19 is because for ERS–2 each 60 seconds three 20-Hz measurements are sacrificed to the internal calibration.

2.3 Range and altitude elements

2.3.1 Altimeter range and orbital altitude

The histogram of the altimeter range (corrected for instrumental effects) H_Alt is plotted in Figure 2.5. Obviously, the histogram for the orbital altitude H_Sat is identical to the eye and is not shown here.

The large number of rejections for ranges between 795 and 797 km is conspicuous, but easily attributable to the large number of sea-ice returns in the Arctic region over which area the satellite maintains an altitude around 796 km.

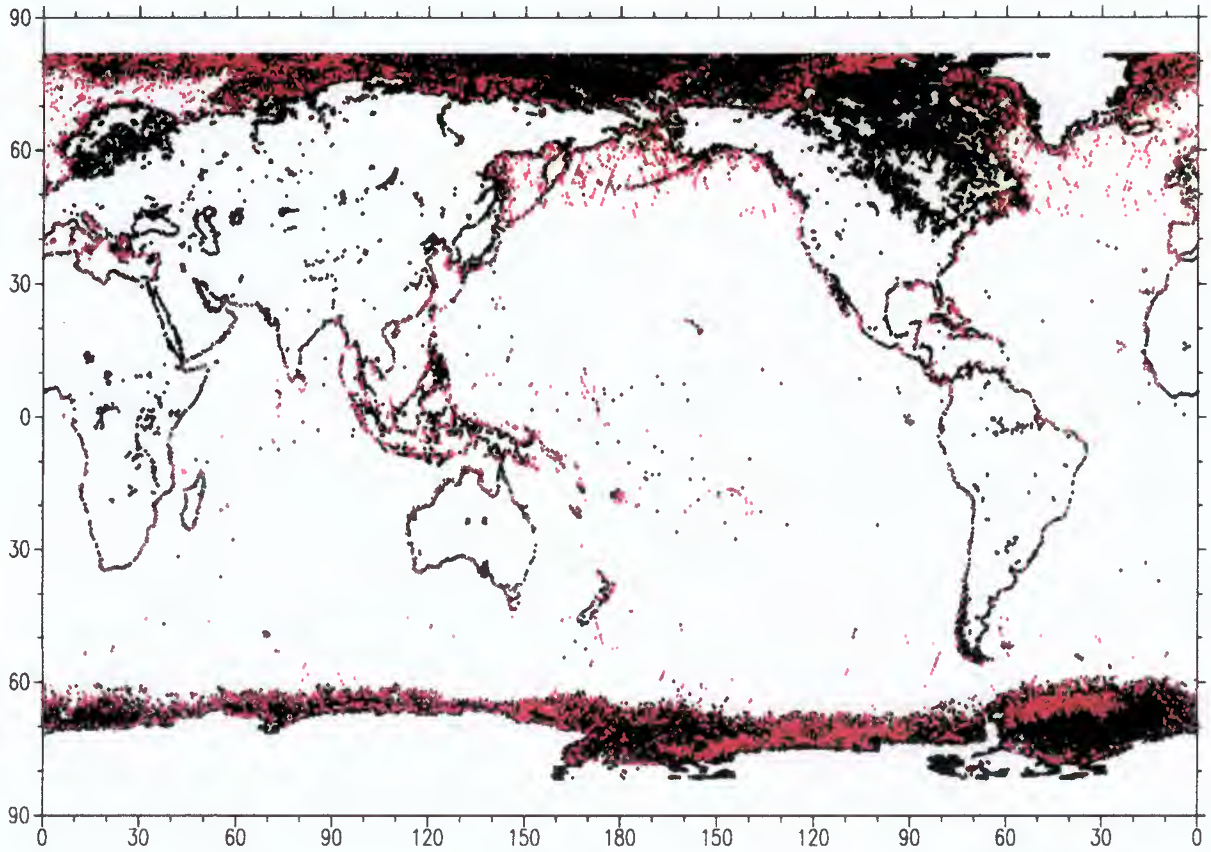

Figure 2.4 Distribution of records with Nval less than 17. Red dots indicate rejection by this criterion only.

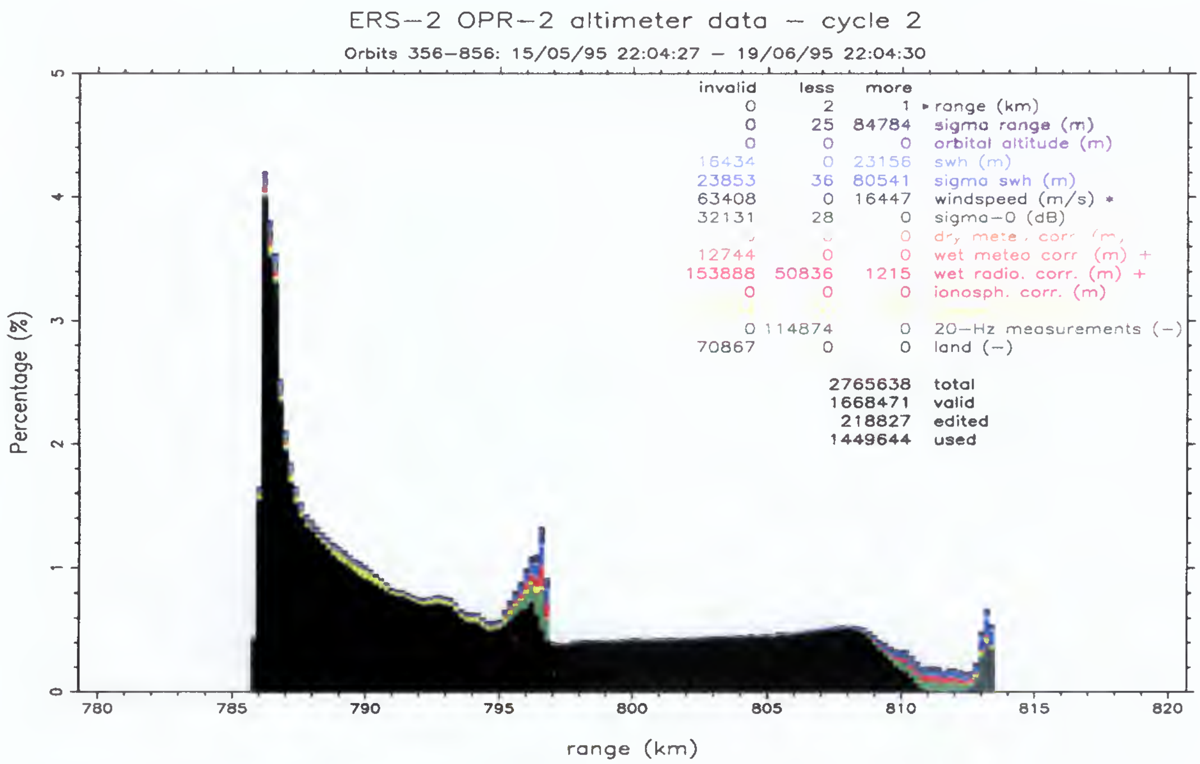

Figure 2.5 Histogram of altimeter range H_Alt.

2.3 Range and altitude elements

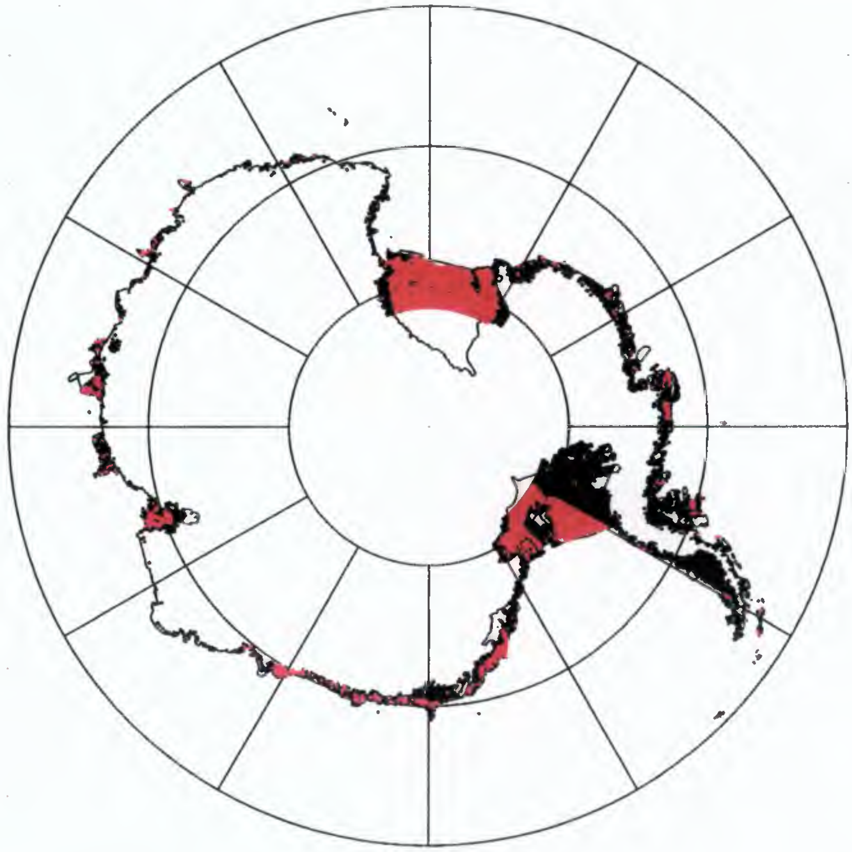

Figure 2.6 Distribution of data rejected by the external land mask. Red dots indicate rejection by this criterion only.

At the far end of the histogram (beyond 811 km) again a large number of measurements is rejected, primarily on the basis of an external land mask. Figure 2.6 shows the locations of the measurements that are rejected by the external land mask.

Note that about 50% of the data over the Amery, Ross, Filchner, and Ronne Ice Shelfs could *only* be rejected by applying the external land mask. All other selection criteria have been passed successfully. Even the ocean tide is given for these areas because the ice is floating. However, between 60°W and 90°W the Enhanced Schwiderski tide model seems *not* to give valid tidal elevations for the ice shelfs.

Still, the fact that we need the land mask to reject the measurements over ice shelfs may also placate us. It suggests that the altimeter is very well equipped to track the ice shelfs even in ocean mode, providing a wealth of observations of the ice thickness (and its variations) in areas that are otherwise poorly monitored.

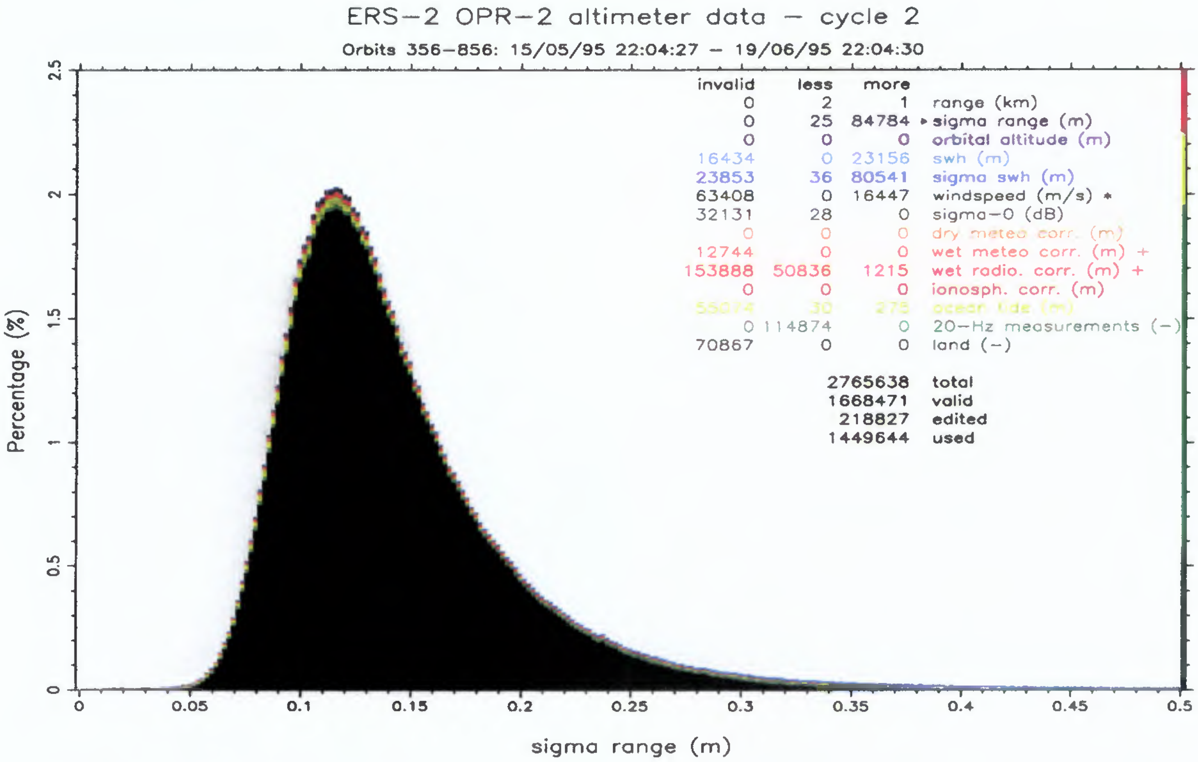

Figure 2.7 Histogram of the standard deviation of altimeter range Std_H_Alt.

2.3.2 Standard deviation of altimeter range

The histogram of the standard deviation of the 20-Hz altimeter ranges Std_H_Alt is plotted in Figure 2.7. Only 25 values were lower than cutoff of 1 mm, but a significant amount of almost 85000 exceed the upper limit of 50 cm. Note, however, that only 750 of these are rejected solely on the basis of Std_H_Alt > 500 mm. The rest coincides with the rejection on various other criteria (mainly SWH).

As suggested in the PUM, the 20-Hz ranges are virtually independent, so we may divide Std_H_Alt by $\sqrt{\text{Nval}}$ to get the standard deviation of the 1-Hz altimeter range, σ_h, so we can compare it to the values given on altimeter products of other satellites, and gives us an estimate of the precision of the 1-Hz range measurement (See also Section 2.4.1).

2.3.3 Dry tropospheric correction

The dry tropospheric correction Dry_Cor is directly related to the air pressure produced by the ECMWF meteorological models. Apart from extreme highs and lows the model pretty well resembles the ground truth.

In comparison with the dry tropospheric correction computed from the NMC meteorological model (Figure 2.9), we see that the path delays determined by either model differ generally less than a few centimetres. The RMS difference is only 8 millimetres. Assuming both models to be independent, but adding some contribution of omission errors (not modelling properly the extremes), we can assume that the dry tropospheric correction is precise to about 1 cm.

Figure 2.8 shows the histogram of the dry tropospheric correction Dry_Cor. None of the values was set to default or out of range.

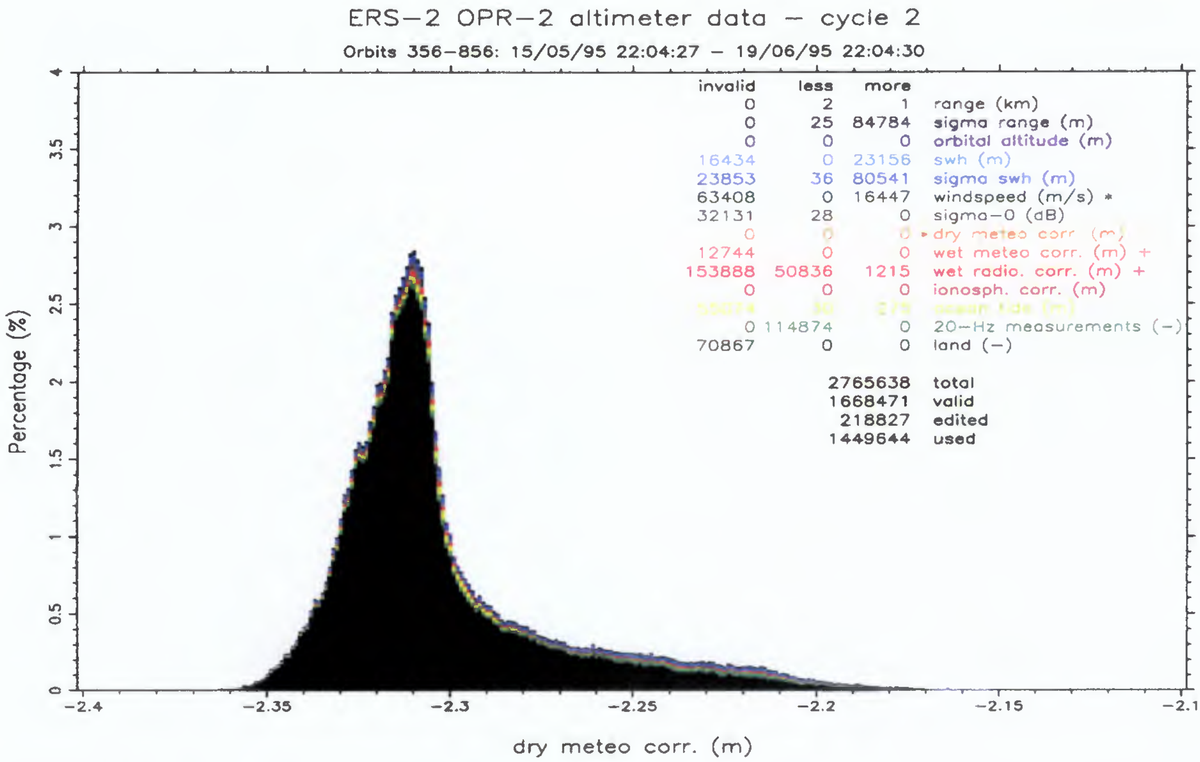

Figure 2.8 Histogram of the dry tropospheric correction Dry_Cor.

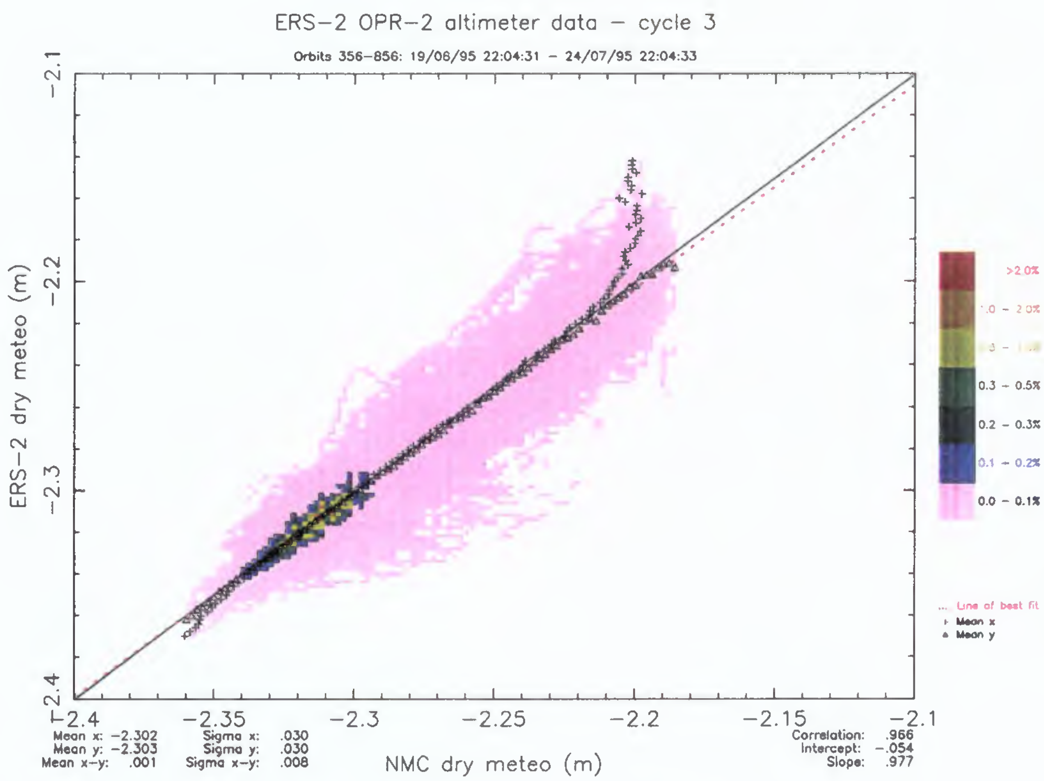

Figure 2.9 Scatterogram of ERS–2 (ECMWF) and NMC dry tropospheric corrections.

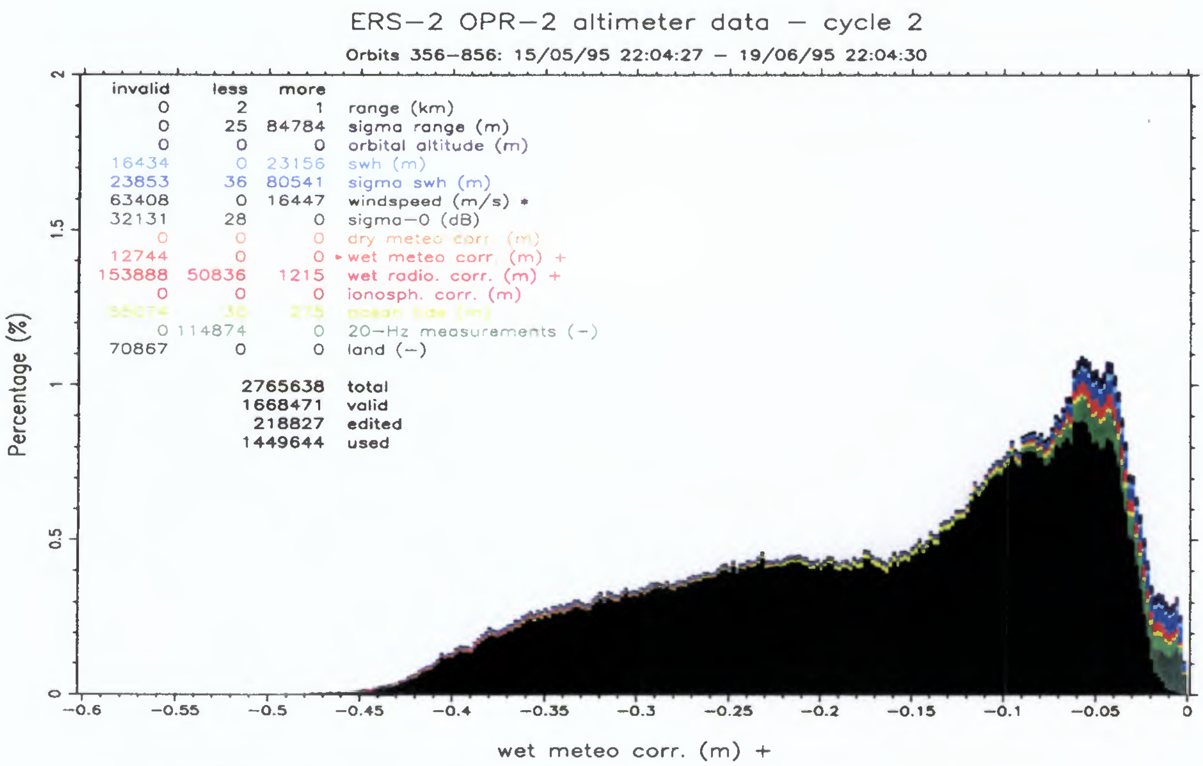

Figure 2.10 Histogram of the wet meteorological correction Wet_Cor.

2.3.4 Wet tropospheric correction

For the wet tropospheric delay two values are provided on the OPR: one obtained from ECMWF meteorological fields, the other measured "directly" by the ATSR/M radiometer on board the ERS satellites.

Figure 2.10 shows the histogram of the wet meteorological correction Wet_Cor. Note that towards the "dry" part of the histogram (values near zero) many of the observations are rejected on the basis of the standard deviations of range and wave height, the number of 20-Hz measurements, and by the external land mask. This suggests that these observations were taken over "arid" areas, like land (possibly small lakes) and ice shelfs. Especially over ice shelfs the humidity is very low. (See also Section 2.3.1).

Apart from less than 1% rejection because the meteorological correction was not available (all of them coinciding with other rejection criteria), none of the corrections are rejected because they are out of the predefined range.

Figure 2.11 shows the global comparison of the ECMWF against the NMC wet meteorological correction. Correlation is 96% and there is hardly any offset or slope between the two corrections. The RMS difference is 3.1 cm, probably equally attributable to errors in either correction. On top of this omission errors should be added.

Figure 2.12 shows the histogram for the wet radiometer corrections Wet_H_Rad. It ranges to larger values (longer delays) than the meteorological correction because the radiometer is able to identify very local extremes in humidity that are obviously smoothed out in the meteorological fields. Yet, longer delays than 60 cm are unlikely, or could indicate rain cells that—in any case—could have contaminated the altimeter measurement, which is also suggested by the high number of coincident rejections based on other criteria. A few observations are rejected because the wet radiometer correction equals zero.

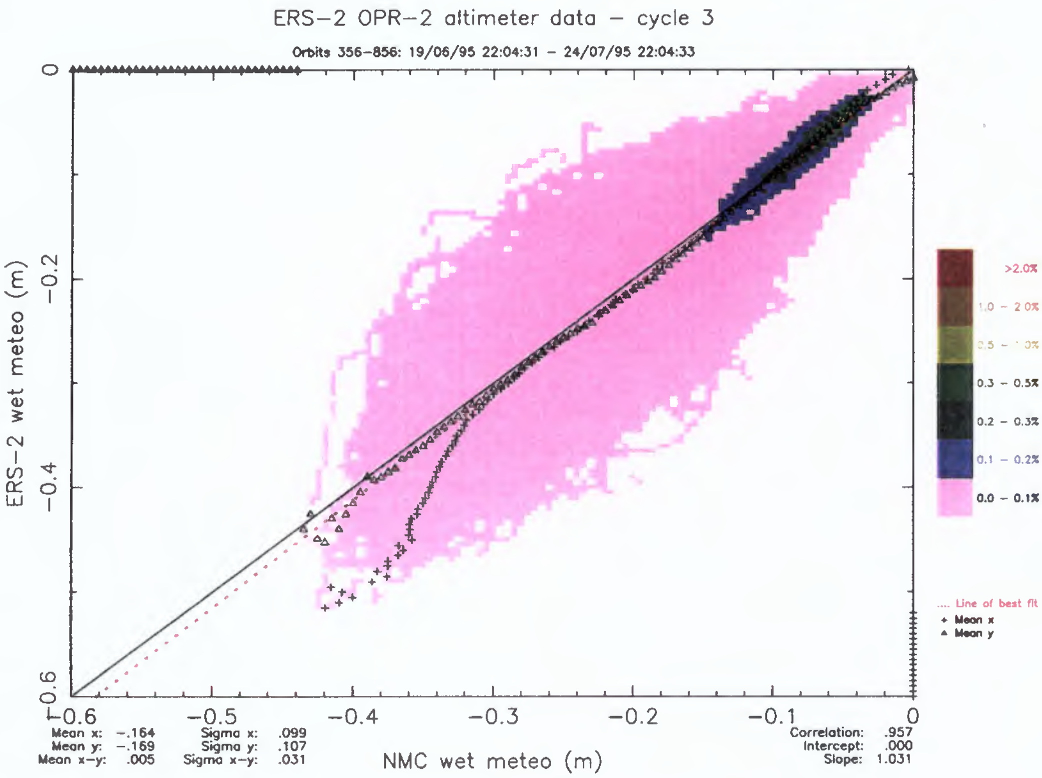

Figure 2.11 Scatterogram of ERS–2 (ECMWF) and NMC wet meteorological corrections.

Because the wet radiometer correction is invalidated over land and close to the coast, this correction is to be replaced by the wet meteorological correction when these areas are of interest to the user. Moreover, the ATSR is very often switched off, thus providing no wet radiometer correction, even over open ocean. In Figure 2.14 the locations marked red are when observations would have been rejected solely because the wet radiometer correction is not available. Because this clearly limits the global use of the altimeter data, we used the following selection:

- Use the wet meteorological correction Wet_Cor by default.
- If the wet radiometer correction is not flagged unavailable (Bits 17, 18, 19, and 20 of MCD are 0) and is not set to the default value (32767) use the Wet_H_Rad.
- Reject the observation when the selected correction is invalid or out of range.

In Figure 2.15 the wet tropospheric corrections are compared along the pass shown in Figure 3.1 of Section 3.1. It is clear that the meteorological correction is a smoothed version of the radiometer correction, that occasionally peaks up to very high values, especially in the tropics.

A global comparison of Wet_Cor and Wet_H_Rad is presented in the scatterogram of Figure 2.13. The primary difference is the cut-off of the meteorological correction at around 50 cm, whereas the radiometer correction extends up to 60 cm. The RMS difference between the corrections is 5.6 cm, which is for the larger part attributable to omission errors in the wet meteorological correction.

The scatterograms of Figures 2.11 and 2.13 suggest that the wet meteorological (Wet_Cor) and wet radiometer (Wet_H_Rad) corrections have a precision of about 5 cm and 3 cm, respectively.

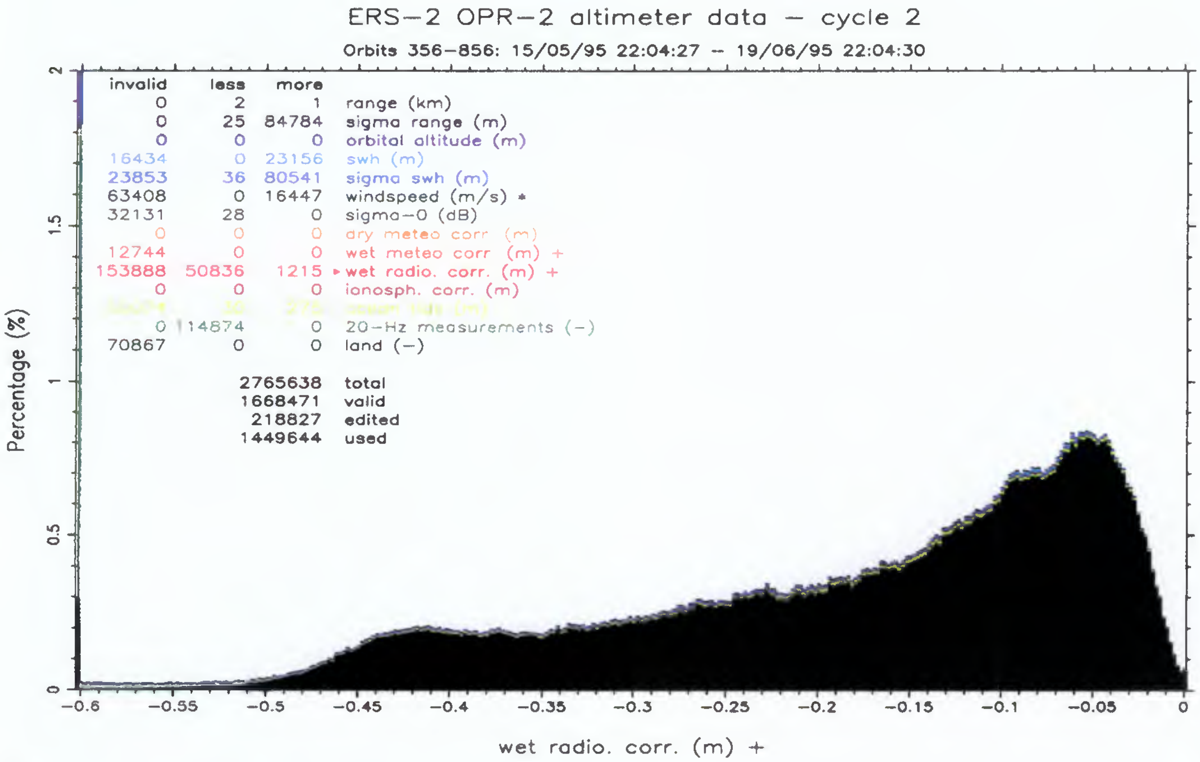

Figure 2.12 Histogram of the wet radiometer correction Wet_H_Rad.

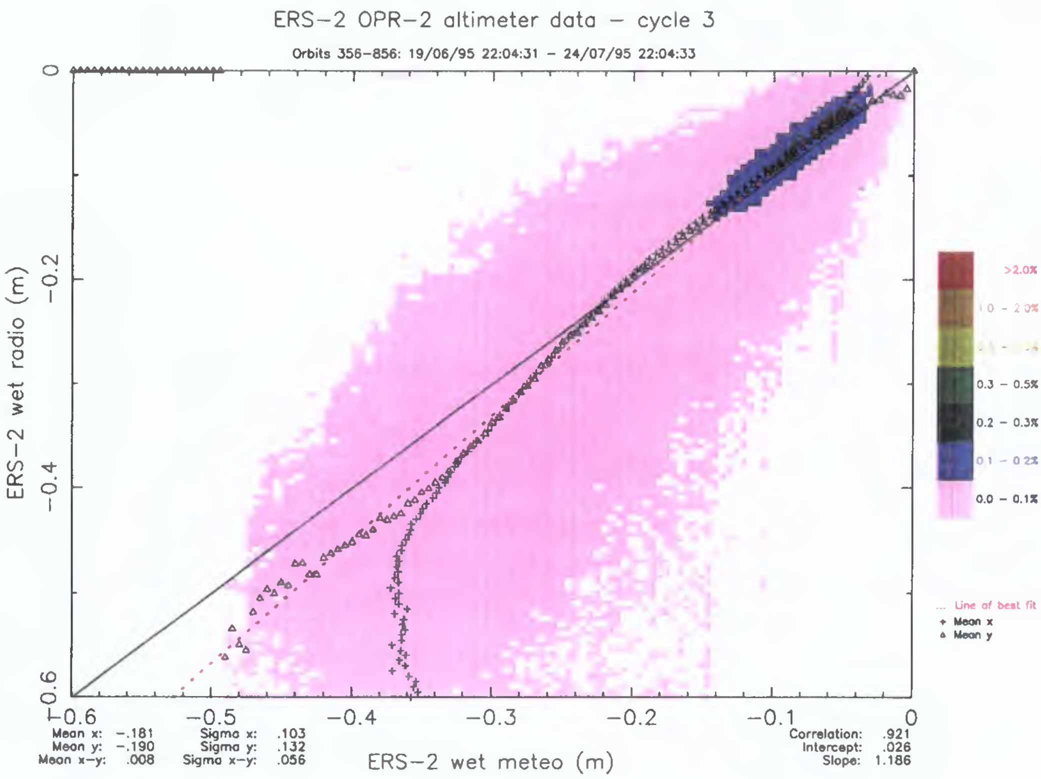

Figure 2.13 Scatterogram of ERS–2 wet radiometer and wet meteorological corrections.

2.3 Range and altitude elements

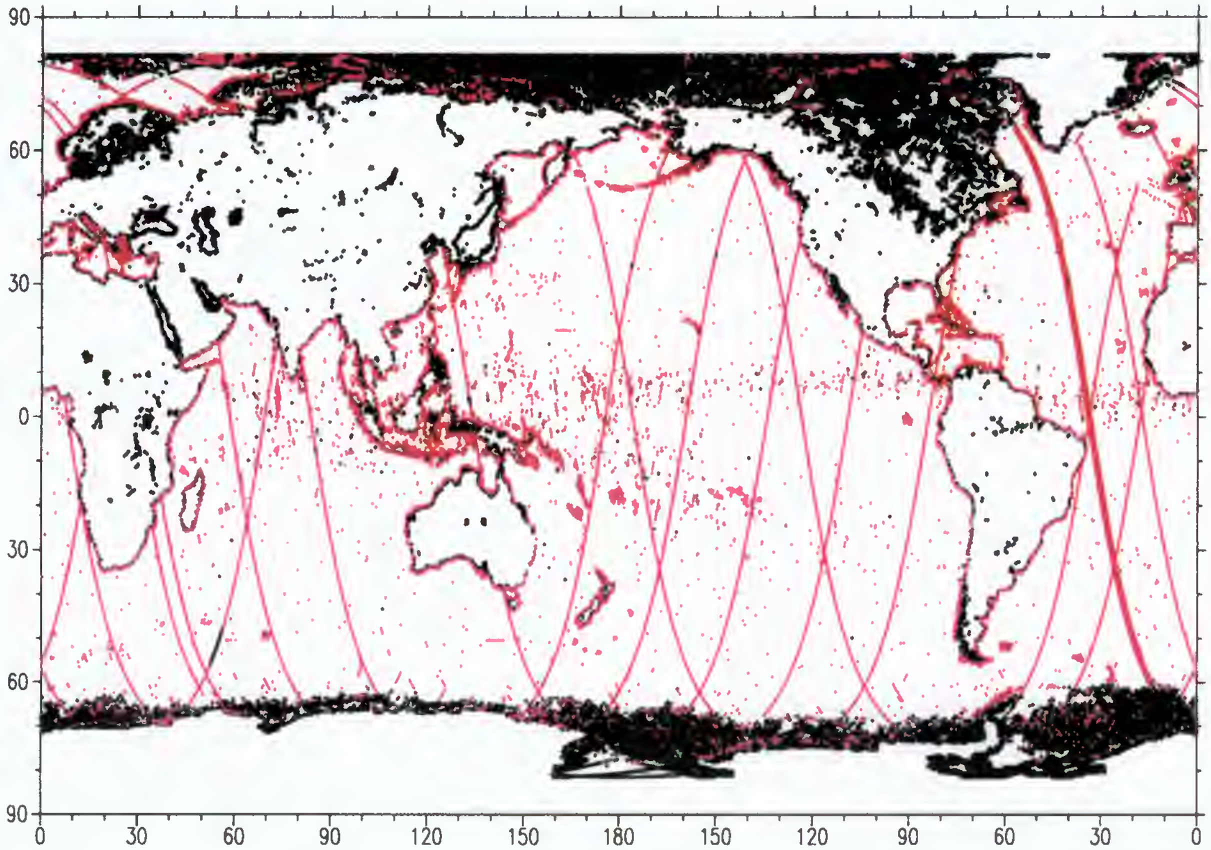

Figure 2.14 Distribution of data under absence of the wet radiometer correction. Red dots indicate when this would be the only reason to reject the record.

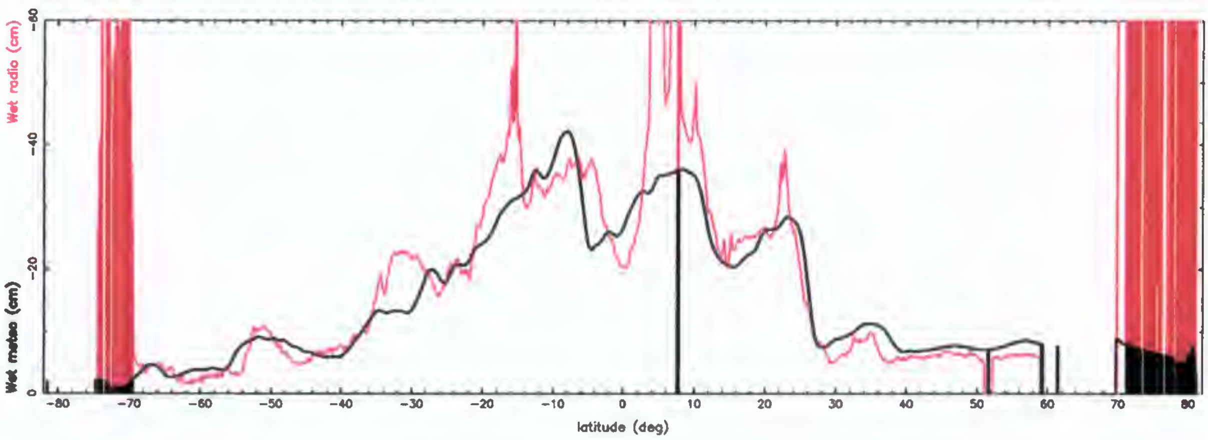

Figure 2.15 Comparison of the wet tropospheric corrections along a single track. **Red:** Radiometer correction. **Black:** Meteorological correction.

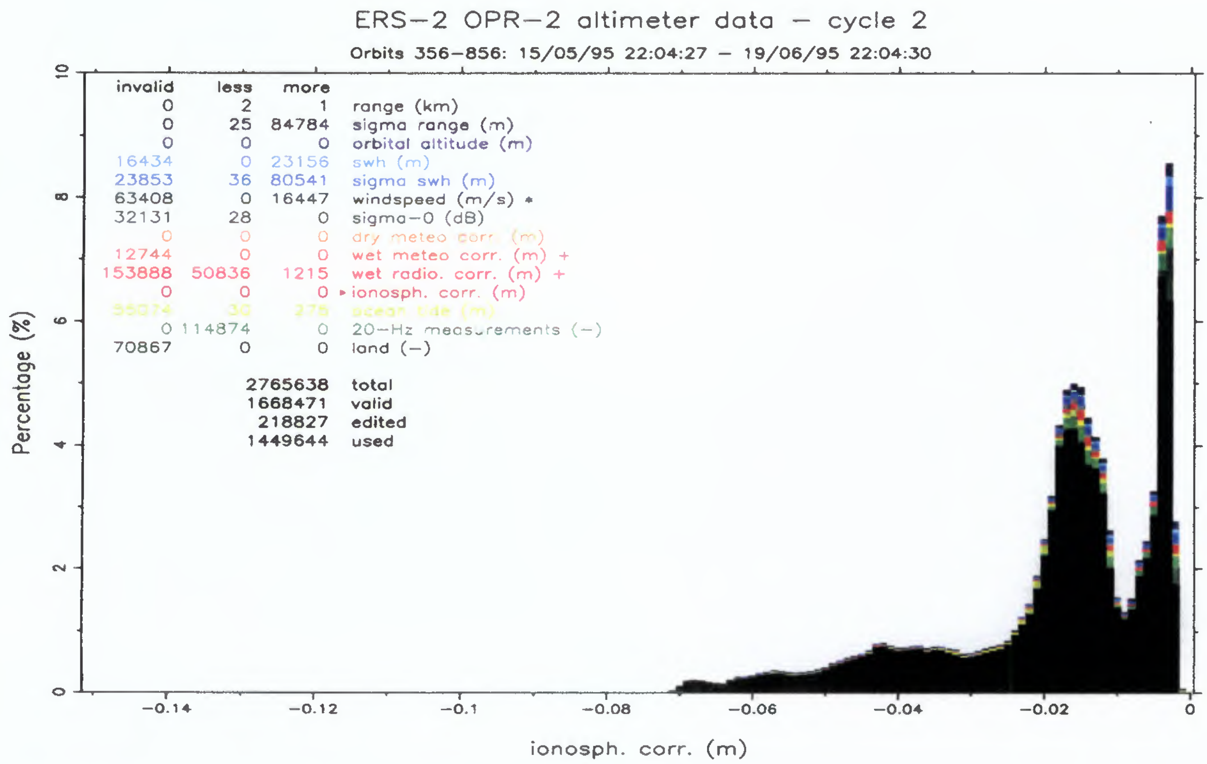

Figure 2.16 Histogram of the ionospheric correction Iono_Cor.

2.3.5 Ionospheric correction

For the ionospheric correction the histogram is plotted in Figure 2.16. As for the dry tropospheric correction the Bent model behaves very well and no default or out of range values are identified.

Comparison with the IRI90 ionospheric model (Figure 2.17) gives an excellent 95% correlation with an RMS difference of only 7 millimetres. Omission errors in both ionospheric will be of a similar magnitude, so we can assume that the ionospheric correction is also precise to about 1 cm.

2.3.6 Ocean tide

The OPR data sets used for this validation process contained the Enhanced Schwiderski ocean tide model. Meanwhile, this is replaced by the Grenoble FES 95.2.1 model. Hence, conclusions given in this section may not be applicable to the common use of the OPR CDROMs.

Figure 2.18 gives the histogram of the sum of elastic ocean tide H_Eot and load tide H_Lt. It is pretty well limited to the range –2.5 to 2.5 metres apart from a few outliers.

The ocean tidal elevation is not provided over some shallow seas (*e.g.*, Sea of Japan), coastal waters, and inland seas and lakes, as shown in Figure 2.19. For the use of altimeter data in these areas, either an alternative tide model should be used, or the ocean tidal correction should be omitted.

However, the tide model *is* given for much of the floating permanent ice shelfs.

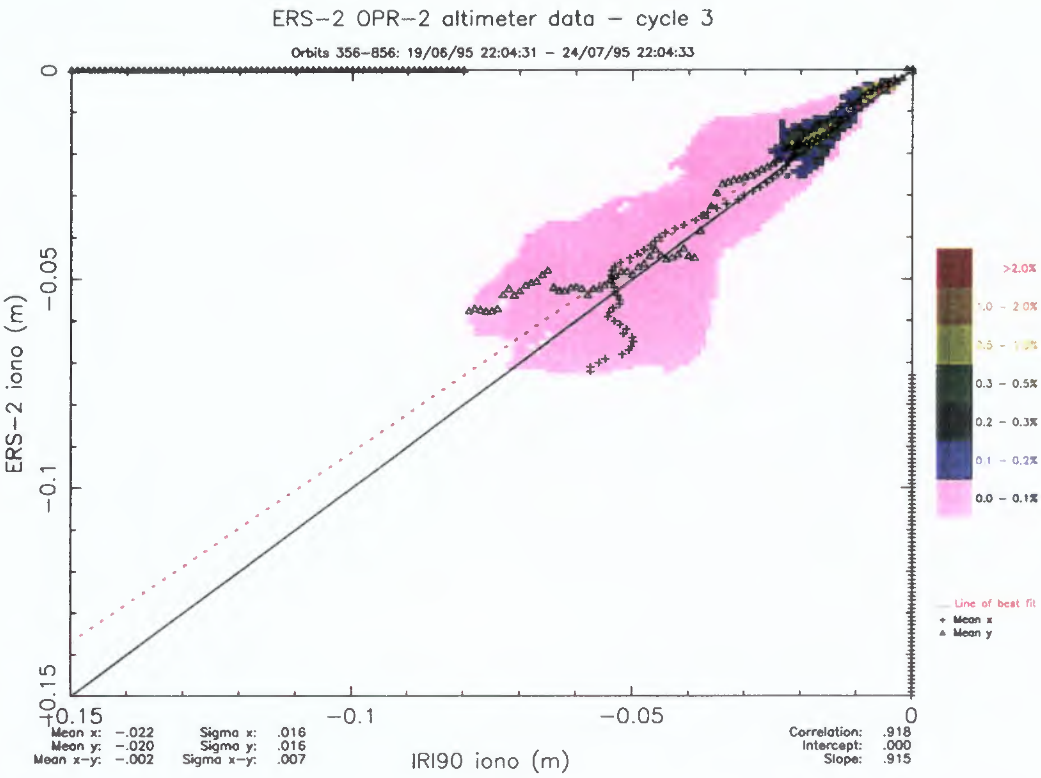

Figure 2.17 Scatterogram of ERS–2 (Bent) and IRI90 ionospheric corrections.

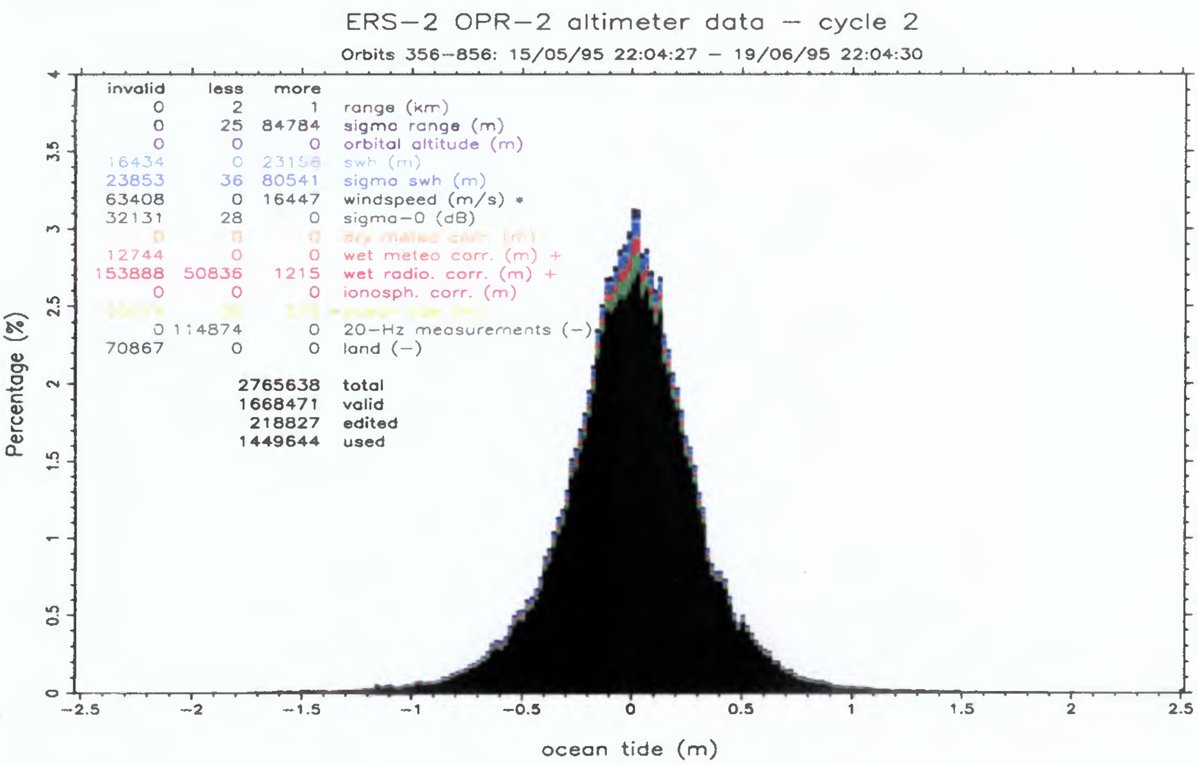

Figure 2.18 Histogram of the ocean tide H_Eot

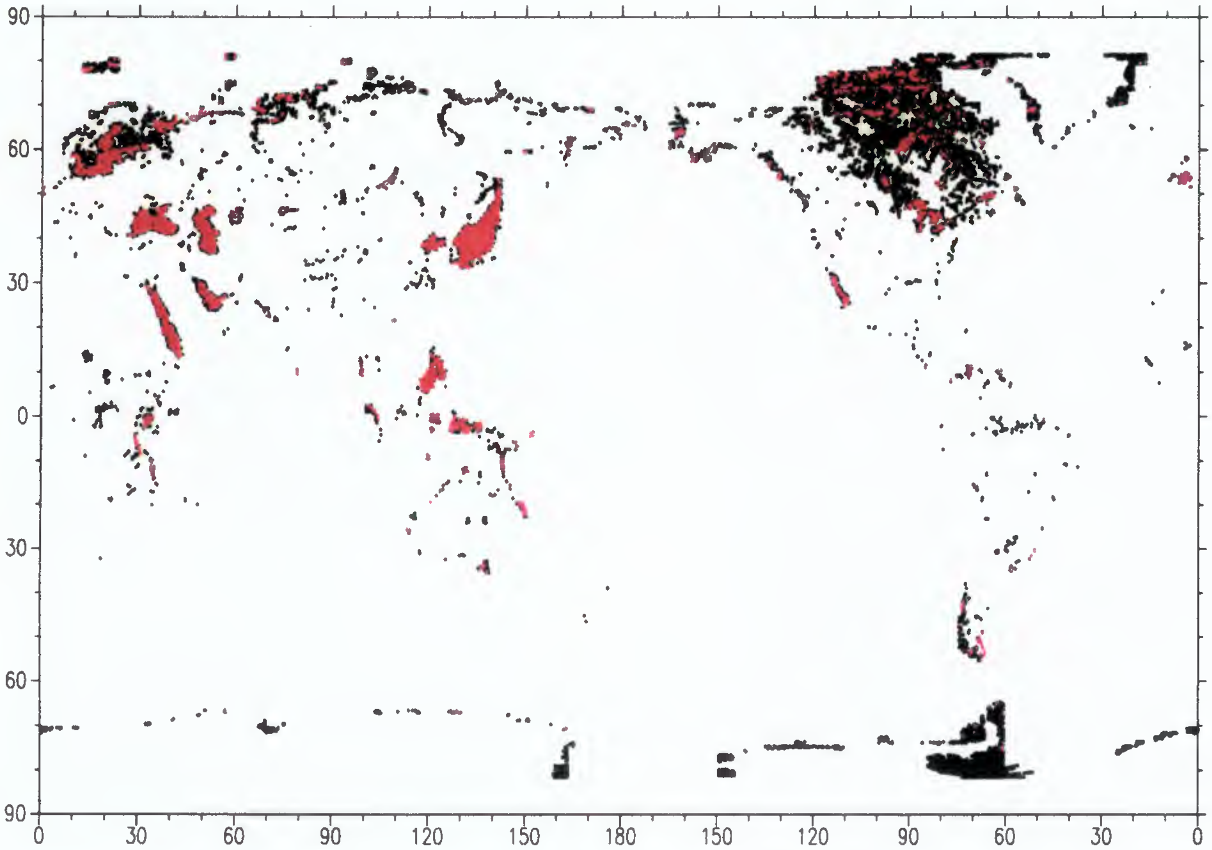

Figure 2.19 Distribution of data rejected because of absence of ocean tides. Red dots indicate rejection by this criterion only.

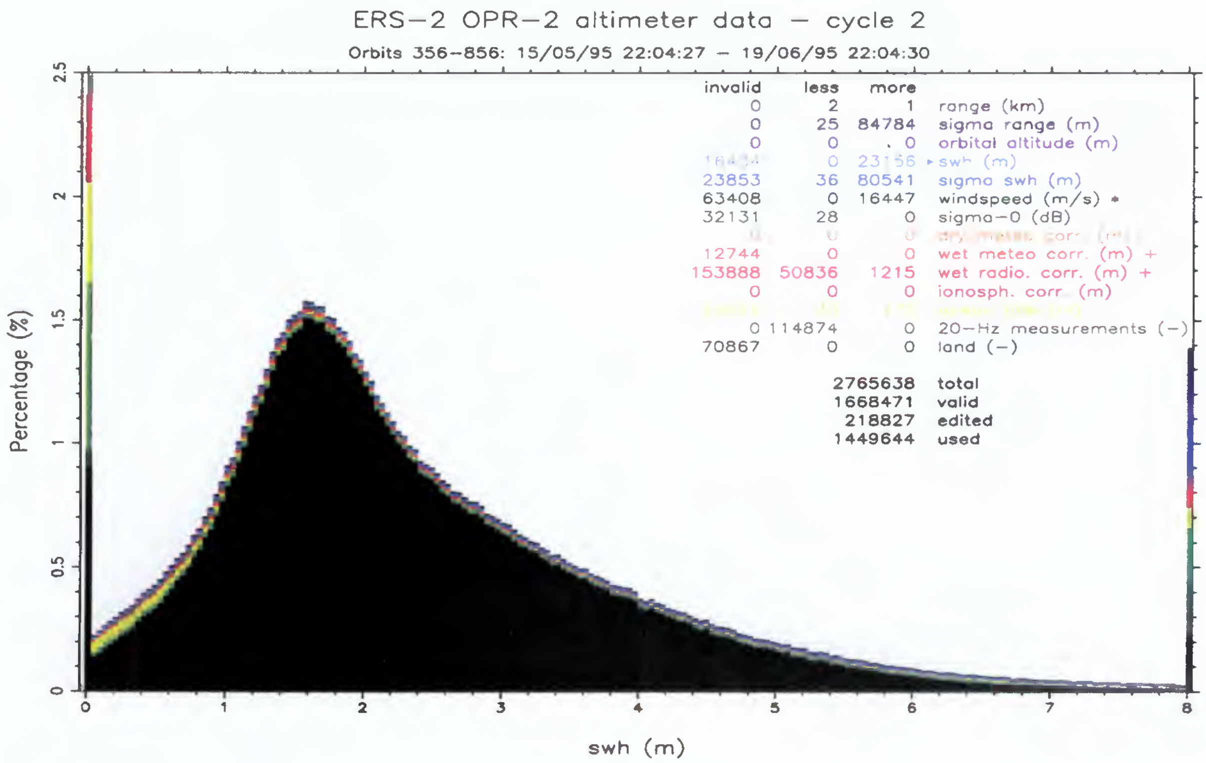

Figure 2.20 Histogram of the Significant Wave Height SWH

2.3 Range and altitude elements

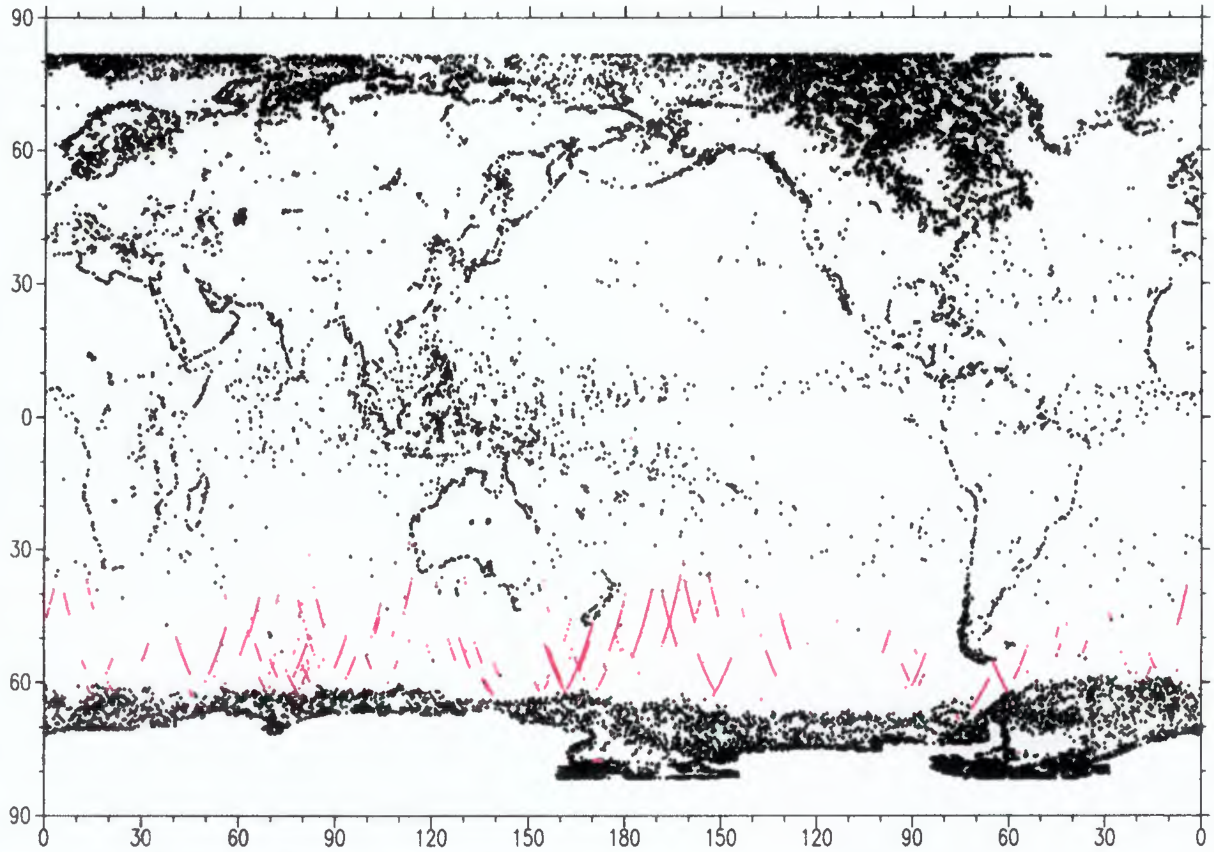

Figure 2.21 Distribution of data rejected because of Significant Wave Heights exceeding 8 metres. Red dots indicate rejection by this criterion only.

2.4 Wave Height elements

2.4.1 Significant Wave Height

The histogram of the Significant Wave Height (corrected for instrumental effects) SWH is given in Figure 2.20. Although the number of SWH values gathered in the first bin (0 cm) is clearly anomalous, we have chosen *not* to exclude the extremely low wave heights, because such wave heights are very common in shallow seas. Figure 2.22 presents the locations of observations with a SWH of 0 that are not deselected by any other criterion except ocean tides. This shows that using a lower limit of 1 cm for the SWH would be over-selective and remove much of the shallow water data.

Except when the altimeter waveform is contaminated by land or ice, wave heights above 8 m rarely occur and are confined mostly to the "Roaring Forties", the zone of strong wind and high waves between 40°S and 60°S (Figures 2.21 and 2.23). This combination of uncomfortable conditions will seriously decrease the precision of the height measurement. On top of this, the sea state bias correction SSB_Cor, which at 8 m SWH already amounts to 44 cm, becomes very uncertain at these wave heights and warrants rejection of these observations.

With increasing wave height, the slope of the leading edge becomes more and more shallow. This implies that the position of the tracker point becomes more uncertain, and the standard deviation of the 1-Hz altimeter range (σ_h in Section 2.3.2) will increase.

Figure 2.24 gives the scatterogram of σ_h against SWH. It is tempting even to

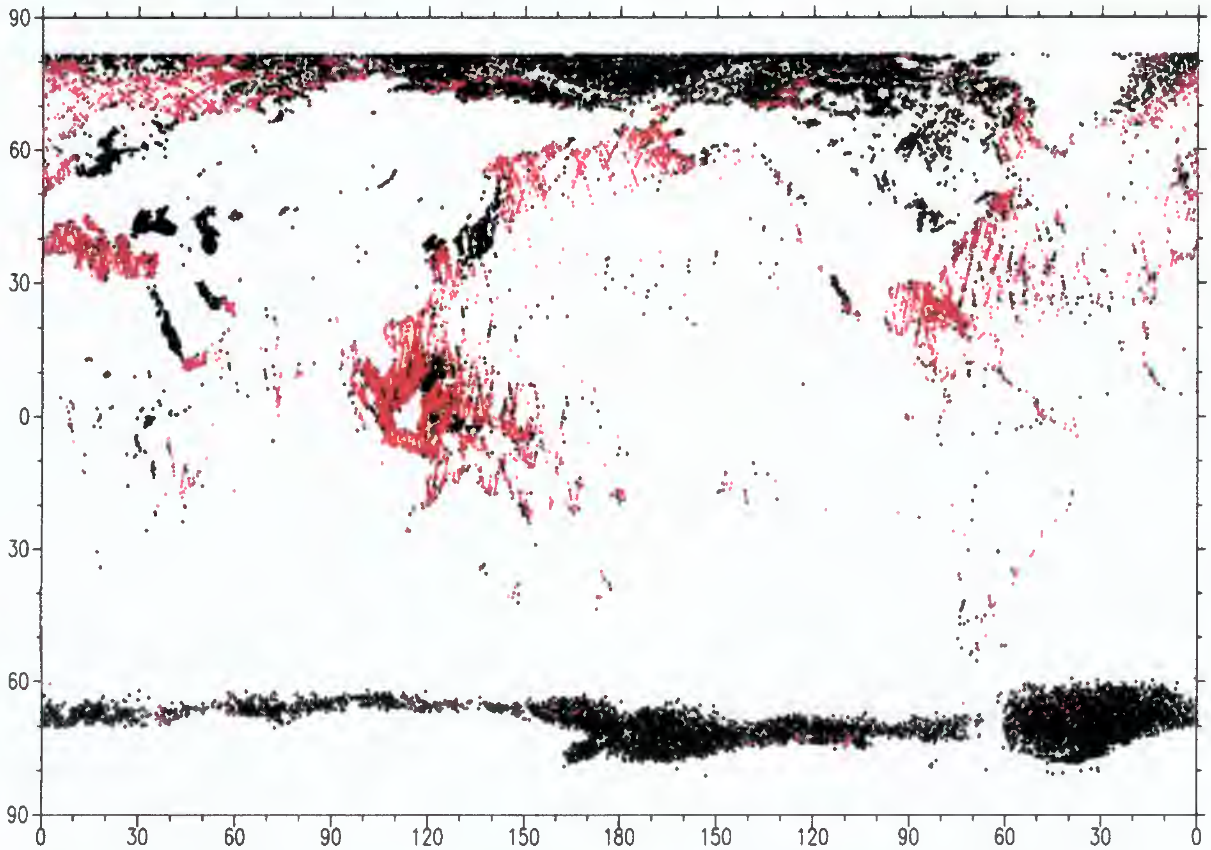

Figure 2.22 Distribution of recorded SWH less than 1 cm. Red dots indicate when this does not coincide with any other rejection criteria except the absence of ocean tides.

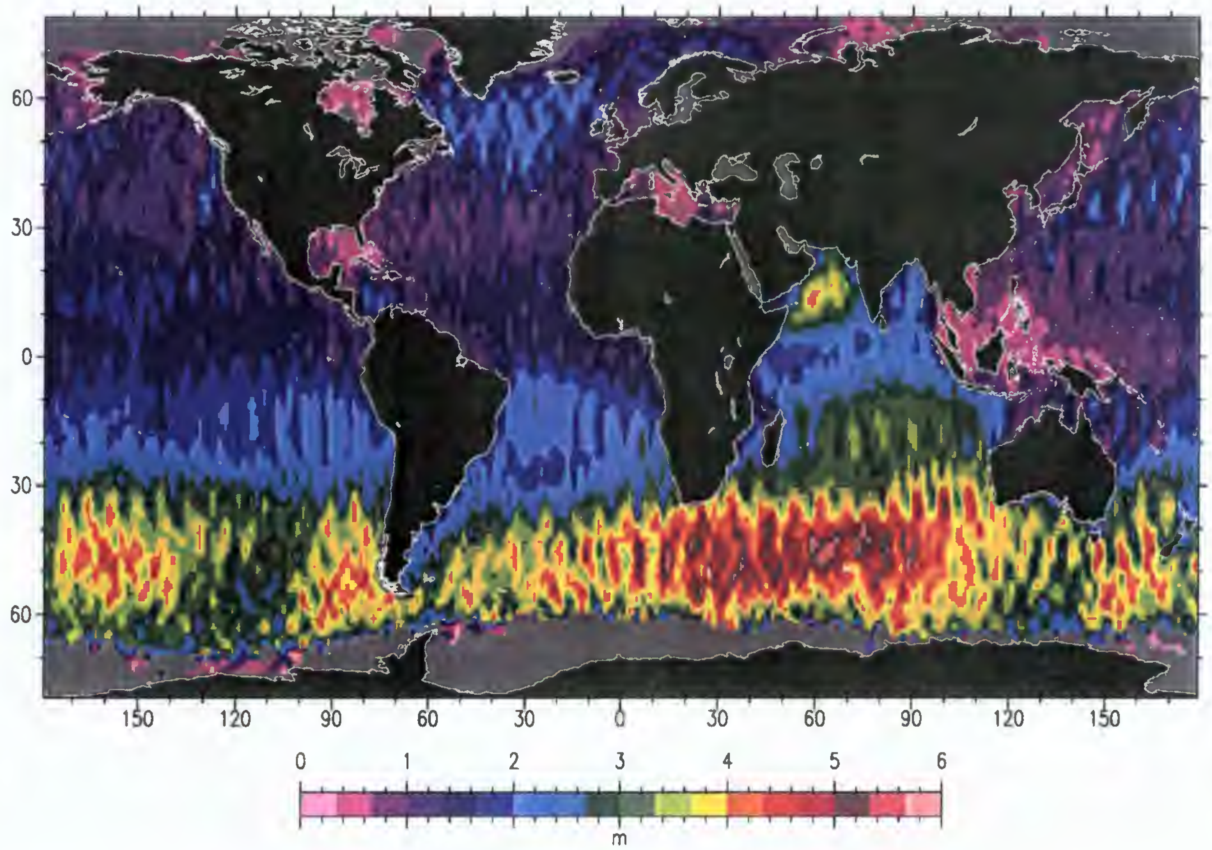

Figure 2.23 Distribution of Significant Wave Height averaged over Cycle 2.

2.4 Wave Height elements

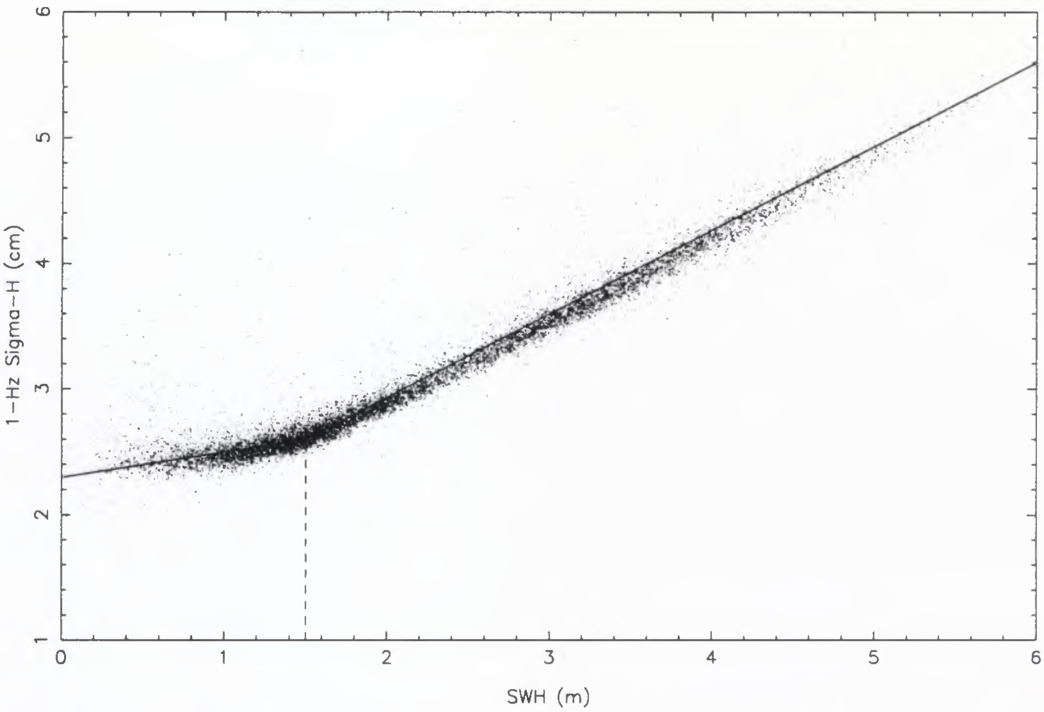

Figure 2.24 Scatterogram of the standard deviation of the altimeter range against recorded Significant Wave Height.

give a functional relationship between the two:

$$\begin{aligned} \sigma_h &\approx 2.3 + 0.20 \cdot \mathrm{SWH} \quad \text{for} \quad \mathrm{SWH} \leq 1.5 \\ &\approx 1.6 + 0.67 \cdot \mathrm{SWH} \quad \text{for} \quad \mathrm{SWH} > 1.5 \end{aligned}$$

with σ_h in centimetres and SWH in metres.

The bottom noise level is approximately 2.4 cm, which compares favourably to other altimeters.

2.4.2 Standard deviation of Significant Wave Height

Figure 2.25 shows that the standard deviation of 20-Hz SWH measurements (Std_SWH) starts at around 30 cm. Given the obvious fact that negative wave heights do not exist, it becomes remarkable that SWH contained values down to 0 cm. This is because of the look-up table and calibration corrections (SWH_LUT_Cor and SWH_Bias) which shift the raw SWH value (SWH_Raw) downwards. Values of SWH could even become negative, but these are set to zero. This explains the large amount of 0-cm wave heights in the previous Section.

When Std_SWH exceeds 2 m, the observation is rejected, mainly because this implies an uncertainty in the sea state bias correction SSB_Cor of 2.5 cm or higher. This criterion appears not to be over-selective; it clearly coincides with a lot of other rejection criteria. The location of measurements that are solely rejected because of Std_SWH or colour coded red in Figure 2.26 which are mainly located in the tropics and suggest contamination by rain cells or high humidity.

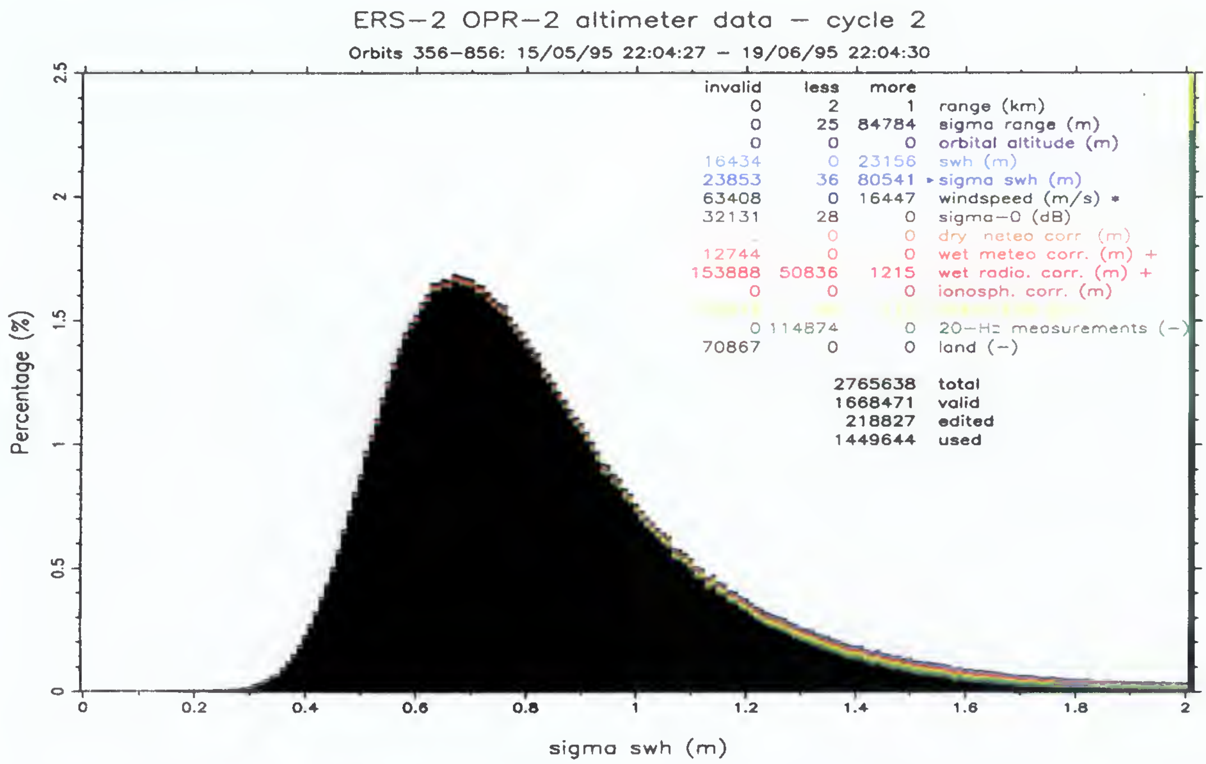

Figure 2.25 Histogram of the standard deviation of Significant Wave Height Std_SWH.

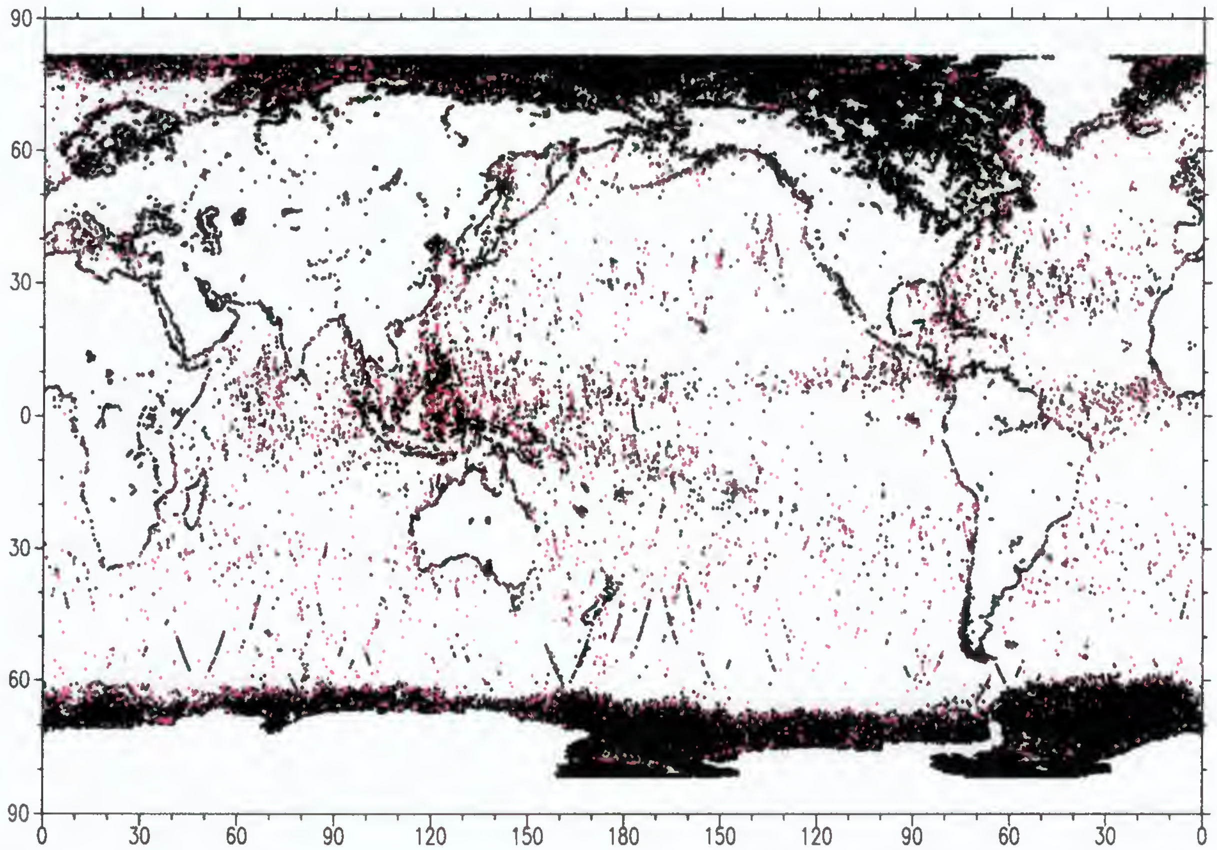

Figure 2.26 Distribution of data rejected because the standard deviation of SWH exceeds 2 metres. Red dots indicate rejection by this criterion only.

2.5 Wind speed elements

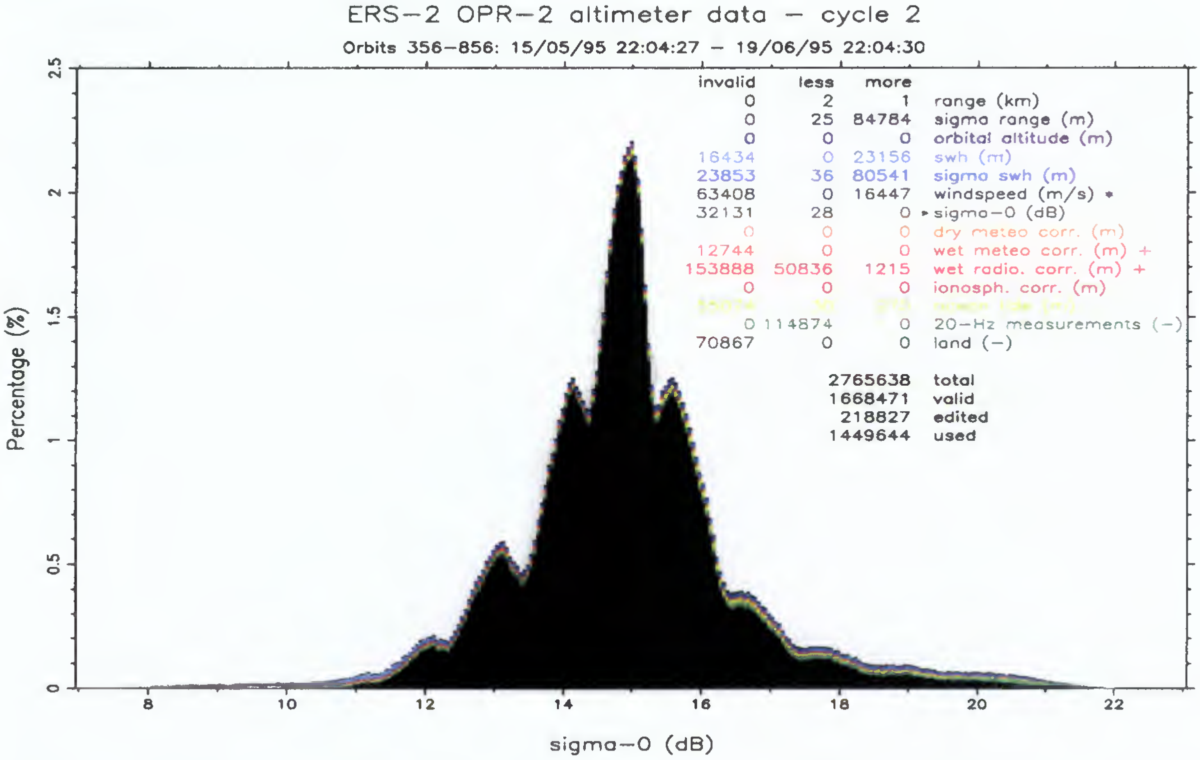

Figure 2.27 Histogram of the backscatter coefficient Sigma0.

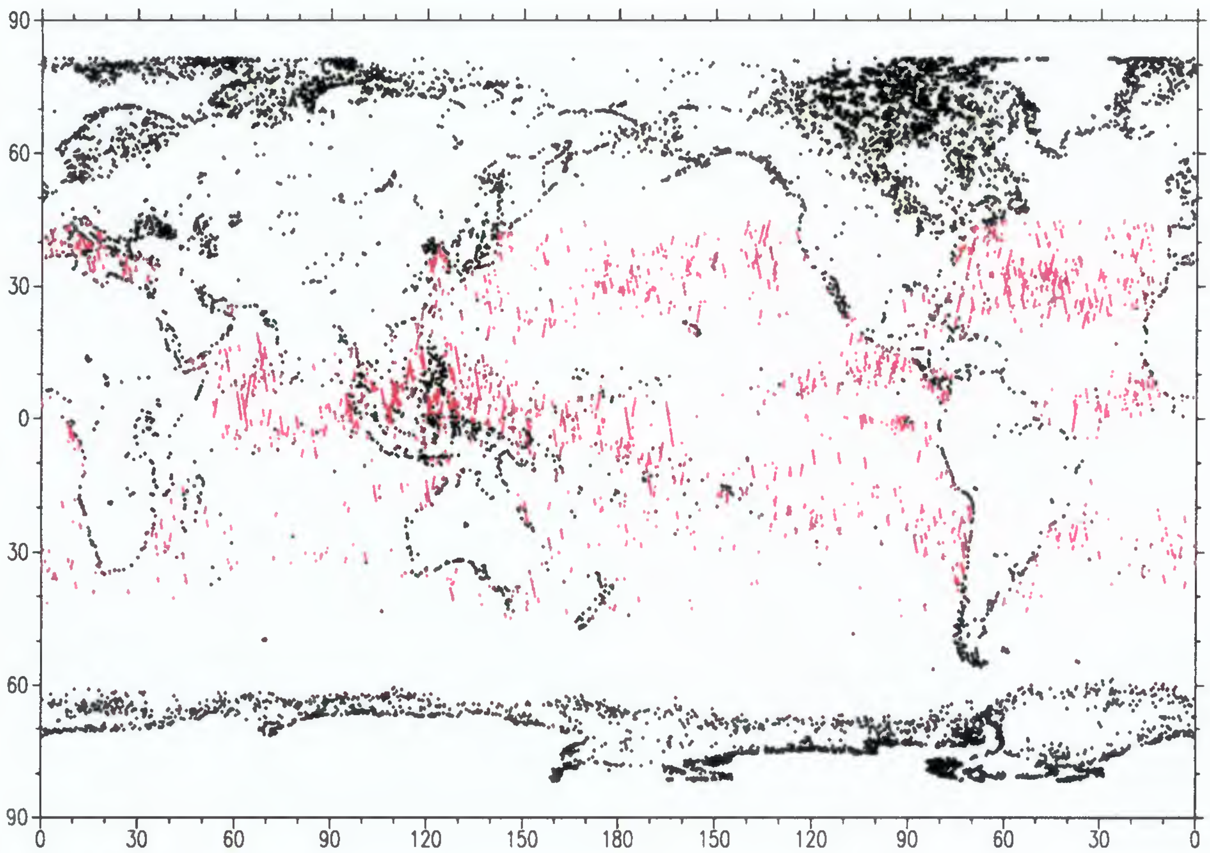

Figure 2.28 Distribution of data rejected because the backscatter coefficient is unavailable. Red dots indicate rejection by this criterion only.

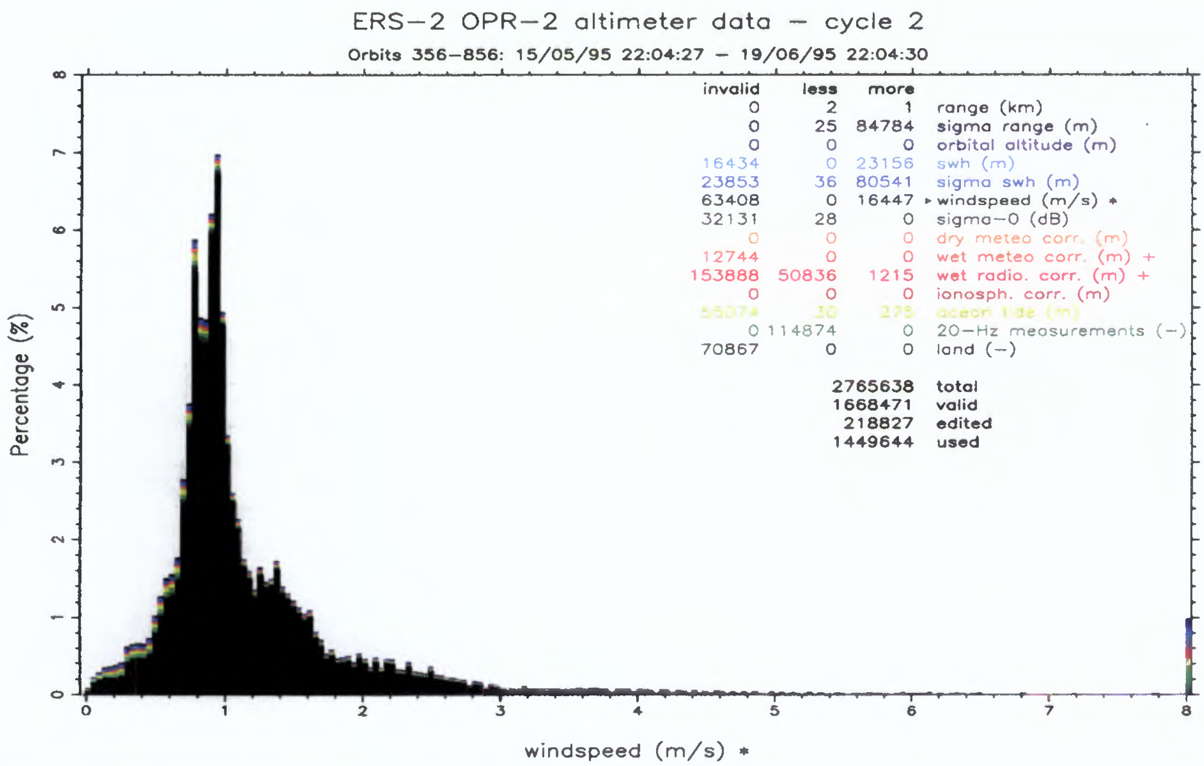

Figure 2.29 Histogram of wind speed Wind_Sp.

2.5 Wind speed elements

2.5.1 Backscatter

The histogram of the backscatter coefficient (corrected for instrumental effects) Sigma0 is shown in Figure 2.27. It has the peculiar shape with several "side-lobes" that is common also to other altimeters. For about 2% of the "valid" observations the Sigma0 is set to the default value; a negligible number of measurements is out of range.

The locations of observations that are to be rejected because of a default Sigma0 or because MCD flag bits 8, 9, or 10 are set (Figure 2.28) coincide with locations of possible contamination by land or rain cells.

2.5.2 Wind speed

The wind speed Wind_Sp is derived from the backscatter coefficient Sigma0 by the Witter and Chelton conversion table. This, however, is only valid for σ_0 values up to 19.6 dB, at which the wind speed is down to 1 m/s. Figure 2.27 has clearly demonstrated that Sigma0 contains seemingly correct values larger than this threshold. Therefore, it is not recommendable to use Wind_Sp for the data screening; Sigma0 should be a sufficient indicator for the validity of the measurement based on backscatter-related information.

2.6 Other elements

2.6.1 Doppler correction

The Doppler correction to the altimeter range H_Alt_Dop_Cor provided on the OPR and applied as a correction to H_Alt_Raw to obtain H_Alt is proportional to the range derivative Range_Deriv by means of the relation

$$\text{H\_Alt\_Dop\_Cor (mm)} = 0.00836 \cdot \text{Range\_Deriv (cm/s)}$$

This relation is *theoretically wrong* because the Doppler effect is proportional to the velocity of the satellite along the direction of its vertical, *i.e.*, the orbital altitude rate. At first glance the orbital altitude rate seems nearly equivalent to the altimeter range rate, because the slope of the sea surface with respect to reference ellipsoid is quite small. However, the slope is certainly not negligible over ice shelfs, where the slope of the surface could by far exceed the slope of the orbit. The slope of the ice is not unlikely to be 1% or more, which equals to 70 m/s; the orbit rate does not exceed 25 m/s, and even nears to zero over the Antarctic.

2.6.2 10-Hz measurements

At one measurement per second, the altimeter measurements are spaced by about 7 km along the satellite ground track. For measurements of wind speed and wave height, which vary on a broader scale, this is quite sufficient. Also most corrections to the altimeter range (except the orbital altitude) do not vary significantly over such a small distance. The sea level, however, may contain gravity related details at shorter wavelengths that do exceed the noise of the 1-Hz measurements. For this purpose the 10-Hz semi-elementary altimeter ranges H_Alt_SME(i) are provided.

Unfortunately, the OPR hardly provides the essential information to convert the 10-Hz ranges to 10-Hz sea level heights. As indicated above, the range corrections may be assumed constant over the 1-Hz interval, but *not* the orbital altitude, which may change by more than 10 m over this interval. Hence, we need the orbital altitude rate to derive 10-Hz sea level heights.

For this purpose the orbital altitude rate can certainly not be replaced by the range derivative, because the slope of the surface may not any more neglected. Moreover, the surface slope was precisely what we were looking for in more detail.

Hence, the only resort we have is to interpolate the orbital altitude from consecutive "valid" measurements. This may fail, however, when there is some gap between them of more then a few seconds. Again, we are faced with an unfortunate feature of the OPR that sets even the orbital altitude to its default when the observation is deemed to be "invalid" (Bit 0 of MCD is set to 1). Interpolation of latitude and longitude is easier because they are not defaulted on the "invalid" observations. Still, it represents a significant amount of coding to do the interpolations correctly.

For the purpose of validation we have extracted the 10-Hz height measurements from the OPR to compare their scatter to the standard deviation of the 20-Hz altimeter ranges Std_H_Alt. A third degree polynomial was fit through the 10-Hz ranges H_Alt_SME(i) and the standard deviation (σ_{SME}) computed using a normalisation factor $\sqrt{N-4}$, where N is the number of valid 10-Hz ranges, and the 4 comes from the number of parameters of the fitting polynomial. To facilitate comparison with the 20-Hz standard deviation, σ_{SME} was again divided by $\sqrt{N}$ and Std_H_Alt by $\sqrt{\text{Nval}}$, so both simulate a standard deviation of the 1-Hz ranges (σ_h).

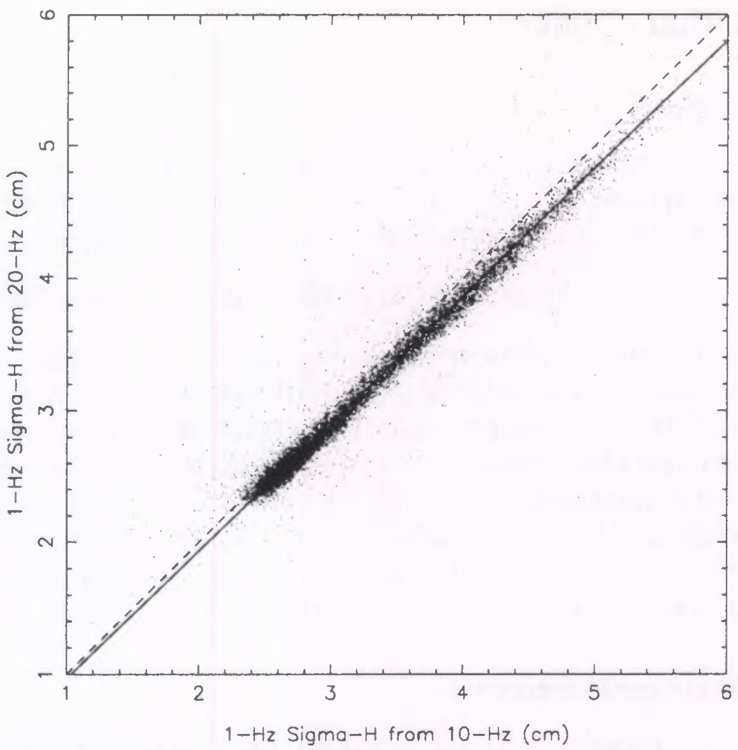

Figure 2.30 Scatterogram of the 1-Hz standard deviation of range deduced from the 20-Hz standard deviation (Std_Alt) against the the one deduced from the 10-Hz semi-elementary ranges H_Alt_SME(i).

Figure 2.30 gives a scatter plot of the two values. The best-fitting slope of 97% is probably do to the different normalisation factors. It shows that the reconstruction of the 10-Hz ranges and the standard deviation of range is possible using the H_Alt_SME(i) values.

2.6 Other elements

CHAPTER 3

Further Analyses

Now the altimeter range observation have been properly screened, we can construct measures of the dynamic topography (H_{dyn} in Chapter 1) from the various data fields provided on the OPR. This Chapter gives the results of some further analyses in the validation of the derived sea level, orbital altitude, wet tropospheric correction, sea state bias, and time tagging.

3.1 Collinear tracks analysis

Inspection of collinear tracks is the best way to spot short-wavelength differences between two sea level profiles and to separate them from the longer wavelengths. The boundary condition that the two tracks should be closely spaced is satisfied. The 35-day time-lag between two consecutive ERS–2 overflights of the same position makes sure most correction errors are completely decorrelated.

In total 1214 collinear pairs were constructed from the first three ERS–2 Cycles of OPR data, comprising about 1.7 million sea height differences. in order to get the best separation of long-wavelength signals (orbit error) and short-wavelength excursions (geophysical corrections) and to have a better picture of the achievable error budget with future enhancements, we have used the Grenoble ocean tide in stead of the Enhanced Schwiderski, and DUT precise orbits in place of the GFZ orbits featuring on the OPR.

Figure 3.1 depicts two pairs of collinear tracks. From left to right the graphs display:

1. The locations of the measurements.
2. The relative sea surface height profile with respect to the MSS95a mean sea surface model. A running average filter is applied to remove the altimeter noise.
3. The Significant Wave Height (SWH) for both collinear tracks derived by the two altimeters. Also here a running average filter is applied.
4. The residual difference between the measured sea surface profiles. An orbit error model (displayed as the thin full line) was fitted through the residuals. Again a smoothing is applied to remove noise. The deviations from the fit are a result of sea level variability and errors in the geophysical corrections.

The orbit error model consists of a constant term and 1- and 2-cpr terms:

$$C_0 + C_1 \cos u + S_1 \sin u + C_2 \cos 2u + S_2 \sin 2u$$

where u is the argument of latitude.

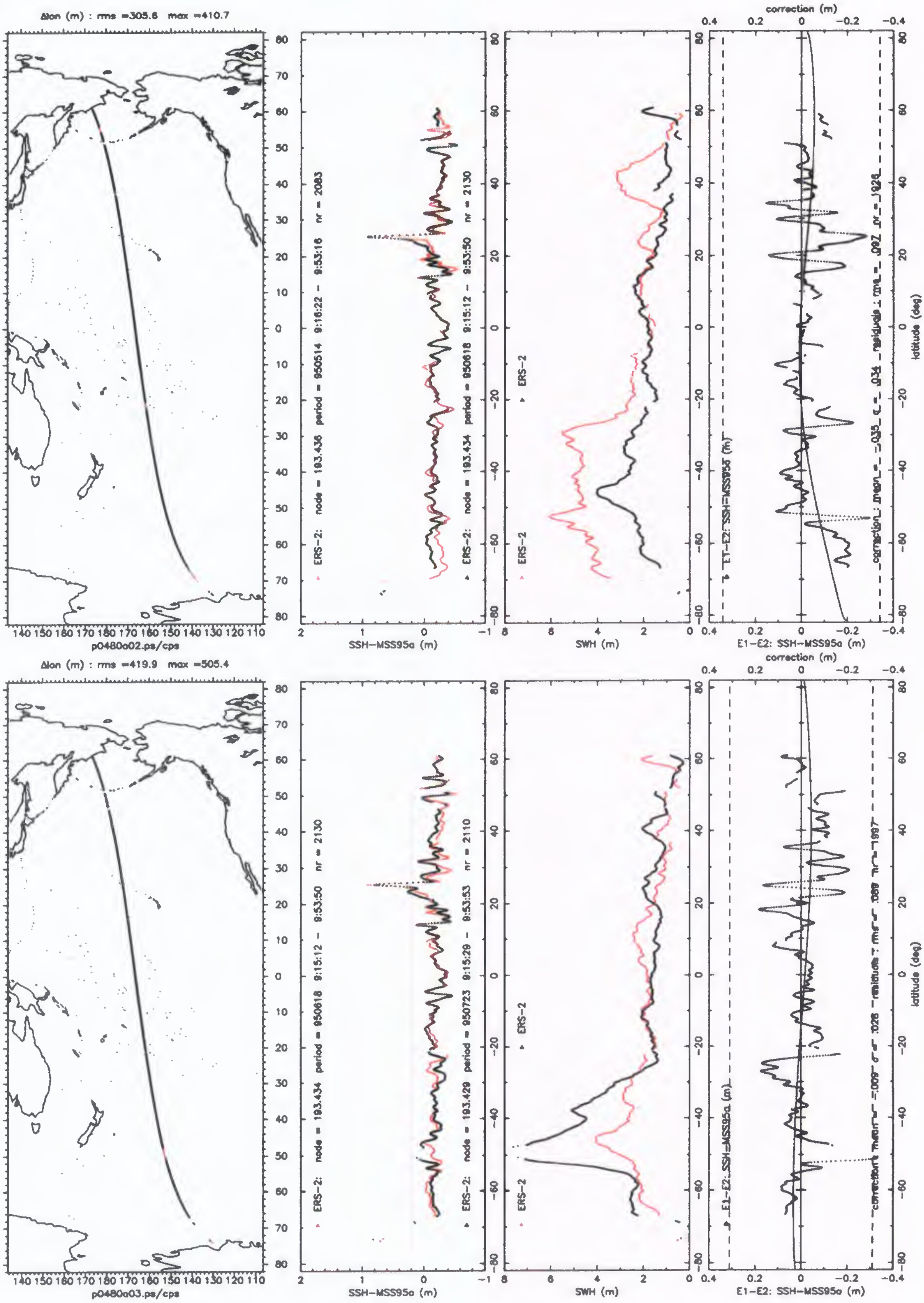

Figure 3.1 Two collinear pairs of sea surface height profiles. Ascending pass 480, 14 May and 18 June (top) and 18 June and 23 July (bottom). From left to right: location, sea surface height wrt MSS95a, SWH, and height difference, including 5-parameter fit.

Error source	Range (cm)
Meso-scale features	
Dry tropospheric correction	0.5–1.0
Wet tropospheric correction	1.5–3.5
Ionospheric correction	0.5–1.0
Ocean tides (Grenoble FES 95.2)	4.0–4.5
Ocean tides (Enh. Schwiderski)	5.0–6.0
Solid earth tides	0.5–0.5
Inverse barometer effect	2.0–3.5
Sea state bias	0.5–1.0
Instrument errors	1.0–1.0
(Meso-scale) sea surface variability	1.0–4.0
Total (Grenoble FES 95.2)	5.0–8.0
Total (Enh. Schwiderski)	5.8–8.9
Large-scale features	
Orbit (DUT)	5.0
Orbit (GFZ/D-PAF)	6.5

Table 3.1 Error budget in OPR derived mean sea level heights. The values (in centimetres) indicate the range of the error. The lower bound assumes heavy correlation over short time intervals (1 day). The upper bound applies when the correction is fully decorrelated.

In both examples, the measured sea level profile deviates significantly from the MSS95a mean sea surface model. The excursions are related to sea-mounts, islands, and trenches. In Figure 3.1 we see spikes in both profiles when the track crosses the Hawaiian Ridge and the Aleutian Trench and Ridge. Note that these spikes completely drop out in the height differences. This is due to the almost perfect collinearity of the tracks.

The RMS residual sea height difference along all collinear pairs (after the removal of the 5-parameter fit) is 11.2 cm, which should be a measure for the global sea level variability, ocean tide errors, and atmospheric delay correction errors. Assuming the contributions are completely decorrelated this gives us an average RSS value of 7.9 cm for each pass, which can be separated into the various contributions as suggested in Table 3.1.

The next important parameter we can derive from the collinear track analysis is an estimate for the radial orbit error. The 5-parameter fit comprises nearly all of the orbit error difference between the collinear pairs and has an RMS value of 5.0 cm. Obviously, this does not include the geographically correlated orbit error, but if we assume that this error is of similar magnitude as the uncorrelated orbit error, this leaves us with an estimate of about 5.0 cm for the total radial orbit error. We will see in Section 3.2 that this is close to what we can deduce from crossover analysis, and shows us the *very* high quality of currently computed ERS orbits.

3.2 Crossover data analyses

Using the first three Cycles of ERS–2 OPR data as they are provided on one of the earlier releases of the product, we have generated a data set (X1) of crossover height differences with a maximum time difference of 17.5 days. A second data set (X2) is constructed from the same OPR data after replacing the GFZ orbit with a DUT precise orbit and the Enhanced Schwiderski tide model with Grenoble FES

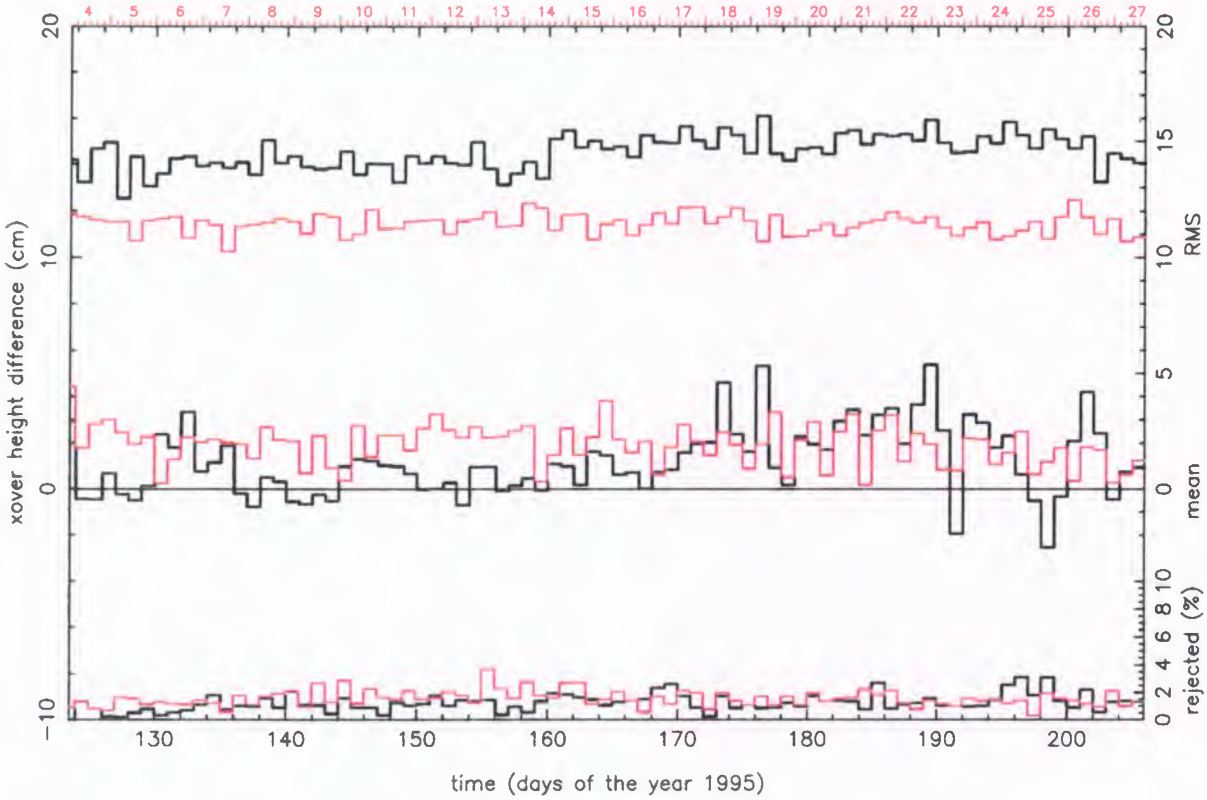

Figure 3.2 ERS–2 single satellite crossover height differences. The lines indicate (from top to bottom) the daily RMS and mean crossover height difference (asc–des), and the percentage of rejected crossovers that do not fulfil the 3.5σ-edit criterion. The time laps between passes is restricted to 17.5 days. **Black:** GFZ orbits, Enhanced Schwiderski tides (X1). **Red:** DUT orbits, Grenoble tides (X2).

95.2, again with the aim to study the result of future enhancements of the OPR. (*Later OPR products are to contain the Grenoble model FES 95.2.1, rather than the Enhanced Schwiderski, and might contain a better (JGM-3) orbit.*)

In both data sets areas that are notorious for large tidal errors or sea-ice coverage were excluded from this data set and a 3.5σ edit criterion is applied to exclude remaining rogue measurements.

3.2.1 Orbit error and geophysical correction errors

Figure 3.2 shows the daily average and daily RMS crossover height differences as a function of time for the period of 3 May till 24 June 1995. The positive average height difference between ascending and descending tracks is a result of the uneven global distribution of the crossovers. Since the majority of the crossovers is on the Southern Hemisphere, where a negative time tag bias causes sea surface heights to increase on ascending tracks and decrease on descending tracks, we have a slightly positive average crossover height difference. If the time tags are corrected the mean height difference is around zero.

Note that partly due to the application of the state-of-the-art tide model, partly because of the superior DUT orbits the crossovers for data set X2 (red lines in Figure 3.2, mean 1.9 cm, sigma 11.3 cm) are significantly better than for X1 (black lines, mean 1.3 cm, sigma 14.5 cm).

Looking at the progress of the crossover height differences with increasing time interval between ascending and descending passes (Figure 3.3), we see a

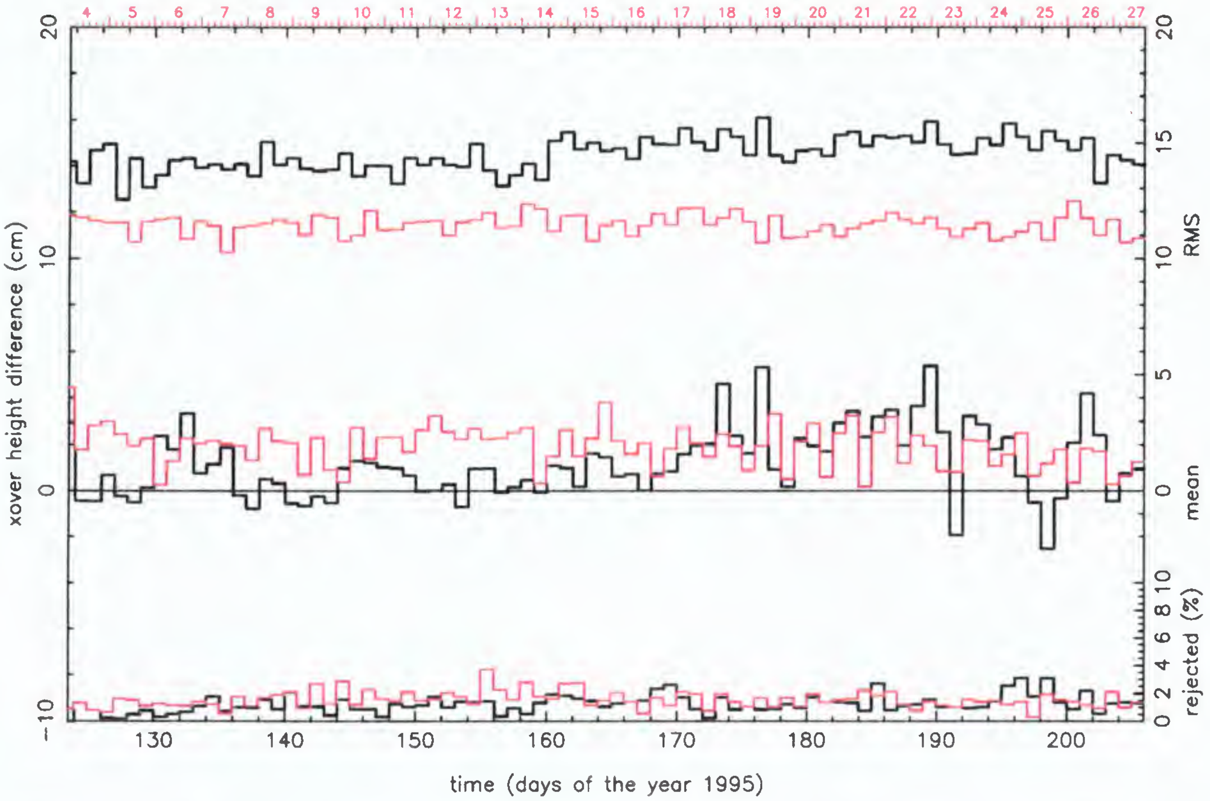

Figure 3.3 ERS–2 single satellite crossover height differences as a function of the time difference between passes. The lines indicate (from top to bottom) the daily RMS and mean crossover height difference (asc–des), and the percentage of rejected crossovers that do not fulfil the 3.5σ-edit criterion. **Black:** GFZ orbits, Enhanced Schwiderski tides (X1). **Red:** DUT orbits, Grenoble tides (X2).

gradual increase of the RMS, from 12.3 to 15.5 cm for data set X1 and from 10.0 to 12.4 cm for X2. This increase can be contributed to the gradual decorrelation of errors in the geophysical corrections along either pass, and partly to sea surface variability, as suggested in Table 3.1.

The crossover RMS values for X1 combine very well with the estimated GFZ radial orbit error of 6.5 cm and geophysical effects increasing from 5.8 to 8.9 cm, which would imply approximately 12.3 to 15.6 cm crossover RMS. Likewise, the DUT radial orbit error of 5.0 cm and geophysical effects (with Grenoble ocean tide) increasing from 5.0 to 8.0 cm would suggest approximately 10.0 to 13.3 cm crossover RMS.

3.2.2 Time tag bias

In crossovers, the height difference (ascending minus descending) to be contributed to a time tag bias Δt equals:

$$\Delta h_x = \dot{h}_a \Delta t_a - \dot{h}_d \Delta t_d$$

With the orbital height rates ($\dot{h}_a \approx -\dot{h}_d$) being known from the orbit determination, a time tag bias ($\Delta t_a \approx \Delta t_b$) can be estimated for each crossover. For the results presented in this Section, we have taken a bit more complicated approach and estimated a single time tag bias per day minimising Δh_x in a least squares sense.

Figure 3.4 shows time tag biases estimated from the X1 (black) and X2 (red) crossover data sets. From both data sets, based on different orbits, we can draw

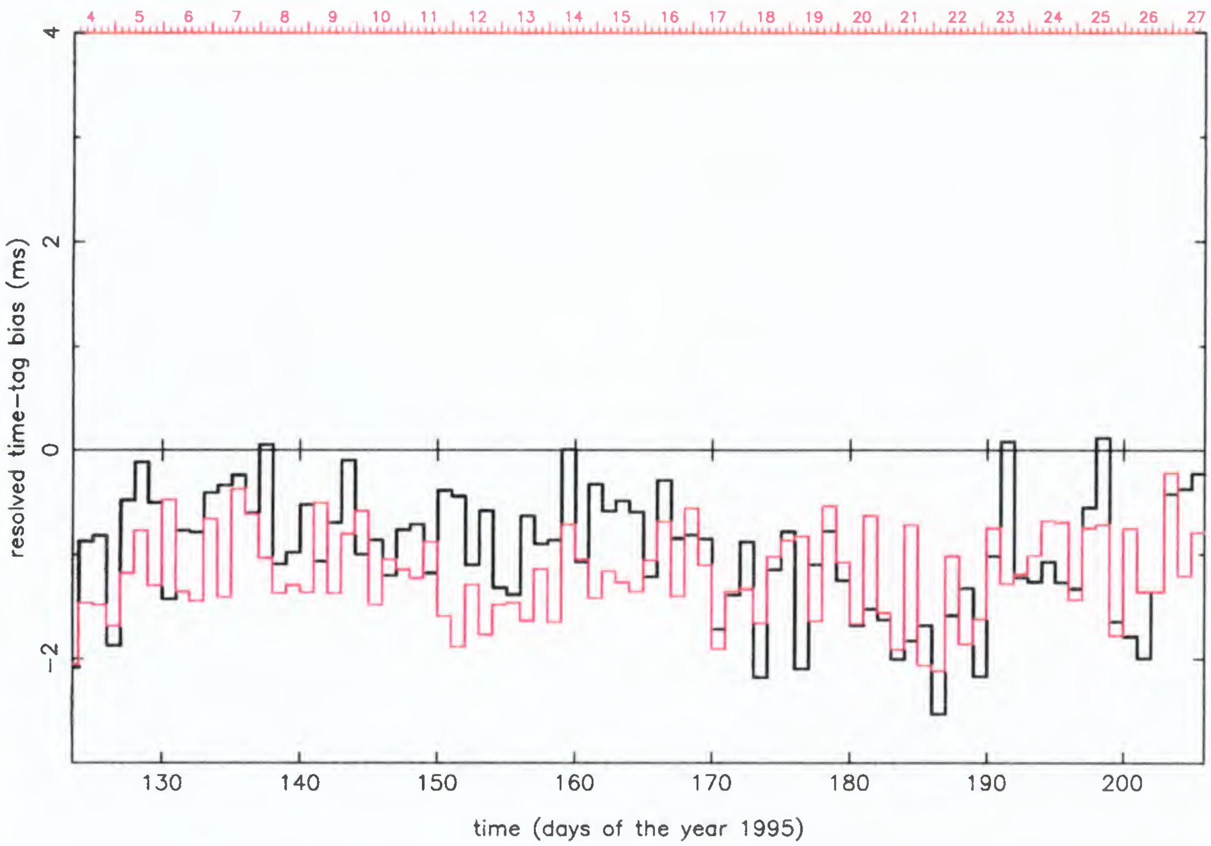

Figure 3.4 Daily estimates of the ERS–2 time tag bias by minimising the crossover height difference RMS. **Black:** GFZ orbits, Enhanced Schwiderski tides (X1). **Red:** DUT orbits, Grenoble tides (X2).

the same conclusion: the time tags of the OPR data are early by approximately 1 millisecond (X1: –1.0 ms, X2: –1.1 ms). Data set X2, which provides the most stable estimate of the time tag bias because it is based on better orbits, reveals a very tiny remnant of geographically correlated orbit errors: a 35-day signal with lows around days 95.151 and 95.186.

When the crossovers are corrected for the estimated time tag biases, the RMS of the crossover height differences decreases by about 3.5 cm in RSS-sense to 14.1 cm for X1 and 10.7 cm for X2.

3.2.3 Sea-state bias estimation

Similar to the time tag bias, we can determine an incremental sea state bias, SSB= b·SWH, for each satellite by minimising the crossover height differences. In stead of estimating a single coefficient b, we have estimated one coefficient b for each interval of one metre of SWH up to 8 metres. A weighted mean coefficient was afterwards computed by weighting each value by the number of measurements and the SWH in each bin.

The results for data set X1 and X2 are shown in Figure 3.5. Main conclusions are:

- For both data sets, the coefficient b drops with increasing wave heights above SWH = 4 metres.
- The 5.50% of SWH applied to the ERS–2 OPR data (circles) appears to be around the correct value. The weighted average sea-state bias increment is be-

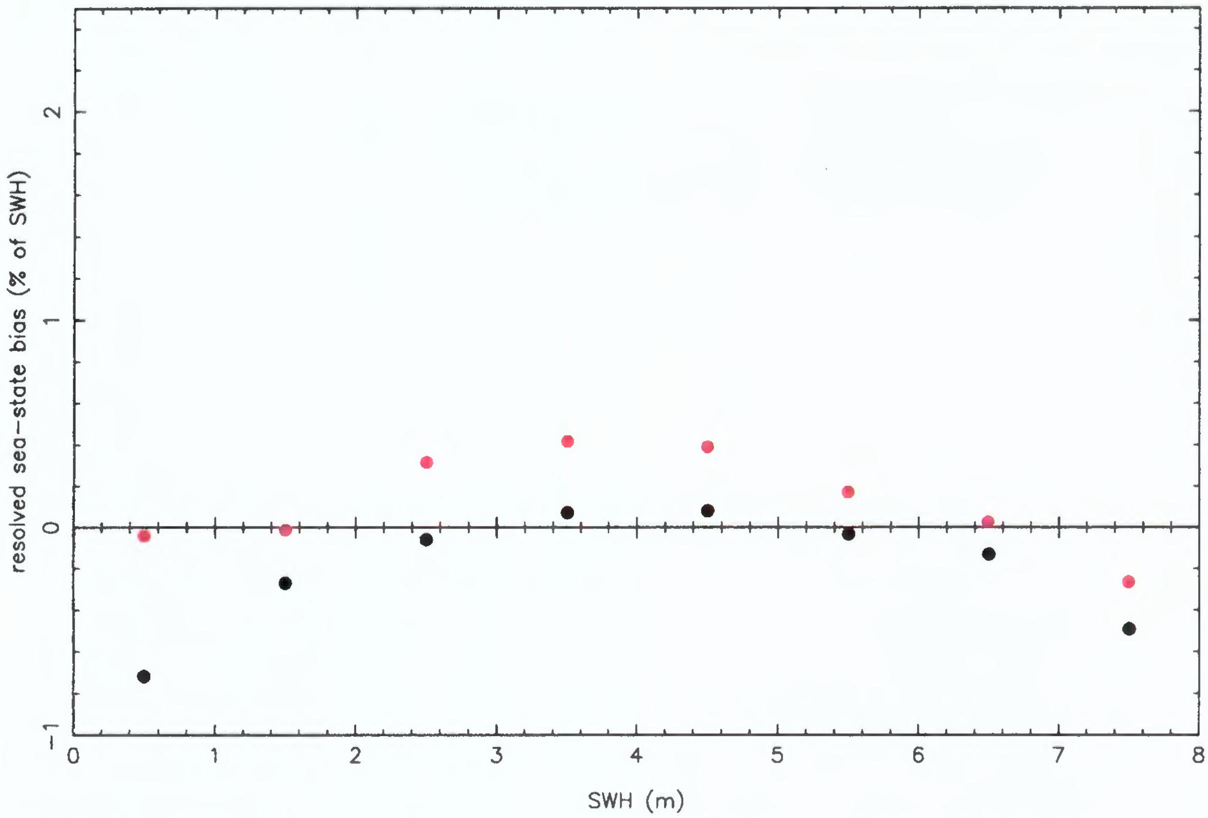

Figure 3.5 Estimates of a correction to the sea state bias of 5.5%, as a function of SWH. **Black:** GFZ orbits, Enhanced Schwiderski tides (X1). **Red:** DUT orbits, Grenoble tides (X2).

tween $-0.08\pm0.18\%$ (X1) and $+0.25\pm0.18\%$ (X2).

- Improvement to the crossover RMS applying either correction is negligible.

3.2.4 Wet tropospheric correction

As discussed in Section 2.3.4 of Chapter 2 two wet tropospheric corrections are supplied on the OPR. The correction based on the wet tropospheric content measured by the ATSR/M radiometer (Wet_H_Rad) is likely to be more precise than the correction based on the ECMWF meteorological models (Wet_Cor). This conclusion from Section 2.3.4 can also be verified by means of crossover analyses.

Two data sets are generated from Cycle 2 OPR: X3 and X4. Similar to X2, both data sets feature the DUT orbit and the Grenoble ocean tide. In addition, a 1.1 millisecond time tag bias is applied. On X3, as on X1 and X2 a mix of the wet radiometer and wet meteorological correction is used as proposed in Section 2.3.4. On X4, the wet meteorological correction is used for all records.

The RMS crossover height differences are 11.1 cm for X3 and 11.4 cm for X4, which suggests that the radiometer correction is more precise than the meteorological one, and their respective error budgets of 3 and 5 cm as suggested in Section 2.3.4 are not unlikely.

CHAPTER 4

Summary, Conclusions, and Recommendations

In Chapter 2 we have discussed the most important altimeter measurement elements and corrections that are relevant for the derivation of high-quality sea level heights for use in oceanographic or geodetic research. We have established edit criteria that are sufficient to reject the rogue data that would negatively influence results. Yet, we have been careful not to be over-selective and reject too much of the valuable data.

In comparison to other state-of-the-art atmospheric corrections, those provided on the OPR are very competitive. Worthwhile is the addition of the wet tropospheric correction determined from the ATSR/M radiometer water vapour content.

In Chapter 3 we have further analysed the available data using collinear and crossover techniques and drawn up a total error budget. It was possible to obtain estimates for errors in the time tagging as well as confirming the applicability of the sea state bias correction of 5.5% of SWH.

4.1 Conclusions

Main conclusions of the validation exercise are:

- After significant enhancement since Version 1.1, the Product User Manual Version 2.0 is clear and rather detailed about the data content and background. This report is intended as a further guideline for the user in judging the quality of the data and how to select the best.
- The OPR product lacks a helpful flag bit or field that would describe whether we are dealing with open ocean, with inland seas, lakes or alike, or with ice shelfs. All these areas are registered as "ocean". The use of the term "over ocean", meaning also over rivers, marshes, lakes, and ice shelfs is therefore very confusing.
- The Doppler correction on the OPR is theoretically wrong. Although the error has little consequence for use over "flat" surfaces like ocean and lakes, it is totally wrong over ice shelfs.
- The fact that many records pass all rejection criteria over ice shelfs indicates the enormous capabilities of the ERS altimeters.
- The extraction of 10-Hz semi-elementary sea level heights is very impractical because of the lack of a field indicating the orbital altitude rate, and the omis-

sion of the orbital altitude on "invalid" records.

- The atmospheric corrections supplied on the OPR are very competitive with other state-of-the-art models. Both dry and ionospheric corrections are believed to have a global RMS error of approximately 1 cm. The wet radiometer and meteorological correction errors are of the order of 3 and 5 cm, respectively.
- The replacement of the Enhanced Schwiderski by the Grenoble FES 95.2.1 ocean tide model is clearly advantages. It brings down the total error budget of the geophysical corrections to 7 cm (excluding sea surface variability).
- A time tag bias of –1.1 ms was found by analysing crossover height differences. This suggests that the time tagging of the OPR records is systematically early by 1.1 millisecond.

4.2 Recommendations to the user

The following recommendations can be made with respect to the use of the OPR data in the current status:

- The MCD flags and default values in the data fields are uncorrelated. Make sure to check both in assessing the quality of the data fields.
- Be aware that the Doppler correction incorporated in H_Alt does not correctly apply to ice shelfs.
- Many data over inland seas, lakes, and ice shelfs are indistinguishable from open ocean data. The term "over ocean" in the PUM applies to all these areas. A check on the presence of a tide model does exclude lakes, but also rejects some shallow seas and does not identify ice shelfs. Take provisions, *e.g.*, by means of an external land mask.
- The following selection criteria are sufficient to reject rogue measurements that are not over *open oceans* (field identifiers and units as supplied on the OPR).

$$\begin{aligned}
\text{MCD bits } 0\ 4\ 5\ 6\ 7\ 8\ 9\ 10\ 16\ 23 &= 0 \\
\text{Nval} &\geq 17 \\
\text{Std_H_Alt} &\leq 500 \\
\text{SWH} &\leq 800 \\
\text{Std_SWH} &\leq 200 \\
\text{Sigma0} &\leq 2300 \\
\text{Sigma0} &\geq 700 \\
\text{External land mask} &= \text{ocean}
\end{aligned}$$

  And the wet tropospheric correction is selected from one of the following, in order of preference:

$$\begin{aligned}
\text{Wet_H_Rad} &\geq -600 \quad \text{and} \quad \text{bits } 17\ 18\ 19\ 20 = 0 \\
\text{Wet_Cor} &\geq -600 \quad \text{and} \quad \text{bit } 21 = 0
\end{aligned}$$

- Correct altimeter time tags by 1.1 ms, making them later. Correct the orbital altitude accordingly by adding the product of the altitude rate and this datation error to H_Sat and the derived sea level.

4.3 Recommendations to F-PAF

The following changes to the PUM or the OPR are recommended:

- Change the computation of the Doppler correction to make it proportional to the orbital altitude rate, rather than the range derivative. The current implementation is theoretically incorrect and is over 100% wrong over steep sloping surfaces like ice shelfs.
- Include the orbital altitude rate as a data field to facilitate the derivation of 10-Hz semi-elementary sea level heights from the 10-Hz ranges. This also allows a correction of orbital altitude because of the datation error.
- Include all relevant data (at least the orbital altitude) also for "invalid" OPR records.
- Include on the OPR a flag or field that makes a further differentiation in areas that are currently all denoted "ocean-covered". Distinguish between: open ocean; inland seas and lakes; marshes and rivers; (floating) ice shelfs.
- Avoid the use of the phrasing "over ocean" in the PUM when "over various wet surfaces or floating permanent ice shelfs" is meant. The original phrasing, combined with the fact that we are talking about an Ocean Product, raises a lot of unnecessary confusion.

Acknowledgements

We gratefully acknowledge the support given by John Lillibridge of the United States' National Oceanic and Atmospheric Administration (NOAA) and for providing atmospheric corrections to be used for comparison with the corrections provided on the OPR.

Bibliography

CERSAT (1996), *Altimeter and Microwave Radiometer ERS Products, User Manual, C2-MUT-A-01-IF, version 2.0*, Toulouse, France, January 1996.

Floberghagen, R. (1995), Geophysical validation of the F-PAF ERS–2 OPR radar altimeter product, *Progress Report 1*, Delft Institute for Earth-Oriented Space Research, 20 December 1995.

Scharroo, R., and R. Floberghagen (1996), Geophysical validation of the F-PAF ERS–2 OPR radar altimeter product, *Progress Report 2*, Delft Institute for Earth-Oriented Space Research, 12 January 1996.

3.3 Geophysical Validation of the F-PAF ERS-2 Altimeter OPR Product

T. Engelis

SpaceTec Ltd.

GEOPHYSICAL VALIDATION OF THE F-PAF ERS-2 ALTIMETER OPR PRODUCT

Theodossios Engelis

SpaceTec Ltd
Attica Technology Park, NCSR Demokritos
Athens 15310, Greece
e-mail : thegge@cyclades.nrcps.ariadne-t.gr

ABSTRACT

This report details the work that was performed to verify/validate the ERS-2 altimeter OPR product as a whole, with emphasis in the geophysical validation of both the altimeter observations and associated corrections, in order to assess the suitability of the data to produce valid oceanographic and geophysical results. Verification of document, media, format and dataset verified that the PUM provides a comprehensive and accurate description of product formats and contents, that header and data record information is consistent and that flagging and default values are properly assigned. Global statistics of range, altitude and corrections indicate that, with minor exceptions, the data are within range and provide a global coverage. The global analysis of three complete and one partial 35 day repeat arcs (from May 3 to August 28, 1995) produce an RMS residual sea surface height value of 50 cm, crossover discrepancies on the order of 19 cm and residual arcs with respect to a mean master arc on the order of 11 cm. Finally, least squares adjustments that solve for the observable part of the orbit error, indicate an error level of 9 cm in the crossover discrepancies and 3 cm in the residual repeat arcs.

INTRODUCTION

The first 120 days of ERS-2 altimeter data, corresponding to 3 complete and a partial 35 day repeat cycles, were provided from ESA-ESRIN in CDs, in order to perform an independent and complete evaluation of the product. The evaluation work consisted of a testing procedure at three different levels.

In a first level verification, an extensive testing of the product was made, in order to certify that the OPR product contents, ie the document, media, formats, and dataset are consistent and accurate. In addition, the proper implementation of applicable algorithms in producing several field values was tested. Finally, testing was made to ensure that the valid range values are within their acceptable magnitude levels.

The second level verification included preprocessing and standard analysis of the data, to provide estimates related to the distribution and behavior of the data (range and corrections) and produce statistics of both global and regional nature. Residual sea surface heights, crossover discrepancies and residual repeat arcs were computed, using standard widely available models, to assess the quality and the inherent accuracy of the range and altitude measurements. Global rms statistics, coverage maps and respective histograms were produced.

The third level verification concentrated in further quantifying the inherent accuracy of the orbital range estimates. Least squares adjustments were performed to solve for the non geographically correlated error of the crossover discrepancies, as well as for the arc dependent orbit errors existing in the residual repeat observations.

All the work was performed in a high end PC and a CONVEX mainframe, using standard FORTRAN processing. Supporting data that were necessary, included the continuous 5 day orbit files at 30 second intervals, received via FTP from ESA ESRIN, the OSU91A gravity field complete to degree and order 360 and a standard SST model complete to degree 10.

FIRST LEVEL VERIFICATION

The testing that was performed included testing of the accuracy, compatibility and clarity of description of the following :

- Naming conventions
- Format conventions
- Format description
- Compatibility of header information, PUM and data files
- Flagging and default values
- Accuracy of algorithms to correct for instrumental effects
- Accuracy of 10 Hz data generation
- Validation and cross-verification of PUM

A thorough reviewing of the PUM concluded that all naming and CCSDS format conventions are consistent throughout the report and are properly applied in the data product. A Fortran software code was developed to read the data from the CD. Two major points in reading the CD, when a 386 or similar processor architecture is used , are in effect : a byte reversal is required in properly reading the record fields, and a bit reversal is required in properly analysing the MCD bitfield, since the most significant bit is the last bit. A final comment in reading the CD is that the CCSDS ASCII header records and the binary data records are not compatible when they are read in a direct or sequential mode, therefore a small reading iteration is required. These coding details are easy and straightforward to apply.

With regards to the compatibility of header information, PUM and data files, it was found that all values are indeed within the geographical limits set by the header records, and that all maximum numbers of valid data, stated in the header records, are properly assigned (i.e. they correspond to the number of valid data in the data files). On the contrary, the min/max ranges of field values stated in the header records and in the PUM field description are indicative ranges, therefore they should only be considered as typical and interpreted as sizing information.

Flagging and default value assignment are very critical in properly editing the data sets and removing invalid and default values. The PUM is very clear in stating that flags and default values represent uncorrelated quality information. A default value is not systematically flagged in the product. Flags, when they exist, are aimed at providing the reason of the default value. On the other hand flagging is a passive processing, i.e. a flagged field is not systematically set to its default value. In this case the computed value is provided in the product, but it is out of range.

More specifically, the flags provide information related to either, validity of the 1 Hz measurement, quality of estimates, presence or absence of geophysical level estimates and measurement characteristics. On the other hand, default values are assigned to missing data, no computation of the field, and when a field value is out of range.

In view of the above, substantial testing was made to quantify the validity of the flagging and default value assignment. As shown in Table 1, a number of data fields have their bit flag(s) assigned to 1 and simultaneously they are set to default (Case 1). This case indicates that data is missing. Case 2, in which the bit flag(s) is set to 1 but there is no default value, indicates that computation of the corresponding data field has been performed, but the resulting value has not passed the threshold set by the quality controls performed at CERSAT.

Table 1 : Testing of Flagging and Default Value Assignment (Cycle 2)

Field name	Field #	Bits tested	Case 1	Case 2	Case 3	Case 4
H_Alt_Raw	7	4 5	0	1	0	1668470
Std_H_Alt	8	4 5	0	1	39677	1628793
H_Alt	29	4 5 6	0	1	0	1668470
H_Alt_Cal_Cor_1	32	6 12	0	0	0	1668471
H_Alt_Dop_Cor	31	11	0	2617	0	1665854
Range_Deriv	34	11	0	2617	0	1665854
Wet_Cor	36	21	12744	0	0	1655727
H_Eot	41	16	55074	0	0	1613397
H_MSS	45	22	102321	0	0	1566150
H_Sat	46	23	0	0	0	1668471
SSB_Cor	40	7	203	16231	154	1651883
SWH_Raw	48	7	4	16430	0	1652037
Std_SWH	49	7	1984	14450	21869	1630168
SWH	50	7	4	16430	0	1652037
Sigma0_Raw	52	8 9	354	31777	0	1636340
Std_Sigma0	53	8 9	2286	29845	21493	1614847
Sigma0	54	8 9 10	354	31777	0	1636340
Sigma0_Cal_Cor	56	10	0	0	0	1668471
Wet_H_Rad	38	17 18 19 20	41717	112084	87	1514583
Sigma0_LW	57	17 18 19 20	41717	112084	87	1514583
TB_23	60	17 18 19 20	41459	112342	0	1514670
TB_36	61	17 18 19 20	41459	112342	0	1514670
WV_Cont	62	17 18 19 20	41459	112342	0	1514670
LW_Cont	64	17 18 19 20	41459	112342	0	1514670
Wind_Sp	58	15	0	63054	354	1605063
Wind_Sp_LW	59	15 17 18 19 20	41717	160387	87	1466280
WV_Cont_WS	63	15 17 18 19 20	41717	160387	87	1466280
LW_Cont_WS	65	15 17 18 19 20	41717	160387	87	1466280

Case 1 : bit=1 (or any of the bits =1) and value is default
Case 2 : bit=1 (or any of the bits =1) and value is not equal to default
Case 3 : bit=0 (or all bits =0) and value is equal to default
Case 4 : bit=0 (or all bits =0) and value is not equal to default

Case 3, in which the bit flag(s) is set to 0 but the data field has a default value, indicates that for some reason there was no computation of the corresponding field, or that the data value is out of range. Finally, Case 4 indicates that the field value is valid and nominal. Note that in case 3, a substantial number of the standard deviation fields have a default value assigned (primarily when the number of 20 Hz measurements is smaller than 3), nevertheless valid values are assigned to associated fields.

Testing of the algorithms for corrections of instrumental effects was straightforward and successful. The 10 Hz times and data generation was also successfully tested, based on the accurate and algorithm description in the PUM.

As an overall conclusion, the test utilisation of the OPR product was straightforward and did not pose to the test user any serious processing problems. The PUM is systematically and clearly describing all necessary issues, and in addition, has substantial additional information that allows the average user to proceed with the data analysis.

SECOND LEVEL VERIFICATION

The second level verification consists of

- editing and data preprocessing
- generation of residual sea surface heights and analysis
- crossover discrepancy analysis
- repeat arc analysis

The analysis work has been performed in all 3 complete 35 day cycles and in 1 incomplete cycle of ERS-2, starting in May 3 and ending in August 28 of 1995. The decision to perform the above analysis work was dictated by the fact that all three alternative observables from satellite altimetry are used by typical users, either in oceanographic or geophysical investigations. In addition they provide complementary statistics, that are all needed to assess the overall accuracy and suitability of the data.

- Editing and data preprocessing

Several editing schemes can be employed to remove the flagged and default field values. Regarding the flagging, the most stringent editing is the removal, at the record level, of all records that do not have a bitfield set equal to 0 (this happens when at least one bit is equal to 1). A lesser stringent editing is to examine all the records, on a field basis, and remove those records when at least one of the significant fields (e.g. correction fields) is flagged. Simultaneously, or sequentially, all the records that have at least one field of interest with a default value need to be edited.

In the present testing a different approach was followed. A set of criteria was established that are more physically oriented. These criteria were the following :

bit0=0	:	ocean only data records
bit23=0	:	nominal orbit
$\sigma_{alt} < 500$	:	std of altimetry less than 0.5 meters
$\sigma_{SWH} <500$	:	std of SWH less than 0.5 meters
$\sigma_{\sigma 0} <100$	:	std of sigma0 less than 1dB
bit11=0	:	valid Doppler correction
bit20=0	:	fields in the ocean

It turns out that this editing scheme is very efficient, removes all the flagged values and is therefore equivalent to removing the records for which field values are flagged. It also turns out that the above conditions are the main physical factors responsible for the flagging of the field values. The editing statistics for the 4 cycles are shown in Table 2 :

Table 2 : Editing Statistics

	Cycle 1	Cycle 2	Cycle 3	Cycle 4
Total	975792	2765638	2870744	2751290
bit0=0	609007	1668471	1646378	1598060
bit23=0	607296	1668471	1646286	1598060
$\sigma_{alt} < 500$	573083	1583687	1593998	1543644
$\sigma_{SWH} <500$	572490	1582366	1593104	1542748
$\sigma_{\sigma 0} <100$	570607	1577686	1589565	1539278
bit11=0	570410	1577120	1589476	1539183
bit20=0	543928	1506556	1532395	1476201

In addition to the above editing, further editing was performed to remove all the default values that are either assigned when the corresponding bit, where it exists, is equal to 0, or simply because no value was computed. Furthermore, editing of computed values that are out of range but are not flagged was made. It turned out that only the radiometer correction field (nominal values are between -0.1 and -0.50 cm) has such values. The results are shown in Table 3 :

Table 3 : Default value Editing Statistics

	Cumulative number of valid data			
	Cycle 1	Cycle 2	Cycle 3	Cycle 4
Valid ocean	543928	1506556	1532395	1476201
Ionospheric cor.	543928	1506556	1532395	1476201
Dry Tropo. cor.	543928	1506556	1532395	1476201
Wet Radio. cor.	532535	1467250	1526338	1447472
SWH	532522	1467188	1526276	1447429
Ocean Tides	527295	1453440	1514775	1433997
Sigma0	521764	1436098	1489268	1433997
Wind Speed	514812	1416240	1468243	1398511
Wet Radio. in range	497755	1377744	1438715	1361886

The last line of the above table represents the total number of valid ocean data with all the geophysical and atmospheric corrections available. The geographical distribution of all the default corrections is shown in Figures 1-5. Note that no default values have been assigned for sigma0 in cycle 4. This is due to the fact that a calculated correction to this field was consistently set to default, at least in the data product version received for the testing, therefore testing in this field was not made.

As it is seen from the Table, the number of data that can be used for processing, is on the order of 50 percent of the total data records available on each CD. Density histograms, with regards to the number of valid 20 Hz elementary data, standard deviation, and magnitudes of SWH, sigma0 and wind speed, have been computed. Note that the histograms are both in tabular form, for convenience and direct identification of the number of observations per unit of measure, and graphs for an easy overview of the density distribution . The graphs have all been prepared considering a normalised set of data and present the histograms in a percentage mode. A set of graphs for the second cycle is shown in Figure 6, and the corresponding tabular histograms are shown in Table 4. This distribution is typical for all cycles.

Table 4 : Histogram distribution of std, Number of 20 Hz measurements, significant wave heights, sigma0 and wind speeds.

Increment	Std (cm)	Nval	SWH (m)	Sigma0 (dB)	Wind Speed (m/sec)
1	117504	0	159177	0	781309
2	612885	0	512038	0	477633
3	397241	5187	355021	0	103938
4	165503	3886	201851	0	27662
5	64767	3039	105991	0	13397
6	26339	2325	48565	0	4873
7	11880	1874	19035	0	3011
8	6736	1542	8394	31	1253
9	4212	1229	3652	580	733
10	2917	1089	1503	1170	518
11	1247	914	625	3639	404
12	848	776	210	25544	323
13	616	684	76	94221	321
14	541	605	52	211163	263
15	425	542	32	483203	236
16	355	551	12	394183	213
17	299	22811	3	125402	113
18	285	551	2	46045	33
19	217	949	1	22957	7
20	206	1367686	0	8102	0
21	139				
22	105				
23	92				
24	86				
25	29				
26	34				
27	34				
28	21				

From the above Table it is seen that in the edited dataset, all fields are indeed within the widely accepted maximum values, i.e. SWH have a practical maximum of 10 meters, with just a few higher (but acceptable) values to 19 meters, sigma0 is between 8 and 20 dB and Wind Speeds reach a maximum of 15-19 m/sec indicating some stormy but acceptable conditions. The altimeter standard deviations have a maximum of 28 cm. In taking the mean of the backscatter coefficient, it is seen that the effective value of 14.9 dB is systematically higher than the corresponding one of ERS-1 (11 dB) by 3.9 dB.

As far as the number of elementary 20 Hz data used for the 1 Hz data generation is concerned, over 98% of the data are 20 per sec data and a much smaller portion is 17 per sec data (resulting from internal calibration). Note that all records with Nval =1,2 have already been removed during the initial editing. Testing has been made to identify any correlation between Nval and the altimeter standard deviation, as well as with other values. No specific correlations have been found, of low Nval with extreme conditions in the other quantities. Therefore, it was decided to maintain all the data, irrespective of their Nval.

As an overall conclusion, a substantial stability has been observed in the distribution of the data. This observation was also supported by a more formal statistical analysis that has been performed (mean, median, mode, variance, kurtosis etc). All the statistics were identical in the three full cycles.

- Generation of residual sea surface heights and analysis

The edited datasets have been used to compute SSH, the sum of all the corrections (including the inverse barometric effect), and the corrected SSH, with respect to WGS84. These have the following global statistics:

Table 5 : Mean and RMS SSH statistics with respect to WGS84

	Mean				RMS			
Cycle	1	2	3	4	1	2	3	4
Uncorrected SSH	-0.97	-0.92	-1.17	-1.39	30.35	30.35	30.23	30.04
Corrections	-2.48	-2.52	-2.51	-2.53	2.51	2.51	2.54	2.56
Corrected SSH	1.51	1.57	1.34	1.13	30.34	30.34	30.22	30.03

To obtain the first measure of quality of the altimeter data in terms of oceanographic quantities, the residual sea surface heights with respect to the geoid need to be computed. It is well known that the expected global statistics of the residual sea surface heights is zero, with respect to the best fit ellipsoid, that is inherently used to compute the geoid undulations. Then, any deviation from the zero mean is either an altimeter bias, an orbit error that gives a global mean attribute, other residual errors, or a combination of all of them. In addition any rms statistic, different from zero, is a combination of ocean variability, orbit errors and other residual effects.

In order to compute the residual sea surface heights, the computation of the geoidal undulations and the sea surface topography for all subsatellite points was necessary.

The computation of geoid undulations was made using the OSU91A gravity field, complete to degree and order 360. To avoid extreme computation times, the geoid was first computed on a regular grid of 7.5*7.5 minutes and then interpolated at each subsatellite coordinate. This procedure has been tested and proved to be accurate at the 1 cm level even at regions of high gravity gradients. For testing purposes, alternative computations were also made, in which the JGM2 gravity field complete to degree and order 70 was used, complemented by the OSU91A coefficients from degree 71 to 360. Both solutions gave insignificant differences, as can be seen from the following table that shows global gridded and along arc (only for the second repeat) statistics.

Table 7 : Grid and Along Arc statistics of geoid undulations

	Grid (Global)		Along Arc (Oceans)	
Field	Mean	RMS	Mean	RMS
OSU91A	-0.039 m	29.189	1.079	30.729
JGM2-OSU	-0.046	29.184	1.075	30.721

So, it was decided that the OSU91A geoid is used to compute the residual sea surface heights. An implied best fit ellipsoid with a=6378136.3 meters was used. Therefore a correction of 70 cm was added to the sea surface heights. In addition, an estimate of sea surface topography, computed from the harmonic synthesis of SST coefficients (up to degree 10), was subtracted from the SSH.

Histograms of the residual SSH indicate that the majority of values are below 5 meters, a discrepancy level that can very well be attributed to the inability of the high degree geoid to resolve very short wavelength changes in the gravity field. Discrepancies higher than 5 meters were also found in all four cycles. In particular several thousand residual SSH exceeding 20 meters were found in the first 2 cycles. These values, generally at latitudes of below 70 degrees and at longitudes centered around 180 and 300 degrees, are obviously ice values that the altimeter tracker has interpreted as ocean values. They are shown in Figure 7.

A final editing was made in all four cycles to remove the residual heights greater than 5 meters. Note that the majority of these edited values have Nval=20 and a very low standard deviation. The final edited datasets exhibit the following global statistics :

Table 8 : Residual SSH statistics

	Mean				RMS			
Cycle	1	2	3	4	1	2	3	4
Number of data	491611	1361048	1438399	1361584				
Uncorrected SSH	-0.50	-0.45	-.48	-0.70	30.24	30.24	30.21	30.01
Corrections	-2.49	-2.52	-2.52	-2.53	2.51	2.55	2.54	2.56
Corrected SSH	1.99	2.07	2.03	1.83	30.33	30.30	30.26	30.07
Geoid Undulations	1.78	1.84	1.77	1.59	30.37	30.36	30.31	30.12
Sea surface topo.	-0.01	0.01	0.03	0.02	0.61	0.60	0.58	0.56
Residual SSH	0.22	0.22	0.23	0.22	0.50	0.51	0.51	0.52

The above Table shows a good stability in the statistics of the residual SSH, on the order of 22 cm for the mean, indicating a possible bias in the altimeter, and 51 cm for the RMS.

Additional statistics have been computed taking into account the orbit error estimates that are included in the OPRs. After removing some observations for which the orbit error field has a default value, the orbit error was applied to the residual SSH and statistics were recomputed. The results indicate that the orbit error is on the order of 8 cm and provides an insignificant reduction in the residual SSH (on the order of 1 cm). Considering though that the orbit error estimates have been computed from crossover analysis, these estimates represent only the geographically uncorrelated portion of the error and not the complete error.

The global representation of all the valid altimeter data is shown in Figures 8 and 9. Figure 8 shows the ascending arcs while Figure 9 shows the descending arcs.

- Crossover discrepancy analysis

Another widely known statistic indicating the quality of the altimeter observations and the accuracy of the orbits, is the rms (global and regional) of crossover discrepancies.

Crossover discrepancies do not contain any time invariable signals. They are primarily functionals of the orbit error and the ocean variations. More specifically they contain the geographically uncorrelated error and the variability of the ocean for the period elapsed between the two occurrences of the crossover. Other minor components do exist and are related to time dependent errors of the geophysical and atmospheric corrections.

Therefore an analysis of crossover discrepancies for small time periods clearly indicates the level of the geographically uncorrelated component of the orbit error (assuming that ocean variability is zero at periods of some days) which in turn gives a qualitative estimate of the total error, since it is known that the two components of the error (correlated and uncorrelated error) have, in a global sense, a more or less similar magnitude.

Since the orbit error is dependent on the initial orbit state vector of each integration arc (5 days for ERS2), it is theoretically and practically correct to produce crossover statistics at least at 5 days time intervals. In addition, and in order to identify the effects of ocean variability and possible inconsistencies between integration arcs, crossover statistics across the 5 day arcs were produced. To produce these statistics, crossover discrepancies for all 5 day arcs and across the 5 day arcs, belonging to the same repeat cycle, have been computed for all cycles.

In order to compute the crossover discrepancies, a semi-analytical method was used. The approximate crossover locations have first been computed, based on well known geometric properties of the orbit. This computation was made for all crossover locations within each repeat cycle. Then, the exact locations were determined, via a 10 point non linear interpolation of the continuous precise state vectors.

The altimeter discrepancy at each of the crossover points was then computed, by linearly interpolating the altimeter datasets and adopting the following two criteria :

- The corresponding undulation crossover discrepancy is less than 3 cm.
- The temporal distance between the observations that precede and follow the crossover location is less that 15 seconds, in either of the two crossover occurrences.

The combination of these two criteria guarantee that no artificial errors due to the high frequency geoid or due to interpolation, contaminate the crossover discrepancies. This has been successfully tested against non linear interpolation of several altimeter points that precede and follow the crossover location.

Maintaining the crossover discrepancies that have a maximum value of 60 cm, the rms statistic for each cycle was found to be on the order of 19 cm. Application of the CD orbit error on the other hand, only reduces this statistic by about 2 cm. The statistics are shown in the following Table :

Table 9 : Crossover discrepancy statistics

	x-vers	rms	cor. rms	Mean
Cycle 1	5329	0.198	0.180	-0.006
Cycle 2	37938	0.192	0.172	-0.001
Cycle 3	42248	0.188	0.174	0.001
Cycle 4	38052	0.189	0.173	0.001

The geographical distribution of the crossover discrepancies for all cycles is shown in Figure 10. Additional statistics of crossover discrepancies within and across the seven 5 day arcs are shown in Table 10, for the second repeat cycle (number of crossovers and rms):

Table 10 : Number of crossovers and rms within and across 5 day arcs

5 day Arc	1	2	3	4	5	6	7
1	470	1167	1282	1150	1189	1220	1254
	.177	.198	.197	.207	.207	.193	.199
2		738	1617	1400	1476	1596	1607
		.169	.189	.199	.184	.193	.211
3			917	1649	1710	1799	1851
			.168	.194	.195	.196	.194
4				776	1556	1616	1680
				.167	.188	.199	.196
5					839	1728	1781
					.159	.181	.198
6						967	1906
						.177	.196
7							997
							.180

In the Table it is seen that the crossover discrepancies within each 5 day arc are systematically lower, on the order of 17 cm, than the ones across arcs. These discrepancies increase marginally, but systematically, to 20-21 cm as the elapsed time of occurrences increase, indicating that orbit errors across arcs and ocean variations start to build up. A final statistic that is produced, is a regional statistic at 30x30 degree geographical blocks. These estimates are shown below for the second repeat cycle and for all blocks (number of points, mean and rms):

Table 11 : Regional crossover statistics

Block	30	60	90	120	150	180	210	240	270	300	330	360
	1961	1250	111	28	172	225	292	250	116	25	225	1077
+60	.000	.030	.015	.027	.004	.023	.014	.025	.033	-.077	.013	-.009
	.224	.175	.252	.390	.277	.288	.296	.299	.296	.311	.171	.193
	185	15	0	0	245	884	877	658	6	206	1031	816
+30	.011	.014	.000	.000	.007	-.004	.001	.029	-.101	.001	-.011	-.029
	.177	.108	000	.000	.200	.162	.154	.129	.264	.218	.186	.173
	25	109	302	226	541	525	604	569	465	388	612	301
0	-.046	-.015	.023	.026	.019	.015	.005	.002	.005	.008	-.020	-.001
	.103	.188	.165	.214	.153	.134	.146	.122	145	.160	.199	.139
	273	380	652	557	158	498	608	616	655	292	213	645
-30	-.034	.000	007	.010	-.001	.013	-.015	-.011	-.027	-.023	-.021	-.020
	.119	.159	.147	.150	.215	.155	.144	.115	.151	.115	.146	.124
	1045	984	1187	1226	888	1032	1132	1110	1057	909	088	1032
-60	.003	-.005	.002	-.017	-.003	006	.003	.031	.006	-.009	.011	.005
	.184	.195	.184	.185	.212	.182	.210	.173	.199	.194	.213	.181
	166	210	189	160	223	361	651	741	615	471	386	206
-90	-.022	-.029	-.040	.003	.013	-.006	-.033	-.038	.059	-.027	.022	.054
	.217	.180	.172	.236	.237	.248	.260	.230	.245	.205	.317	.283

These regional statistics show smaller discrepancies in the equatorial and mid-latitude regions and higher discrepancies in the polar regions.

- Repeat arc analysis

Repeat arc analysis presents validation results of the altimeter data in terms of their level of consistency of repeated observations. It is important to note that the available repeat cycles (only three complete and one incomplete) are not sufficient to clearly define a long term mean arc and therefore long term ocean variations. The following analysis only determines variations with respect to a mean surface defined over 120 days. It is therefore expected that these residual variations are smaller, as compared to annual or longer term variations.

The first concern in a repeat arc analysis is always the generation of a reference arc, through the determination of time equidistant points, which is used to provide a common reference for all cycles and on which all the altimeter data are mapped. This reference arc is necessary, primarily because the individual altimeter observations are not generally occuring at repeated geographical locations. In addition, the density of observations (7 km apart) is unnecessarily high for studies related to ocean variations, since the minimal half-wavelengths of ocean variations, that are reported in the literature, are on the order of 30 km. Therefore normal points are computed, generally at 5-10 sec intervals.

In this validation analysis, normal points were computed every 30 sec, since the purpose was not to actually compute the ocean variations, but to establish a global level of consistency between the repeat cycles. The choice of 30 sec intervals was dictated by the availability of the rectangular earth fixed coordinates of the subsatellite track of the satellite orbits. These coordinates have already been converted to geodetic coordinates in order to be used for the generation of crossover discrepancies.

One shall have to bear in mind that not all studies can be performed with this type of data representation. For example, the determination of the effective wavelength of the altimeter noise requires the availability of all 1 sec repeated observations. Such determination though does not require the global dataset but only a few arcs and therefore it can be treated separately. On the other hand, it requires several repeat arcs that are not available. So this type of analysis was not performed.

To compute the coordinates of the normal points of the reference arc, the geodetic latitudes and longitudes of the orbit files have been considered. The corresponding coordinates of the 30 sec reference arc were simply the mean values of the corresponding latitudes and longitudes of all three complete repeat cycles. To test the representativeness of this reference arc, its deviations with respect to any of the three cycles have been computed, in terms of latitude and longitude difference, total distance on the sphere and across track and along track distance components. These values are shown in Table 12 (in degrees) :

Table 12 : Deviations of the reference arc from any of the repeat cycles

	D-lat	D-lon	Total dist	Across dist	Along dist
Max	0.109	0.736	0.112	0.029	0.112
Mean	0.045	0.055	0.051	0.003	0.051
Std	0.024	0.089	0.023	0.002	0.023

As it can be seen from the Table, the mean deviations of the normal points from the original points of the subsatellite track are, in terms of spherical distance, on the order of 0.05 degrees, or about 7 km. Most important, the reference arc is in practice coincident with the individual repeat arcs, since the across track distance is minimal.

The normal point estimates for each repeat arc (i.e. mapping of all altimeter observations on the reference arc) have been computed as a weighted mean of all individual residual sea surface heights that were within 15 sec from the normal point. The weights that have been used in the averaging were the inverse distances of the original observations from the normal point. Corresponding standard deviations have also been computed through standard error propagation.

Normal point estimates have been computed even when only one altimeter observation existed in the 30 sec time window. The global statistics of the residual sea surface heights for all four repeat cycles, based on the computed normal points, are shown in Table 13 :

Table 13 : Residual SSH statistics based on the normal points

	Number of normal points	Mean	RMS
Cycle 1	17709	0.22	0.49
Cycle 2	49248	0.22	0.49
Cycle 3	52330	0.23	0.51
Cycle 4	49913	0.21	0.51

These statistics are very similar to the statistics when the global set of data has been used. The standard deviations of the normal point estimates are mostly less than 10 cm, although there exist several estimates with higher standard deviations, primarily in regions of high variability and in cases of just a few altimeter observations in the 30 sec interval.

To test the sensitivity of the results to the specific choices made, alternative computations have been attempted that have considered either a different weight (e.g. simple average or square root of inverse distance), or a different maximum distance from the normal point (e.g. 7 sec), or finally a minimum number of data (e.g. 5 or 10 altimeter observations). In all these tests the global statistics have been changed slightly, to reflect the different degrees of smoothing and data representation, but in all cases the results were practically identical.

Having computed the normal point estimates for each cycle, the mean estimates and the residual repeat observations have been computed for the 3 full cycles. For this computation, only the points that had all three estimates available were considered. The global statistics are shown in Table 14 :

Table 14 : Global statistics of mean and residual surfaces

	Number of normal points	Mean	RMS
Mean surface	40478	0.23	0.45
Cycle 2	40478	0.002	0.117
Cycle 3	40478	0.014	0.114
Cycle 4	40478	-0.017	0.112

The above computations have been repeated using different constraints, e.g. removing differences greater than 50 cm, not considering points with standard deviations greater than 10 cm, or points being generated by less than 10 original altimeter observations. The corresponding results have an rms magnitude ranging from 9 to 11 cm. These results are for all practical purposes, considered to be identical to the above.

A final test that was made, was to compute the differences between all the individual arcs, at common normal points. The corresponding results gave an rms of 16 cm for all differences.

In concluding with the second level verification, it has been found that the ERS-2 altimeter data are complete and accurate at the 18 cm level in terms of crossover discrepancies and 11-12 cm in terms of repeat arcs, for the time period of 120 days. These results indicate that an average user may very well use these observations for oceanographic and geophysical analysis, without having to necessarily resort to orbit error improvement. The orbit errors themselves, are expected to be at the 15-20 cm level.

THIRD LEVEL VERIFICATION

The third level verification concentrated in further quantifying the inherent accuracy of the orbital range estimates. Least squares adjustments were performed to solve for the non geographically correlated error of the crossover discrepancies, as well as for the arc dependent orbit errors existing in the residual repeat observations.

- Crossover discrepancy adjustment

It is well known that the radial orbit error arises from errors in the gravity field that was used for the orbit integration and errors in the determination of the initial state vector of each integration arc. The two types of errors are distinctly different. Indeed, the first type of error has, in principle, amplitudes at all orbital frequencies (in practice up to 3 cy/rev) and is only dependent on time within each repeat cycle. This error can easily be expressed in terms of Fourier series at known orbital frequencies. The second type of error evolves as a bias, 1cy/rev and 2 cy/rev with constant and time dependent amplitudes, thus creating a bow-tie pattern. This error is dependent on each integration arc and is generally different among integration arcs, subject to the accuracy of the respective initial state vectors. This error is expressed as a bias and first degree Fourier term for each integration arc.

For a certain geographic location, the two types of errors have a portion that is different at the ascending and descending arcs (geographically variable error) and a portion that is identical at the two arcs (geographically correlated error). Therefore, in a crossover discrepancy, only the geographically variable errors are observable.

The geographically variable error within a cycle can be modeled as a differenced Fourier series and a differenced set of bias, 1cy/rev and 2cy/rev terms within and across integration arcs. To remove singularities that exist in any crossover adjustment solution, the bias and the cosine term of the first integration arc are typically set to zero. In addition, a constraint is imposed on the frequencies of 1cy/rev - 1cy/day and 2cy/rev - 2cy/day, since these are fully correlated with the frequencies 1cy/rev + 1cy/day and 2cy/rev + 2 cy/day.

Using such a model, a least squares adjustment was made to compute the relative biases and the coefficients of the 1 and 2 cy/rev for each integration arc, as well as the coefficients of the differenced Fourier series. The orbital frequencies of the Fourier series have been defined for a maximum gravity field order of 70, which corresponds to the maximum order of the gravity field that was used for the orbit integration. Of these frequencies, only the frequencies that are smaller than 3 cy/rev were retained, since it is well known that no significant signal exists beyond this limit. The resulting number of frequencies was 417 (834 unknowns). For each 5 day integration arc (a total of 24 arcs) there were 7 unknown coefficients, with the exception of the first arc of each repeat cycle, that had 5 unknowns, due to the removal of singularities.

The data that were used for the adjustment, were all the crossover discrepancies, within each repeat cycle, with a magnitude smaller than 60 cm.

The results of the adjustment for the arc dependent parameters are similar for all cycles and are typically shown for the second cycle in Table 15. The amplitude spectrum of the differenced Fourier series solution is shown in Figure 11.

Table 15 : Solution for the arc dependent parameters (Cycle 2)

Arc	A_0	A	B	A^t	B^t	A^{2t}	B^{2t}
1	.000	.000	.013	.003	-.003	.004	-.007
2	.014	.006	-.017	-.003	.005	-.002	-.003
3	.020	-.027	-.023	.002	.002	.001	-.003
4	.001	-.071	.076	.001	-.004	.001	-.001
5	-.006	-.029	.032	.000	-.001	-.002	-.001
6	.019	-.014	.031	.001	-.001	.000	-.001
7	.010	.038	-.060	.000	.002	.000	-.001

From the Table it is seen that the coefficients of the time dependent 1 and 2 cy/rev terms are all insignificant. This was expected due to the small duration of the integration arcs. The 1cy/rev effects, that create a bow-tie pattern, are on the order of 5 cm with the exception of some arcs where the amplitude reach 10cm and higher. The relative biases are also very small.

Figure 11 indicates errors on the order of about 4 cm for some frequencies, the majority of them being below the 1 cm level.

Using the above solution, adjusted crossover discrepancies have been computed and their statistics were compared with the original crossovers. Table 16 shows the global statistics for each repeat cycle and for the total number of crossovers.

Table 16 : Original and adjusted crossover discrepancies

Repeat	Number of crossovers	Original RMS	Correction	Adjusted
1	5329	.198	.088	.189
2	37938	.192	.092	.169
3	42248	.188	.092	.166
4	38052	.189	.090	.167
Total	123567	.191	.092	.168

Table 16 indicates that the overall correction in on the order of 9 cm reducing the crossover discrepancies from 19 to 16.8 cm. This implies that the orbits have a geographically variable error on the order of 9 cm. If one assumes that the geographically correlated error is of the same order of magnitude in the RMS sense, then the total orbit error is on the order of 13 cm. Such assumption is not necessarily valid, since the crossover discrepancies, that do not contain the geographically correlated error, have already been used for the orbit adjustment, and possibly for the gravity field development, therefore the data has been optimised for the crossovers, leaving an undetermined geographically correlated error in the sea surface heights.

To observe the effect of the adjustment in each integration arc, statistics have been computed and are shown in Table 17 for all arcs of the second cycle :

Table 17 : Number of crossovers, Original, corrections and adjusted rms discrepancies

Arc	1	2	3	4	5	6	7
1	470	1167	1282	1150	1189	1220	1254
	.177	.198	.197	.207	.207	.193	.199
	.073	.083	.085	.095	.086	.084	.086
	.164	.182	.182	.186	.187	.184	.182
2		738	1617	1400	1476	1596	1607
		.169	.189	.199	.184	.193	.211
		.080	.088	.097	.083	.087	.098
		.156	.166	.168	.167	.171	.182
3			917	1649	1710	1799	1851
			.168	.194	.195	.196	.194
			.089	.099	.095	.089	.094
			.147	.170	.168	.171	.173
4				776	1556	1616	1680
				.167	.188	.199	.196
				.087	.095	.103	.110
				.150	.160	.169	.164
5					839	1728	1781
					.159	.181	.198
					.077	.094	.101
					.138	.158	.164
6						967	1906
						.177	.196
						.086	.093
						.149	.168
7							997
							.180
							.093
							.147

From this Table one can observe that the adjusted RMS across arcs tend to stabilise since the arc dependent corrections remove small arc inconsistencies.

In any case all these corrections are small and indicate that the altimeter data set is accurate at the 13 cm level (subject to geographically correlated errors). In addition, these corrections are very similar to the corrections implied by the orbit error estimates that are included in the OPR. The corresponding RMS of OPR corrected crossovers are 0.181, 0.174, 0.175 and 0.173 m for each repeat cycle respectively.

- Residual repeat arc adjustment

In a repeat arc analysis, when the mean sea surface is computed, by averaging all the normal point estimates, the orbit error that is inherent in the normal points of each repeat cycle is propagated into the mean surface in an averaged form. This means that the effective orbit error is composed by the full error implied by the errors of the gravity field and an unspecified average of arc dependent errors, primarily at 1 and 2 cy/rev. On the contrary, the residual arcs do not contain any gravity field implied error, since this is canceled out in the differencing, but they do contain arc dependent errors.

In order to remove these errors a typical bias, 1cy/rev and 2cy/rev adjustment was performed for each integration arc. The solution indicated that the orbit error is on the order of 3 cm for all three repeat cycles. After removing this error, the statistics shown in Table 14 change as follows : the mean residual for each repeat becomes effectively equal to zero, while the rms value only reduces by half a centimeter.

The quantification of orbit errors both in crossover discrepancies and repeat arcs, has indeed confirmed the conclusions drawn from the standard analysis of the altimeter data, that indeed the data is accurate at the 13-15 cm level, an accuracy adequate for geophysical studies, and that the residual arcs are practically free from errors, having an amplitude at the order of magnitude of the expected seasonal ocean variations.

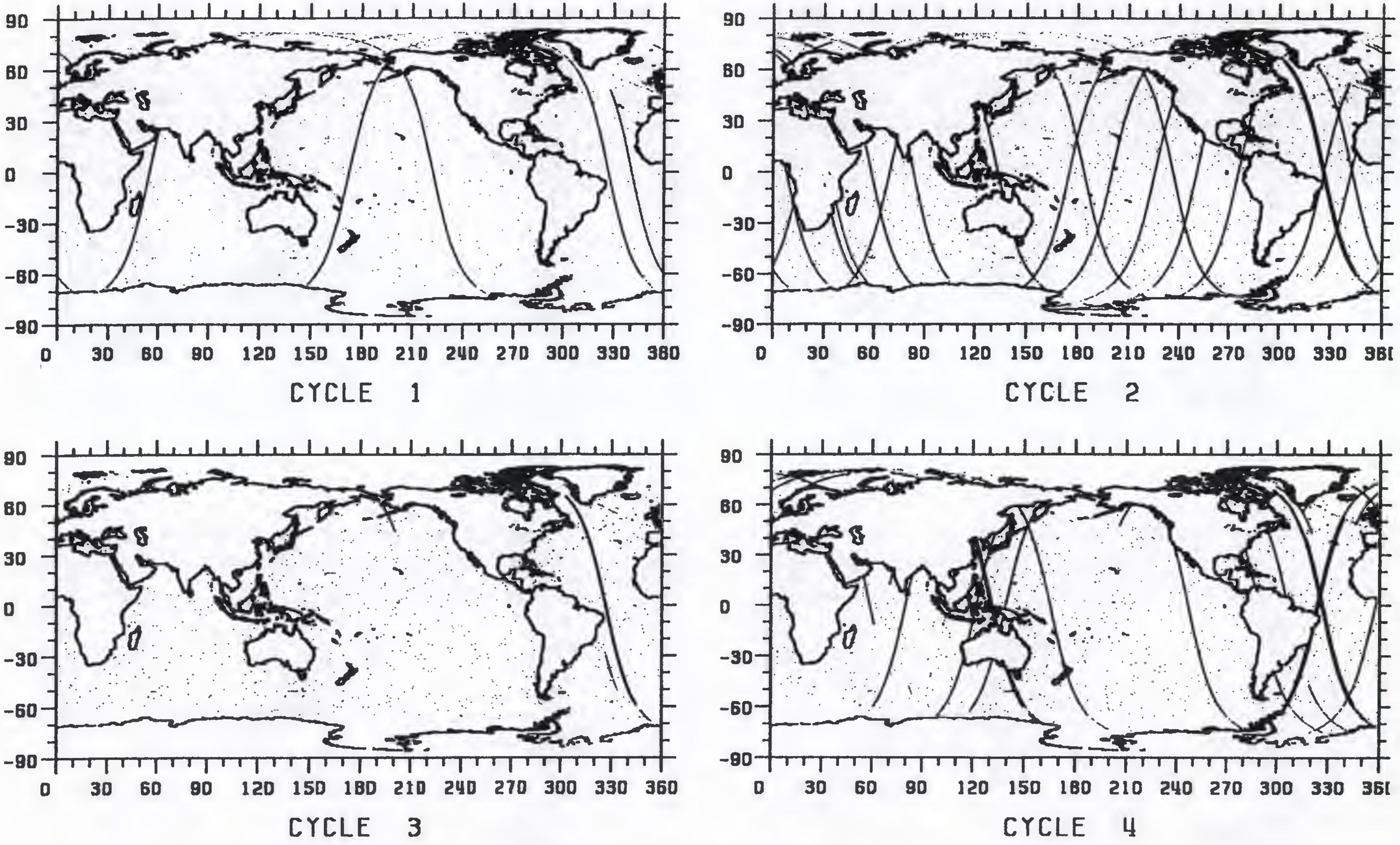

Figure 1 : Geographical distribution of the default values of the Wet Radiometer correction field

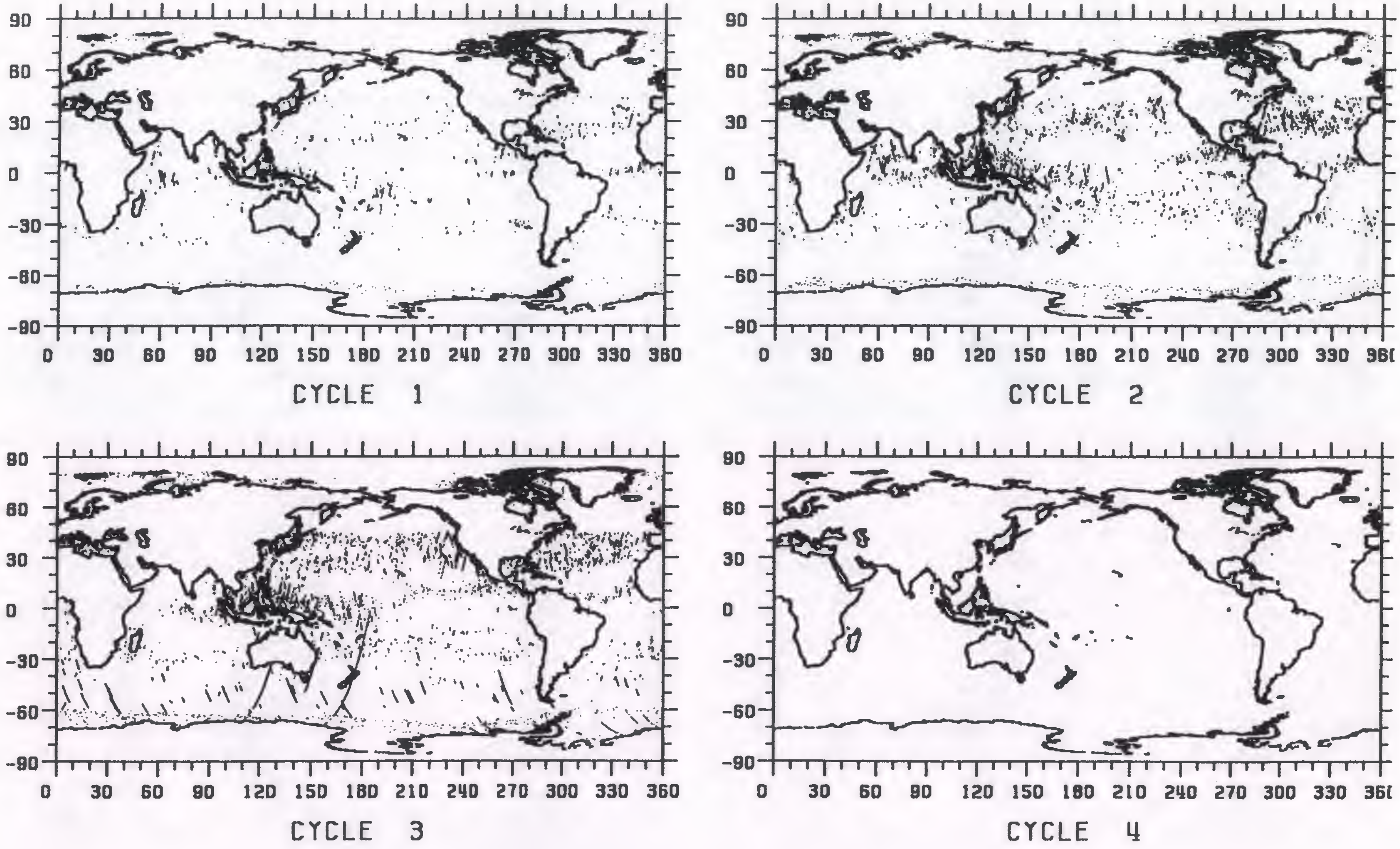

Figure 2 : Geographical distribution of the default values of the backscatter coefficient field

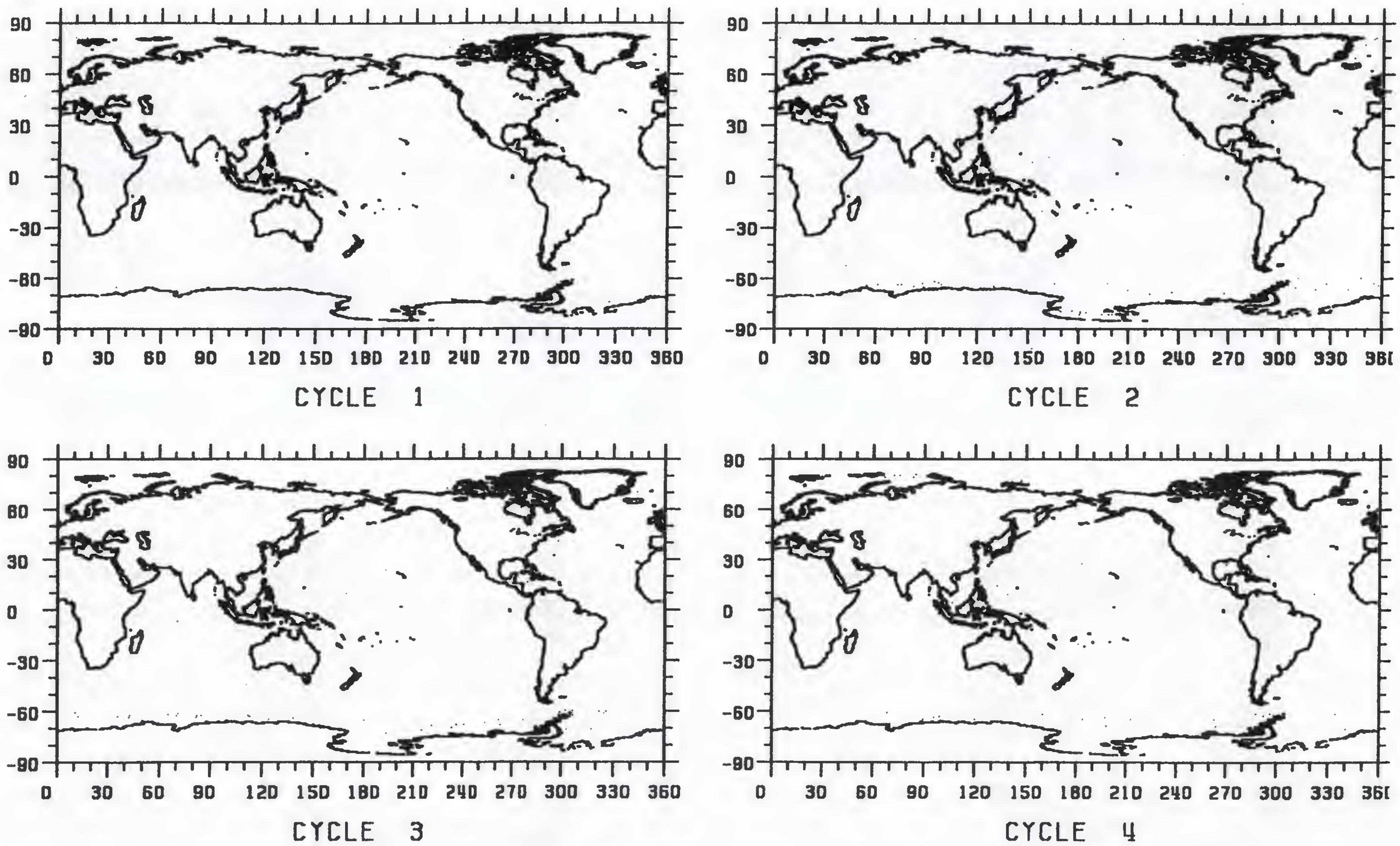

Figure 3 : Geographical distribution of the default values of the Significant Wave Height field

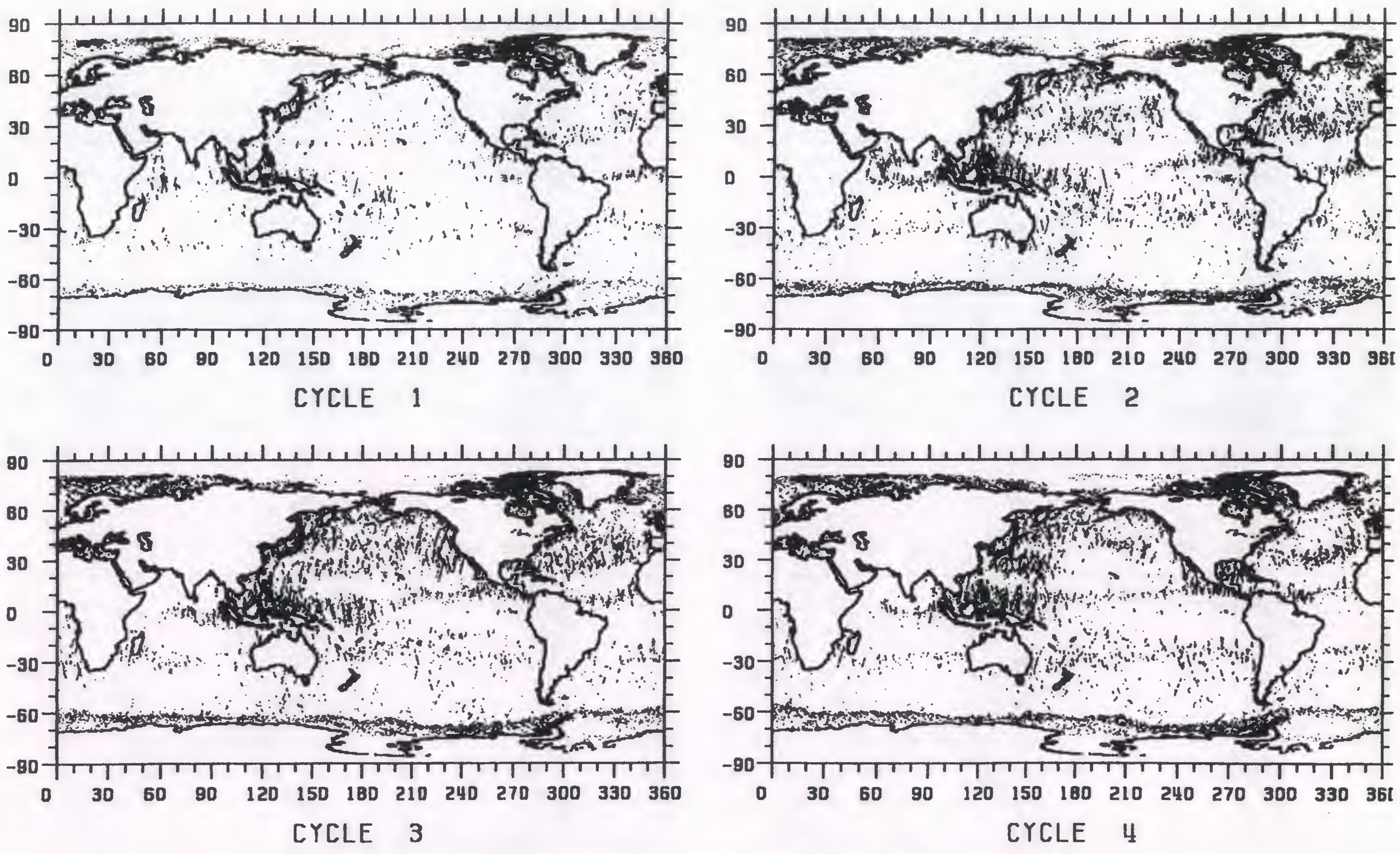

Figure 4 : Geographical distribution of the default values of the Wind Speed field

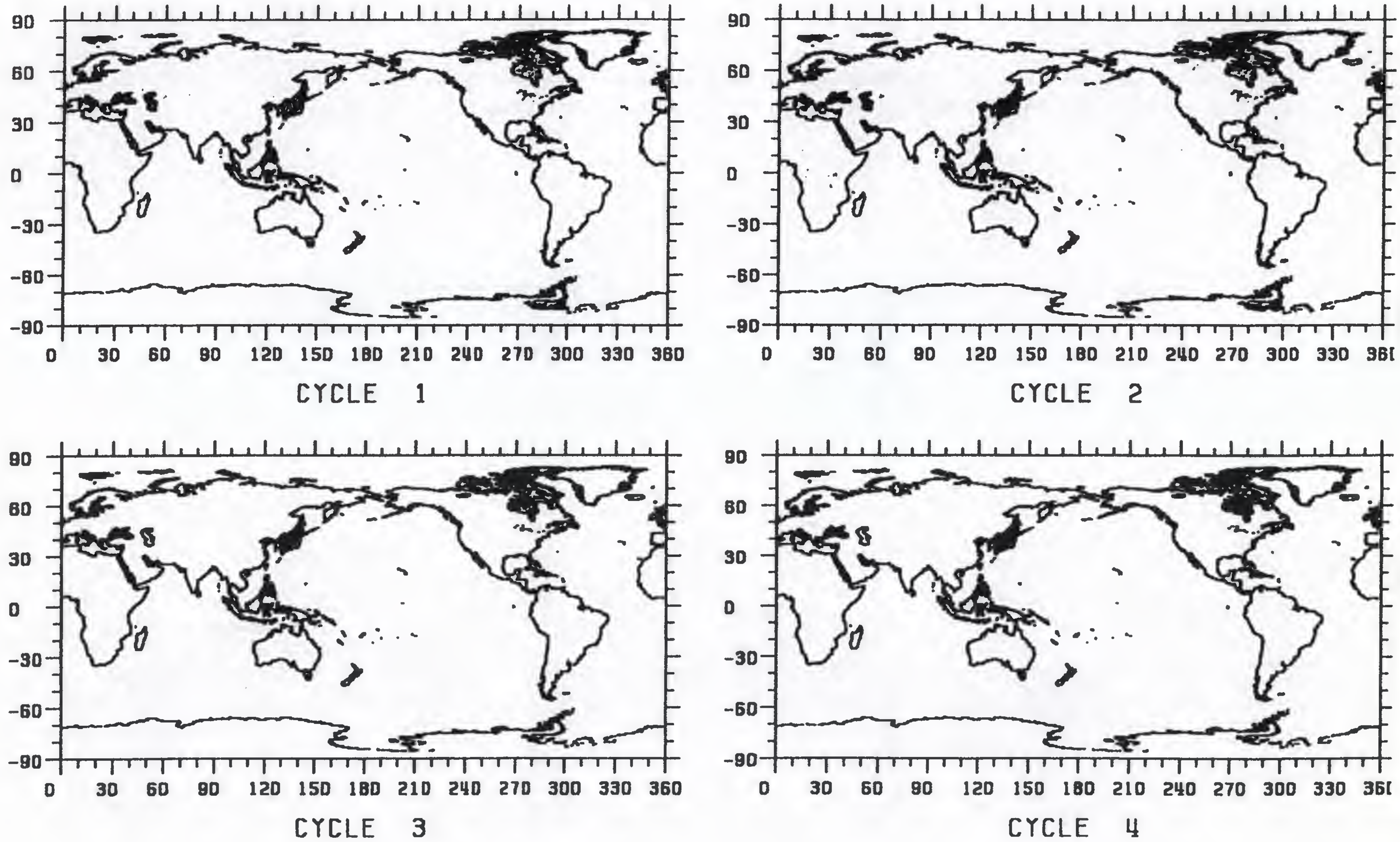

Figure 5 : Geographical distribution of the default values of the Ocean Tide correction field

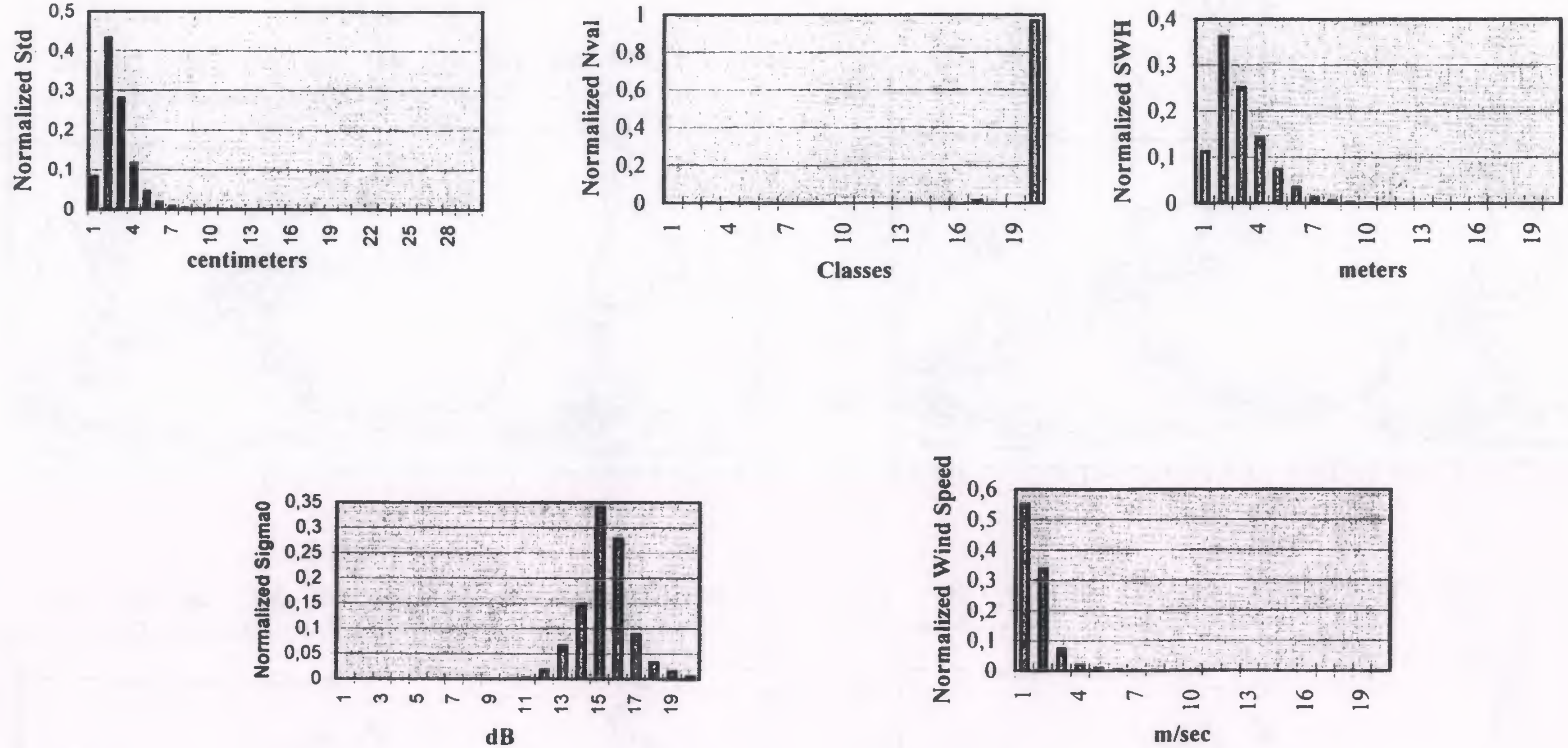

Figure 6 : Histogram of percentage distribution of std, Number of 20 Hz measurements, significant wave heights, sigma0 and wind speeds

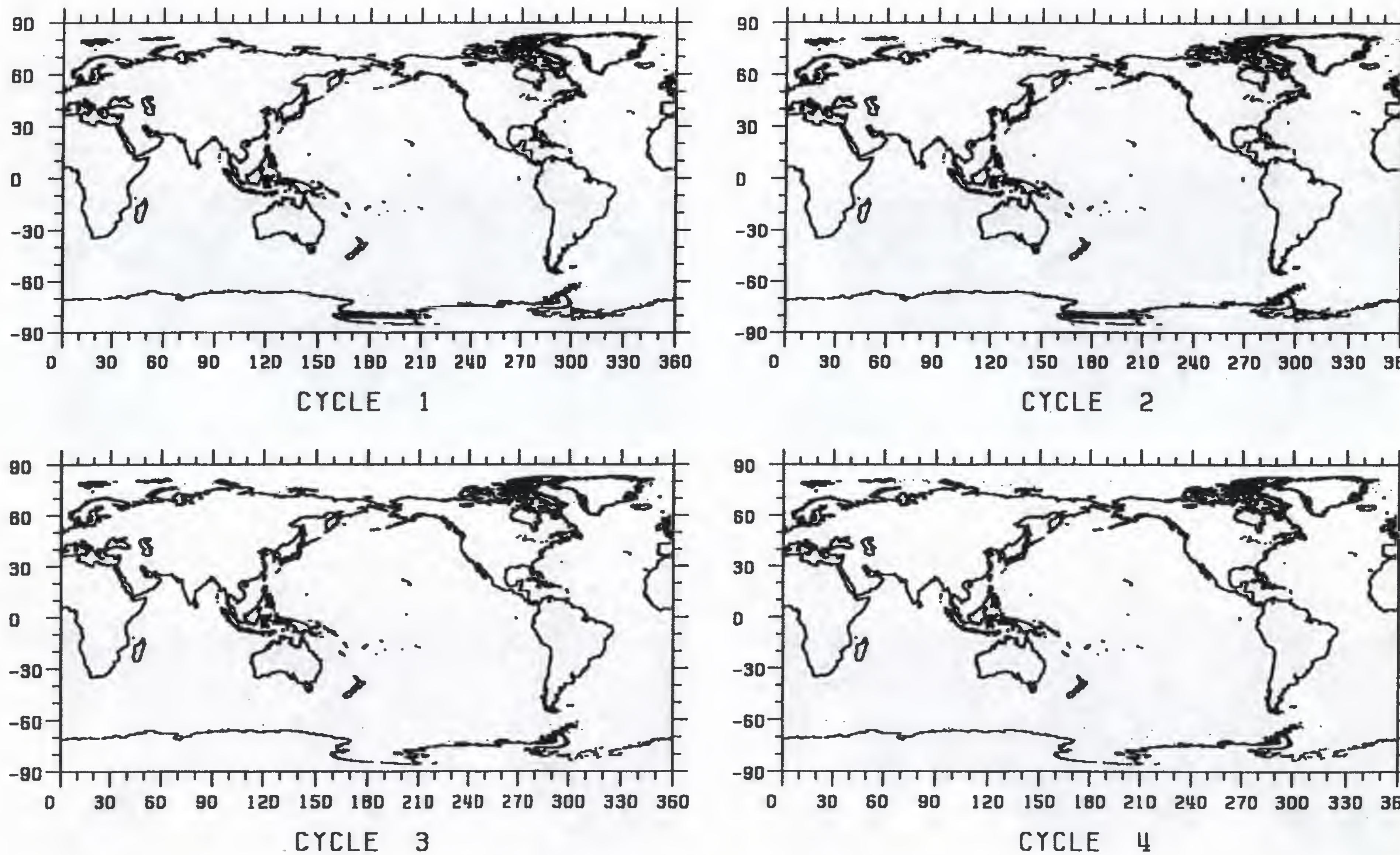

Figure 7 : Geographical location of residual sea surface heights greater than 20 meters

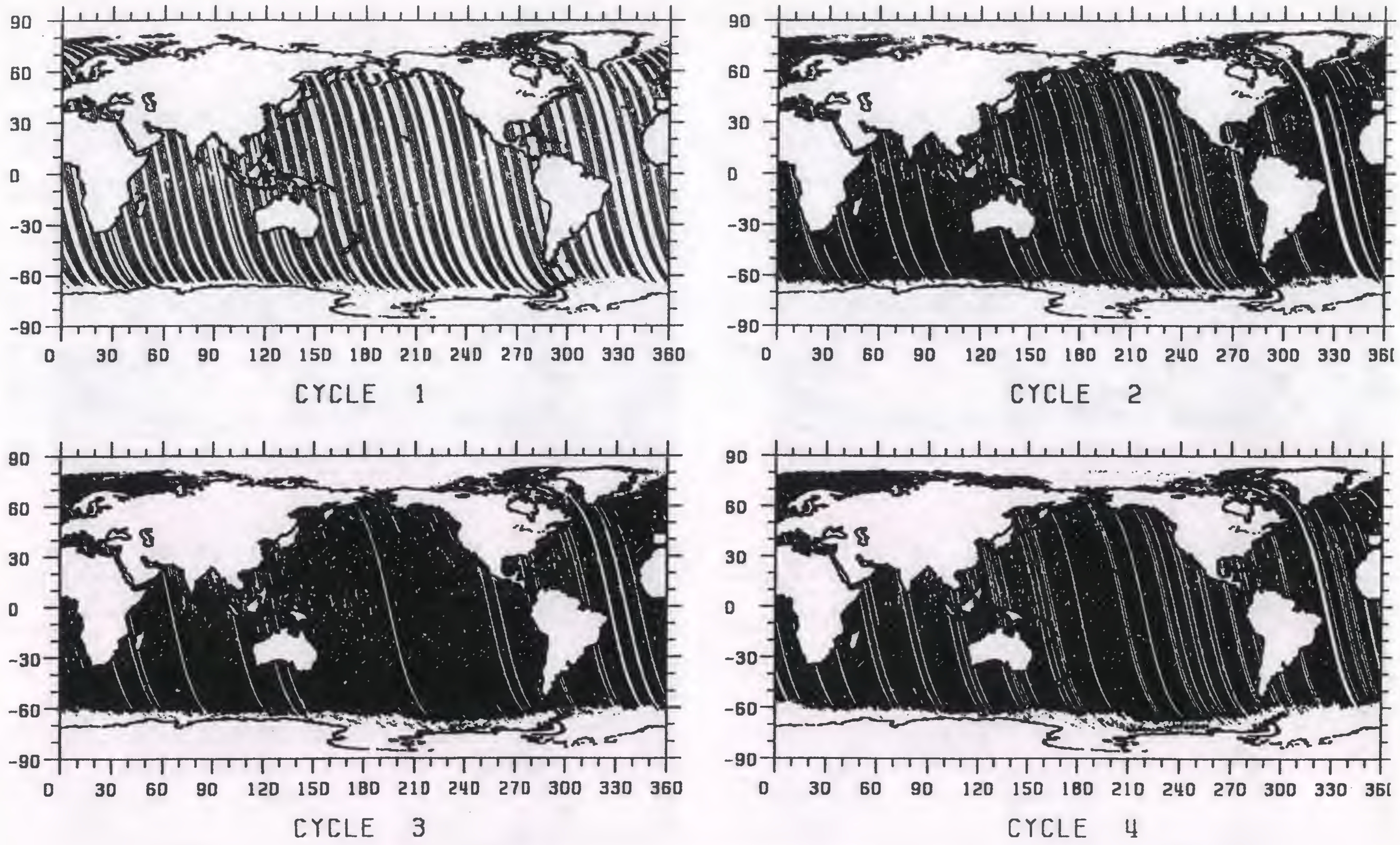

Figure 8 : Global coverage of ascending arcs of valid residual sea surface heights

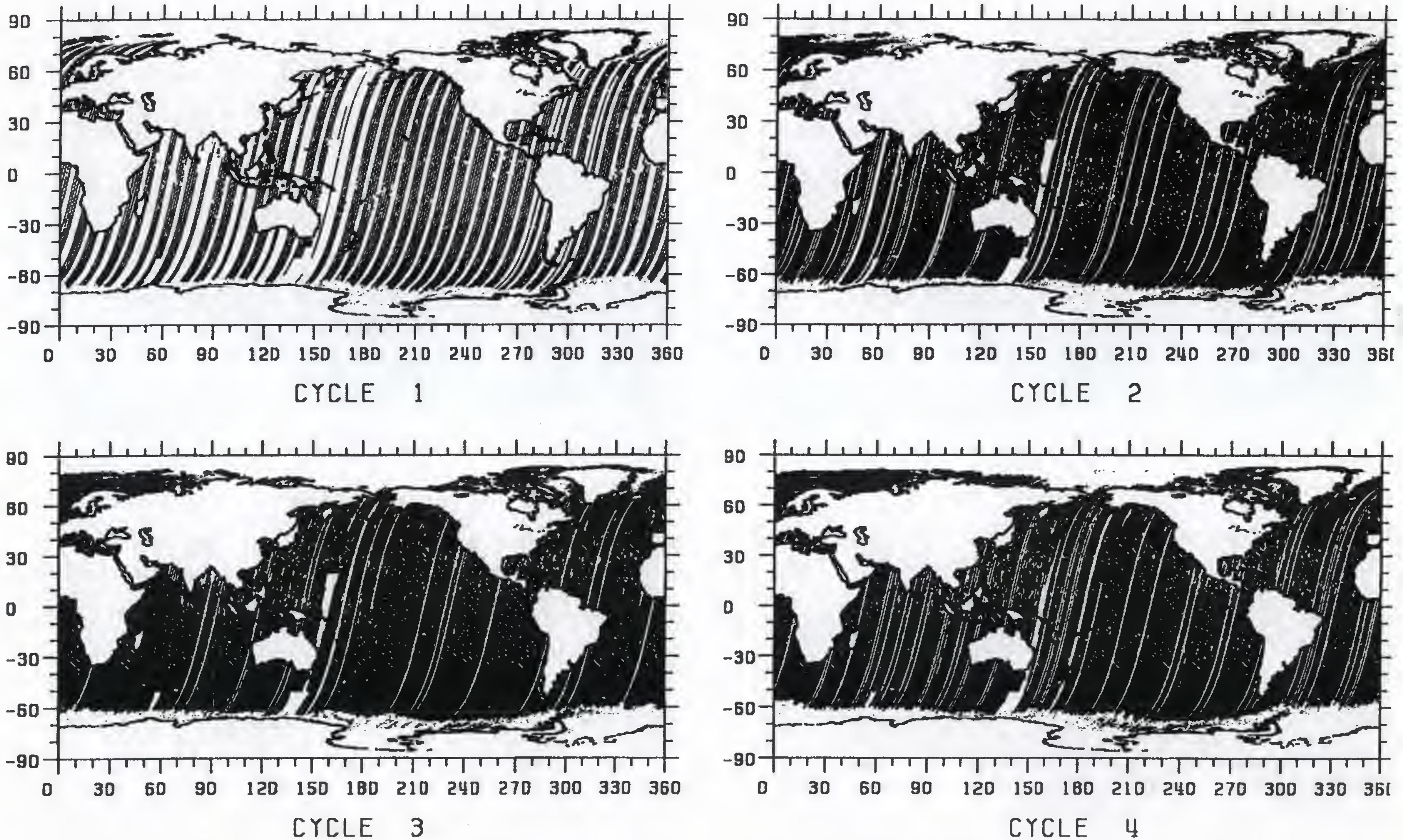

Figure 9 : Global coverage of descending arcs of valid residual sea surface heights

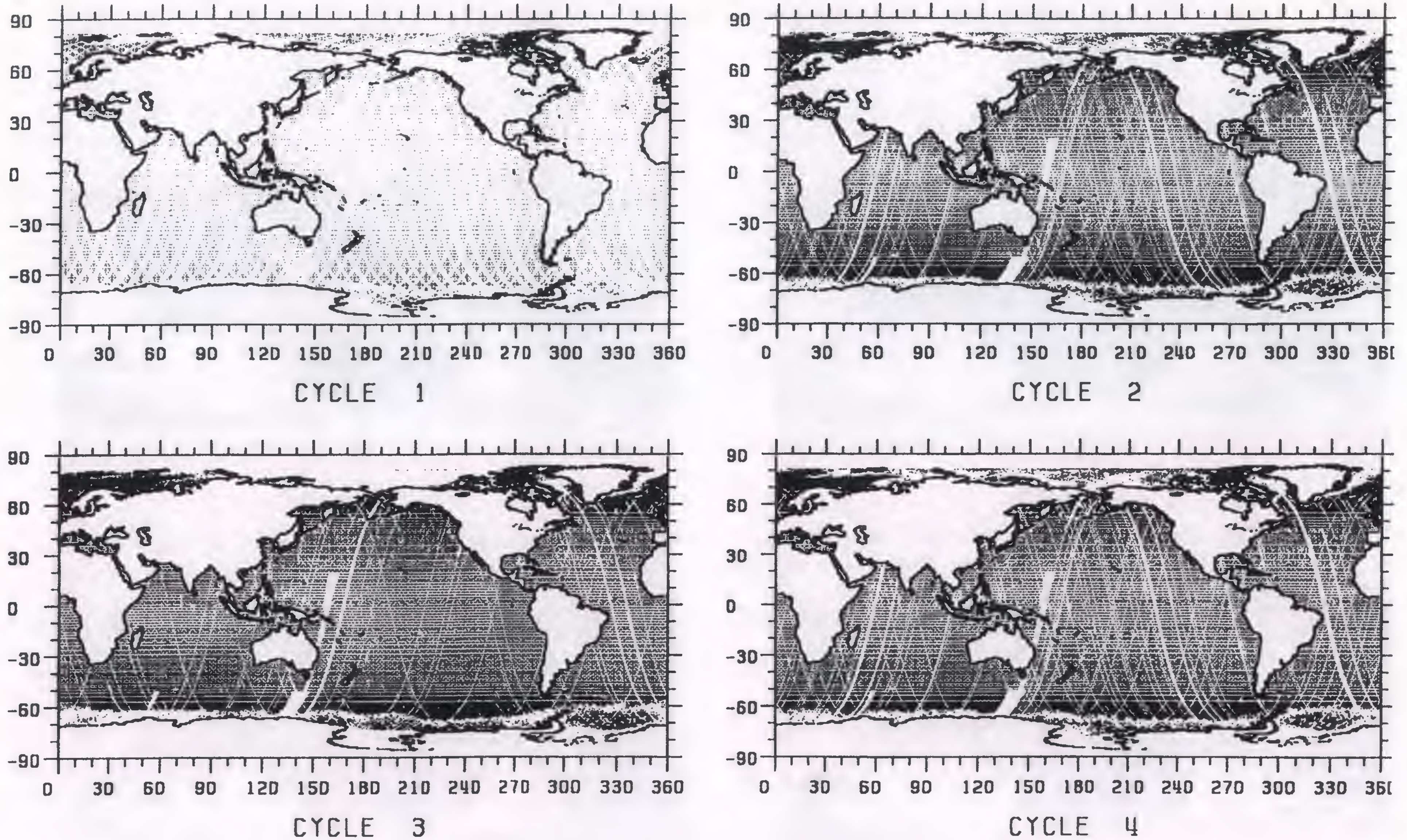

Figure 10 : Global coverage of crossover discrepancies

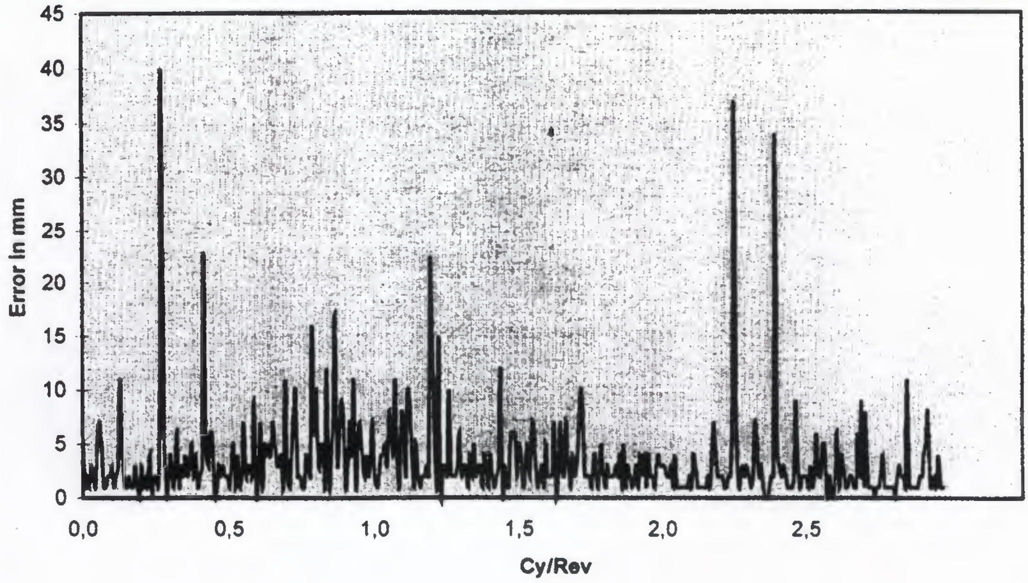

Figure 11 : Amplitude error spectrum of the differenced Fourier series solution

3.4 CETP Contribution to the validation of the ERS-2 OPR Products

C. Guérin, S.-A. Boukabara and
L. Eymard

CETP

Centre d'étude des Environnements
Terrestre et Planétaires
Vélizy, Issy-les-Moulineaux, Saint-Maur-des-Fossés

IPSL

CETP contribution to the validation of the ERS-2 OPR products

Validation of the CERSAT OPR products

March, 3rd 1996

Christine Guérin, Sid-Ahmed Boukabara & Laurence Eymard

Documents in reference:

ER-TN-CRP-AT-045	(1)
ER-IS-ESA-GS-0002	(2)
ER-TN-CRP-AT-0250	(3)
CLS.OC/NT/94.020	(4)
C2-MUT-A-01-IF	(5)

This is a summary of the work undertaken in CETP as part of the contract between CETP and IFREMER on the validation of the F-PAF products. It is also a part of the ERS-2 commissioning phase works.

1. Introduction:

We propose to examine in details the products processed in CERSAT (F-PAF) by comparing them to those processed here at CETP. There are two levels of validation:

- Validation of the brightness temperatures (MBT products): It concerns the two channels of the MWR2 radiometer, the 23.8GHz channel and the 36.5GHz one.
- Validation of the geophysical parameters (OPR products): It concerns the wet tropospheric correction, the integrated water vapour and the integrated water content.

In addition to CETP data (available since launch), we disposed of CERSAT data of one ERS2 35-days cycle (during September month). We selected then the coincident ones, it means 165 sequences. The TB's are integrated every 1.2 seconds in order to be coincident with the altimeter data for which they are used to correct the range.

2. MBT products validation:

We have filtered the CERSAT data using two flags, the validity one (data conserved when equal to zero) and the indicator of position (data conserved when equal to zero , for sea). We have also made coincident the two measurements by correlating their times. Time at CETP is processed using the predicted orbitographic data and those of CERSAT are processed using the restituted ones.
The systematic comparisons between CETP brightness temperatures and those of CERSAT, have showed that a significant bias between the two quantities exists. This bias is dependant on the brightness temperature value itself. As shown in the figures below, the bias presents some fluctuations which could reach a bit large values (more than 50 °K). The figures presented on the next page are an example of only one representative file. We will see later the explanation of these anomalies and the corresponding correction.

Visual results:

See next figures numbers 1 and 2. We see that in general, the discard between the 36.5GHz CETP brightness temperatures and those of CERSAT is around zero. For the 23.8GHz channel, the discard is a little bit over zero (dependant on the TB value). The first figure shows the evolution during time of the discard between the CETP brightness temperatures and the CERSAT ones (in both channels). The second figure shows the evolution of the 23GHz TB's discard versus the 23GHz TB value itself (it shows the relative variation).

Statistical results:

We present here the numerical-statistical results of this comparison, obtained by using all the MBT files.

Mean 23GHz T	Δ TB23	Δ TB36	Std. Dev. TB23	Std. Dev. TB36	Δ TB23 / TB23
178°K	0.39	-0.03	0.83	0.89	0.0022

Conclusion

We can see that the bias concerning the 36.5GHz TBs is almost zero, so we can say that the 36.5GHz TBs produced by CERSAT are conform to those processed at CETP.
On the contrary, the mean bias concerning the 23.8GHz TB's is too important to be ignored (a error of 0.39 °K could produce about 0.176 cm error on the wet tropospheric

correction). We have searched then what was the reason of this discard. Some recalls are necessary: The brightness temperature is calculated using the antenna temperature taking into account the effects of the secondary lobes. The formula giving the TB is:

$$TB=(Ta\text{-}contrib)/effic \qquad (1)$$

We find the same values of "contrib" at CETP and at CERSAT.

contrib=5.92	channel A
contrib=4.51	channel B

The values of "effic" are the same at CETP and CERSAT for the 36.5GHz channel (effic=0.95).

On the other hand, the values of "effic" in the 23.8 GHz channel are not the same: ("effic" represents the efficiency of the main antenna reflector and the efficiencies of the antenna main and secondary lobes)

effic=0.928	in CETP
effic=0.93	in CERSAT

The difference in the "effic" values is Δeffic = 0.002 . According to the formula number (1), we can get:

$$\mathbf{\Delta Tb/Tb=-\Delta effic/effic \quad = \quad +0.00215}$$

So, when taking the mean value of the 23.8GHz brightness temperature (178°K), this gives an error on the TB of about 0.38°K which corresponds well to the mean bias found when comparing the CETP 23.8 GHz TB's and those of CERSAT (the CETP TB is greater than the CERSAT one of about 0.39°K).
The problem of the difference between the CETP brightness temperatures and those of the CERSAT, found in the 23.8 GHz channel could be resolved just by taking the same value for the "effic" parameter : 0.928.

Remark:
- The fluctuant points for which the difference could reach big values (more than 50 Kelvins) are due to the fact that CETP and CERSAT do not use the same method in order to integrate the elementary measurements (every 150 ms). In the figures we can see that the only the coast contaminated points are concerned by this problem. Indeed, in CETP, we make an average of 8 scans values, as in CERSAT they fix absolutely a 1.2 seconds interval where they do the average, which is not the same.

-The problem mentioned before concerning the "effic" value will be completely eliminated in the new version of the CERSAT processing chain (version 6.1)

3. OPR products validation:

By OPR products, we mean the wet tropospheric correction, the integrated water content and the integrated water vapour. For this validation, we have processed only the CERSAT products in order to avoid the MBT discard found in the precedent chapter. This has been done by comparison between the official OPR products given in the files and the results obtained when applying the retrieval algorithms on the CERSAT brightness temperatures (given in the same files). Theoretically, the difference should be zero. Of course, we applied the same algorithm on the TB's values as the one applied to obtain the OPR official products (retrieval algorithm of July 1991)

Visual results:
See next figures (numbers 3 and 4). We could see that in general, the discard between the theoretical values and the delivered ones, present quite important anomalies. The example presented here concerns only one OPR file (sequence number 1954). This has been the subject of a lot of error simulations until the source of error was found. Figure 3 shows the results of the comparisons (tropospheric correction and water vapour). Significant differences appear. In addition, they are not constant. The figure 4 shows the results after modifying the processing chain (version 6.0, file example of sequence number 1000), no difference appears between the theoretical values and those delivered in the OPR files.

Statistical results:
We present here the numerical-statistical results of the OPR comparisons obtained using all the OPR files.

ΔWV	ΔWV (precise)	ΔWV simulated(precise)	Δ DH (precise)
-0.0091 g/cm²	0.2972 g/cm²	-0.0006 g/cm²	0.791 (cm)

We can see that an important bias appears in the water vapour precise products. A simulation of a sign error in the code of the retrieval algorithm removes the error (it becomes zero), after verification of the CERSAT processing chain, it appeared that an error of this kind has been found. We can also see the large bias in the case of the tropospheric correction.

Conclusion
The OPR precise products are not valid. A correction is necessary for their official use. The version 6.0 of the CERSAT processing chain has eliminated these problems.

Remark:
- Same remark concerning the fluctuant points: As we have fluctuant points for the TB's, we obviously have fluctuant points for the geophysical parameters (deduced from the TB's).
- The problem mentioned before concerning the OPR values, has been completely eliminated in the new version of the CERSAT processing chain (version 6.0), the new retrieval algorithms have also been implemented (algorithms of February 1996).

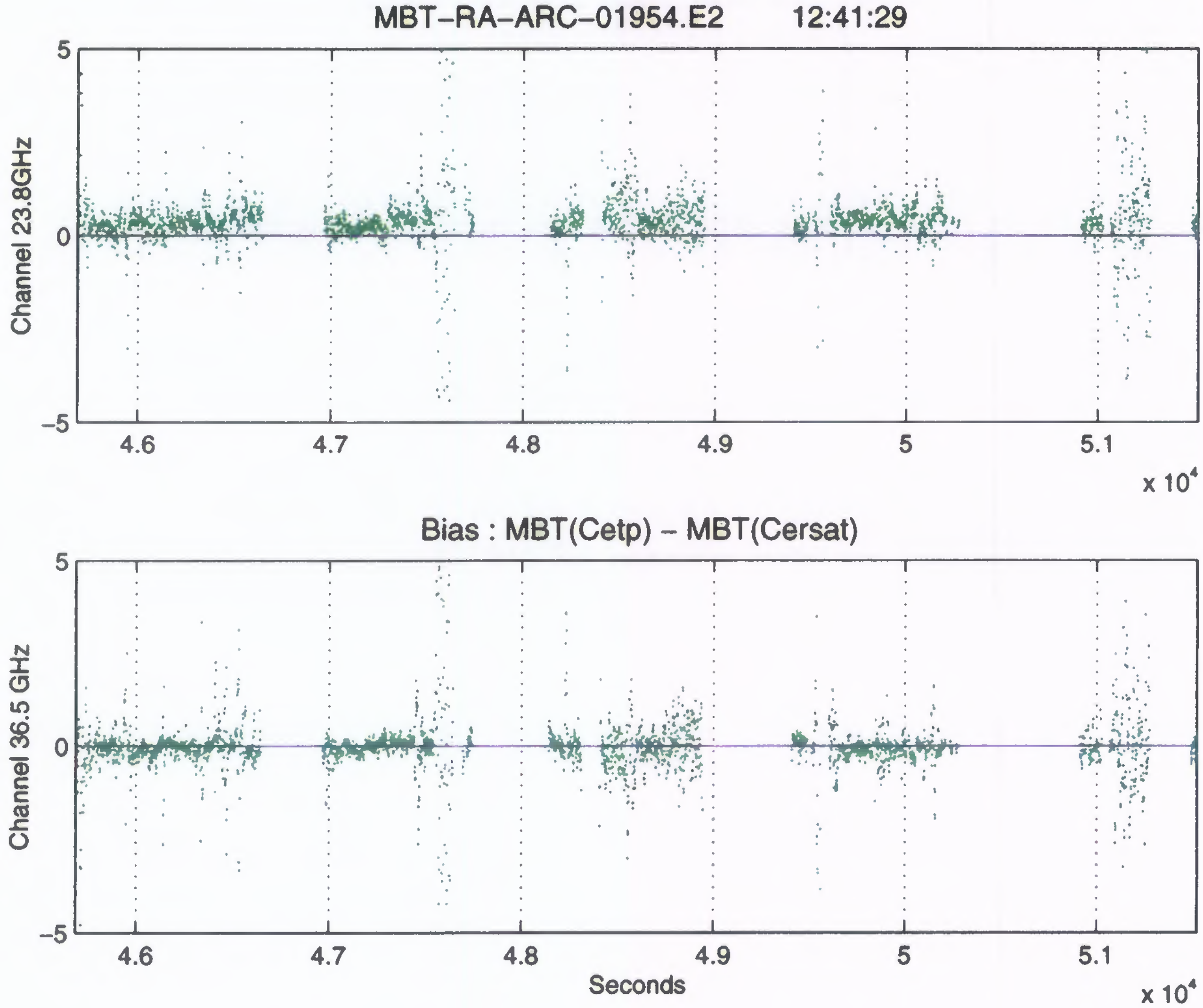
MBT-RA-ARC-01954.E2 12:41:29
Channel 23.8GHz
5
0
-5
4.6
4.7
4.8
4.9
5
5.1
x 10^4
Bias : MBT(Cetp) - MBT(Cersat)
Channel 36.5 GHz
5
0
-5
4.6
4.7
4.8
4.9
5
5.1
Seconds
x 10^4

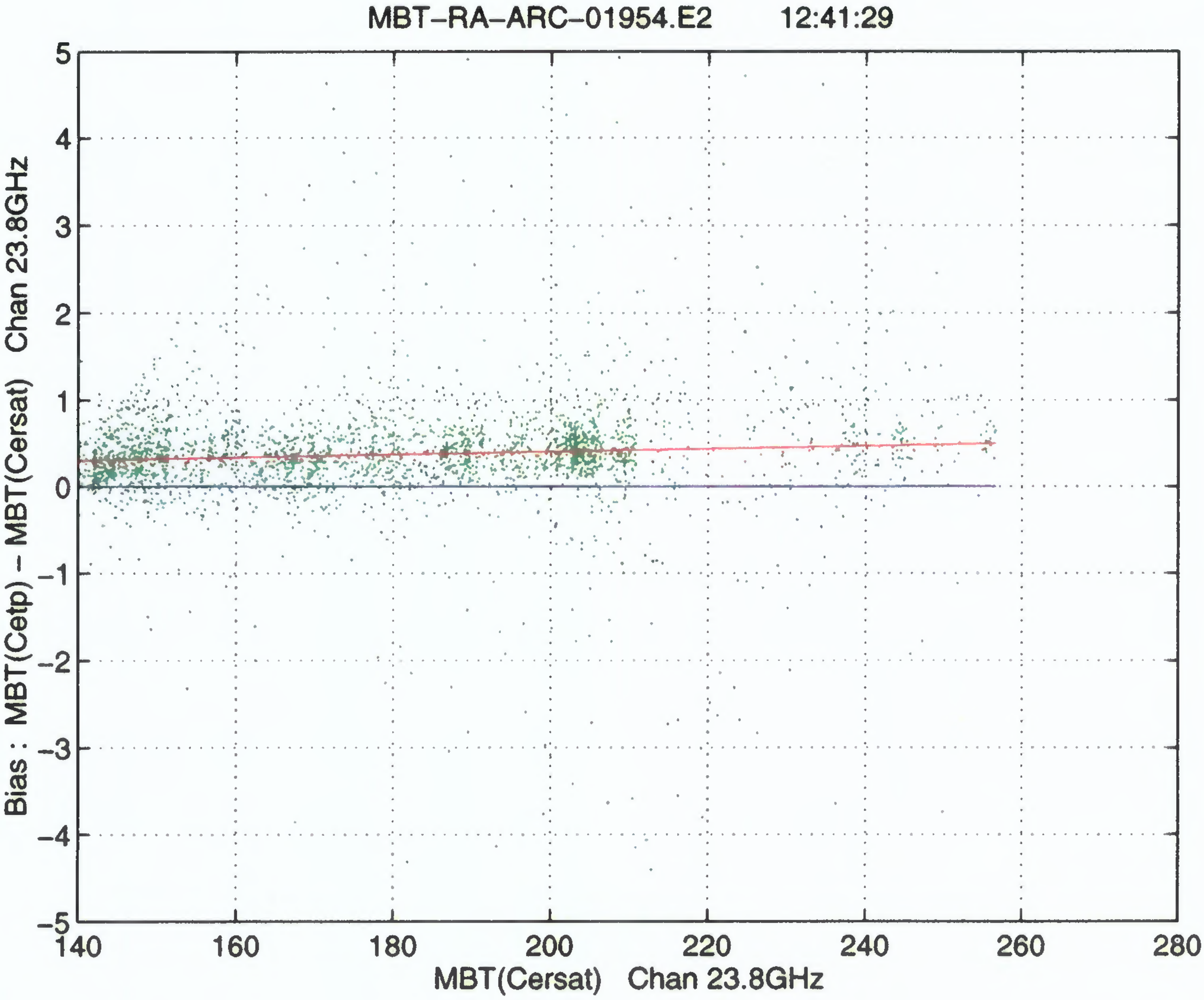

MBT-RA-ARC-01954.E2 12:41:29
Bias : MBT(Cetp) - MBT(Cersat) Chan 23.8GHz
MBT(Cersat) Chan 23.8GHz
5
4
3
2
1
0
-1
-2
-3
-4
-5
140
160
180
200
220
240
260
280

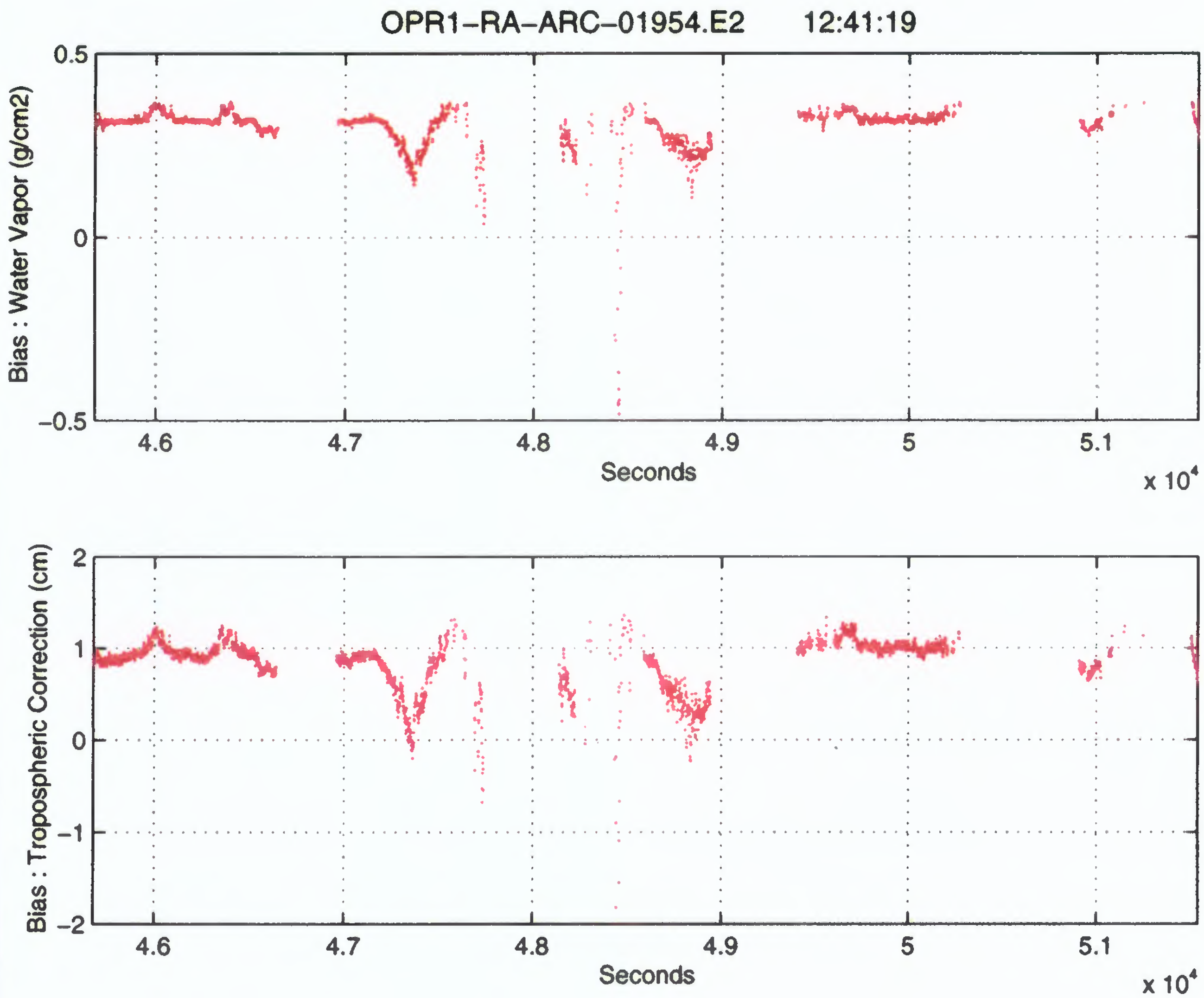
OPR1-RA-ARC-01954.E2 12:41:19
Bias : Water Vapor (g/cm2)
0.5
0
−0.5
4.6
4.7
4.8
4.9
5
5.1
Seconds
x 10^4
Bias : Tropospheric Correction (cm)
2
1
0
−1
−2
4.6
4.7
4.8
4.9
5
5.1
Seconds
x 10^4

OPR2-RA-ARC-01954.E2 12:41:19

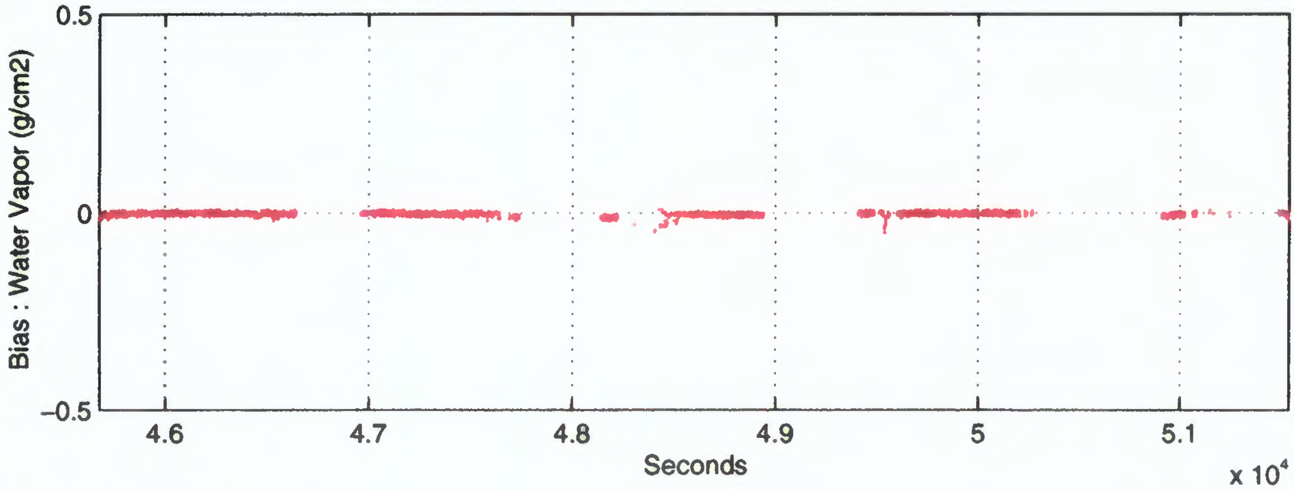

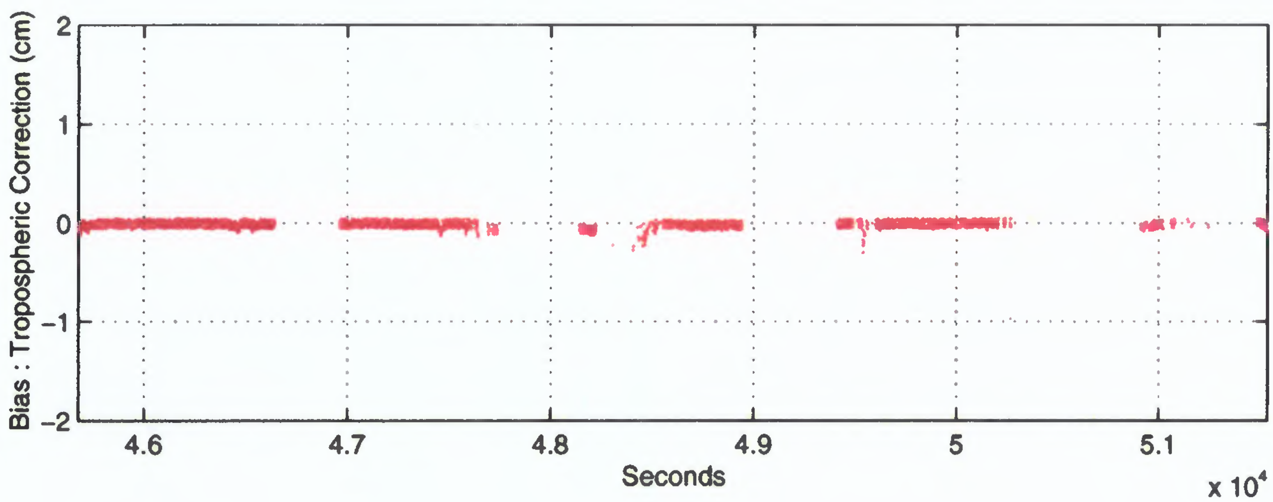

3.5 A comparison of ERS-2 OPR issued from software versions number 5 and software version 6

J. Stum, J.-P. Dumont, J. Durandeu, F.Ogor, P.-Y. Letraon, O.-Z. Zanifé and P. Gaspar

CLS

A comparison of ERS-2 OPR issued from software versions number 5 and software versions number 6

Jacques Stum, Jean-Paul Dumont, Joël Dorandeu, Francoise Ogor, Pierre-Yves Le Traon, Ouan-Zan Zanifé and Philippe Gaspar

CLS Space Oceanography Division, Toulouse, France

October 1996

1. INTRODUCTION

The results of the ERS-2 RA/MWR Calibration Working Group (CWG) were obtained with Ocean Products (OPR) processed with versions 5 of the radiometer and altimeter ground processing softwares. New software versions (version 6) are now operationally used by CERSAT to produce OPR. These new softwares should not be confused with the first release of the version 6 softwares used to process 5 ERS-2 cycles (number 2 to 6) which were distributed on CD-ROMs between February 1996 and June 1996. It has been shown that this first release of version 6 produced a too large number of zero significant wave heights (SWH) and contained an inaccurate radiometer calibration. These problems have been removed from the new version 6 softwares which results are analysed here.

As version 6 softwares include significant modifications relative to version 5, it is important to determine how these modifications affect the CWG results. This is the goal of this study. Notice however that this work was performed using a single repeat cycle of version 6 data (cycle 2 of ERS-2). The results obtained here thus need to be consolidated when more V6 data become available.

Section 2 of this report summarises the main modifications of version 6. The next sections are devoted to the comparison of the data produced with version 5 and 6 softwares

2. THE NEW OPR IN V6

As explained in a short note entitled « The new OPR software version 6 » (CLS.OC/NT.96.012, issue 1) sent to the OPR users, the OIP (altimeter instrumental level), MBT(radiometer instrumental level) and OPR (altimeter and radiometer geophysical level) softwares in version 6 include important modifications relative to version 5. These modifications impact on:

a) the altimeter range, significant wave height (SWH), backscatter coefficient (σ_o), and their respective standard deviations.
b) the radiometer wet tropospheric correction (through brightness temperatures calibration and new retrieval algorithm)
c) the altimeter sea surface height (through new ocean and loading tide model, and SSB change)

As previously mentioned, a first release of the version 6 softwares caused problems that requested:

- a modification of the OIP software to eliminate the problem that caused a too large number of zero wave heights
- a tuning of the MBT software to introduce a better radiometer calibration.

These changes finally led to the following version numbers for the threesoftwares :

- for ERS1 : OIP 6.3, MBT 6.5, OPR 6.2
- for ERS2 : OIP 6.3, MBT 6.4, OPR 6.2

In the rest of this report we will constantly refer to these softwares as V6 softwares. Accordingly, the version 5 softwares, used to produce the OPR data that were analysed by the CWG, will be referred to as V5 softwares.

For the sake of completeness we shall mention that the first (problematic) release of the version 6 softwares included OIP 6.2, MBT 6.2 and OPR 6.1. We will not further comment on this as the 5 ERS-2 cycles that were produced with these software versions will be reprocessed with V6. There have been no ERS-1 data released with these problematic software versions.

2.1 MODIFICATIONS IMPACTING ON ALTIMETRIC ESTIMATES

We recall here the major differences between the products issued with V5 and V6 softwares. The OPR user is referred to the Altimeter and Microwave Radiometer ERS Products User Manual (Version 2.1) for more details.

a) Correction of the on-board anti-aliasing filter effects

Anti-aliasing filtering is applied on-board before performing the FFT (which outputs waveforms), to account for the periodicity of the discrete Fourier transform. Waveforms are affected by the imperfections of this filtering (i.e. ripples, global slope, etc.). Up to V5, the effect of these imperfections on the altimeter range estimates was corrected using a look-up table deduced from simulations (see field H_Alt_Lut_Cor in the User Manual). In V6, the correction is applied to the waveforms themselves. This correction is directly deduced from a pre-launch measurement of the filter shape.

b) Waveforms retracking

The retracking algorithm deduces the altimetric parameters from the waveforms. It provides precise estimates of the altimeter range, SWH and σ_o. The estimation is an iterative process performed by fitting the measured waveform with a mean return power model, using Maximum Likelihood Estimators. Up to V5, the curvature effects of the earth in the footprint were not accounted for. In V6, this approximation is removed, i.e. the earth curvature effects are taken into account through the echo model expression. Also, the loop gain of the iteration algorithm is increased to improve convergence.

c) Refinements of instrumental parameters

The following parameters have been updated in V6 for ERS-2 data processing:

- Field H_Alt_COG_Cor : distance between the antenna reference for the altimeter range measurement and the satellite centre of gravity (accounting for its final precise value). Its value was 85.83 cm for V5. It is 83.78 cm in V6.
- Field Sigma0_Bias : engineering calibration correction added to σ_o (removal of the relative bias with respect to ERS-1 σ_o). Its value is -3.9 dB.

2.2 MODIFICATIONS IMPACTING ON RADIOMETER WET TROPOSPHERIC CORRECTION

In V6, ERS-1 and ERS-2 brightness temperatures (23.8 and 36.5 GHz) have been tuned to account for the latest CETP results on radiometer calibration (Boukabara and Eymard, 1996). The wet tropospheric correction is computed from the brightness temperatures by using a new retrieval algorithm.

2.3 MODIFICATIONS IMPACTING ON SEA SURFACE HEIGHT

a) Ocean tide

In V6, the ocean tide is computed using the FES95.2.1 hydrodynamic model of Le Provost et al.(1994)

b) Tidal loading

In V6, the tidal loading is recomputed according to Francis and Mazzega (1990), using the FES95.2.1 tidal model.

c) Sea state bias

The V5 OPRs feature the Barrick and Lipa (1985) sea state bias (SSB) correction. In V6, the SSB correction is equal to -5.5% of SWH. This is the correction recommended by Gaspar and Ogor (1994) based on the analysis of 18 cycles of ERS-1 V5 OPRs.

3. IMPACT ON RANGE

Figure 1 shows the histogram of the V6-V5 range differences, for ERS2 cycle 2. The mean difference is -38 mm ± 12 mm. As V6 includes an updated value for centre of gravity offset (83.78 cm instead of 85.83 cm for V5, see section 2.1c), the real mean range difference induced by the new altimeter processing is -17.5 mm ± 12 mm. Histogram assymetry is due to the change in range dependency with SWH induced by the V6 modifications listed in section 2.1. For example, implementing only the curvature effects of the earth in the altimeter footprint would decrease the altimeter range of about 1% of SWH (i.e., 2 cm for SWH = 2 m), a non-gaussian modification since the SWH distribution is notgaussian.

Figure 2 shows the V6-V5 range difference, plotted as function of SWH (top), and wind speed (bottom). The variations of the range difference as a function of SWH and wind speed are very weak. Deviations from the mean value (38 mm) are generally below 5 mm. A fraction of it can probably be attributed to sea state bias differences between V5 and V6.

Figure 3 shows the histogram of the range standard deviation for V5 (top) and V6 (bottom). Clearly, the 20-Hz range estimates are noisier in V6 than in V5 (peak at 13.5 cm for V6, 11.5 cm for V5). Note also that the scatter around the peak is increased in V6. The same patterns are also observed for the significant waveheight standard deviation. Fine analysis of this behaviour showed that the increased noise is mainly due to the application of the anti-aliasing filter at the waveforms level (described in section 2.1a), and to a less extent, to higher decorrelation of individual 20-Hz estimates consecutive to a better convergence of the retracking algorithm (see section 2.1b).

The noise level of the 1-Hz range estimates was then estimated using power spectra of collinear sea surface height differences between two consecutive ERS-2 cycles (cycle 2 and 3). As V6 OPR for cycle 3 was not available at the time of this study we actually used the range data obtained with the first release of the version 6 softwares. This is legitimate because the range values are virtually unaffected by the software modifications that led from the first release of version 6 to V6.

Spectra were computed for nearly 3000 pairs of arcs of about 2200 km. These spectra were averaged to produce Figure 4. Power spectral density in cm^2/cy.km is plotted versus wavenumber in km^{-1}. The V5 and V6 spectra exhibit the same variations of power density as a function of wavenumber. In particular, in the low wavelength (high wavenumber) portion of the spectrum, the values are identical, showing that the 1-Hz range noise is the same for both versions. The exact noise level is difficult to estimate, because the noise floor is not clearly visible : the noise floor spectral density value is about 300 cm^2/cy.km. Then, the noise level is obtained by integrating this value of the spectral density over the frequency domain, and dividing the result by $\sqrt{2}$ (because SSH differences are between two repeat cycles) :

$$(\text{Noise})^2 = [300 \times (1/\lambda_1 - 1/\lambda_2)] / \sqrt{2}$$

where λ_1 is twice the shortest observable wavelength (about 13 km), and λ_2 is the longest wavelength (about 2200 km). This calculation leads to a noise value of about 3.4 cm. It is also important to notice that since the 1-Hz range noise is the same in V5 and V6:

$$\text{20-Hz V6 range variance}/N(V6) = \text{20-Hz V5 range variance}/N(V5) = \text{1 Hz range variance}$$

where N is the number of non correlated elementary (20-Hz) measurements. Using the range variance estimate given above one obtains:

$$(13.5)^2/N(V6)=(11.5)^2/N(V5)= (3.4)^2$$

This yields $N(V6) \approx 16$ and $N(V5) \approx 11$. Thus, among the 20 elementary measurements used in average to compute the 1-Hz measurement, about 16 are non correlated in V6, whereas about 11 were non correlated in V5.

4. IMPACT ON SIGNIFICANT WAVE-HEIGHT

Figure 5 shows the SWH histogram for V5 (top) and V6 (bottom). The zero wave heights have been removed from the plot. This population actually corresponds to negative SWH values provided by the retracking algorithm and then arbitrarily set to zero in the OPR. For ERS-2 cycle 2, V5 generated 15217 measurements (1.1%) with SWH = 0. V6 only generates 2807 (0.2%) such measurements. The first release of version 6 software generated as many as 63171 zero values (4.5 %).

The comparison of the V6 and V5 SWH histograms shows that V6 yields a smaller number of low wave heights, and a larger number of high wave heights. This is further quantified in figure 6. This figure shows the V6-V5 SWH difference plotted versus SWH(V6). The average difference is 19 cm but this difference exhibits marked variations as a function of SWH. The difference is minimum (12 cm) for SWH = 1.4 m, but reaches values as high as 30 to 35 cm at large wave heights. The shape of the difference is also very characteristic. It largely explains the fact that all SWH calibration studies performed with SWH(V5) values show the need to use different calibration relations for SWH below and above (about)1.5 m. For example, Queffeulou (1996) compared TOPEX wave heights with ERS-2 V5 wave heights. He found the following relations between the two:

for SWH < 1.5 m : SWH(TOPEX) = 0.90 x SWH(V5) + 0.35 (1)
for SWH > 1.5 m : SWH(TOPEX) = 1.075 x SWH(V5) + 0.10 (2)

On the other hand, figure 6 shows that the V6-V5 SWH difference is well fitted by straight lines in the range [0.5, 1.5 m] and [1.5, 6 m]. Linear regressions yield:

for 0.5 m < SWH < 1.5 m : (V6-V5) SWH difference = -0.139 x SWH(V6) + 0.305 (3)
for 1.5 m < SWH < 6 m : (V6-V5) SWH difference = 0.046 x SWH(V6) + 0.063 (4)

The differences for SWH<0.5 m were not considered as they are mostly differences between small SWH(V6) values and SWH(V5) values that were arbitrarily set to zero. Also, fitting was not performed for SWH > 6 m because the slope of the V6-V5 difference clearly changes at such high SWH value. Notice that SWH values above 6 m are very few (only 2.1% of the data set).

Using (3) and (4) to express SWH(V5) as a function of SWH(V6) and then introducing the result in (1) and (2) one obtains:

for SWH < 1.5 m : SWH(TOPEX) = 1.025 x SWH(V6) + 0.075 (5)
for SWH > 1.5 m : SWH(TOPEX) = 1.026 x SWH(V6) + 0.032 (6)

This shows that the slopes of the regression lines below and above 1.5 m are now virtually identical and close to 1. Even the intercept is very small (between 3 and 8 cm). The new SWH(V6) values thus seem to be in excellent agreement with TOPEX measurements. Of course, this little algebraic calibration exercise only provides a crude approximation of the actual relation between SWH(TOPEX) and SWH(V6). Direct intercalibration between ERS2 and TOPEX data is needed to precisely assess this relation. This is done by P. Queffeulou (see **annex TBD)**

5 - IMPACT ON SEA STATE BIAS

The Sea State Bias (SSB) associated with V5 range measurements was estimated by several CWG teams. The estimation was obtained using the simplest linear model in which the SSB is expressed as a constant fraction of SWH:

$$SSB = b\ SWH$$

The parameter b is classically determined by a simple regression, to minimize the variance of the crossover or collinear differences. As part of the commissioning activities performed at CLS, Dorandeu and Stum (1996) estimated b = -0.056, based on the analysis of 4 ERS-2 cycles (cycles 1 to 4). Estimates of b obtained with the same data by different CWG members are generally in the range -0.05 to -0.06 (that is -5 to -6 % of SWH). This variability in the SSB estimates is essentially due to slight differences in the data editing and data processing performed by the different groups. To avoid such differences we applied exactly the same processing to V5 and V6 data. We obtained the following regression results based on the minimisation of the cycle 2 crossover differences :

V5 : SSB = -0.0597 SWH
V6 : SSB = -0.0587 SWH

The V6 estimate thus appears to be 0.1 % of SWH above the V5 estimate.

We also performed the following regression:

$$DR = c\ SWH + e$$

where DR is the V6-V5 range difference. This regression yields c = -0.0005, that is only -0.05 % of SWH. Looking at figure 2 (top) where DR is plotted as a function of SWH, such a very low linear correlation coefficient between DR and SWH is no surprise.

The SWH-correlated fraction of DR is the difference SSB(V5) - SSB(V6) (watch the sign !). Therefore, the regression result implies

$$SSB(V6) = SSB(V5) + 0.05\ \%\ of\ SWH$$

This further suggests that the SSB is a bit less negative in V6 than in V5. The difference in the estimated value of b is nevertheless very small: between 0.1 % and 0.05 % of SWH depending on the estimation method. Such a difference is, by no means, significant. We can thus reasonably assume that the SSB is well represented by the same constant fraction of SWH in V5 and V6. The value of this constant must be precisely estimated using more data cycles

Finally, it is worth mentioning that, even if the estimated value of b is the same for V6 and V5, the mean value of SSB is different because the mean values of SWH are different:

$$\langle SSB(V6) - SSB\ (V5)\rangle = b\ \langle SWH(V6) - SWH(V5)\rangle$$

where $\langle\rangle$ denotes an average. As indicated in section 4, $\langle SWH(V6) - SWH(V5)\rangle = 19$ cm. Taking b = -0.055, one obtains :

$$\langle SSB(V6) - SSB\ (V5)\rangle \approx -1 \text{ cm.}$$

This means that, if a SSB of -5.6 % of SWH is applied to both V5 and V6 range data, the corrected range bias (V6-V5) will be equal to the uncorrected range bias minus 1 cm.

6- IMPACT ON BACKSCATTER COEFFICIENT

Figure 7 shows the V6-V5 σ_o difference, plotted versus σ_o(V6). The V6-V5 difference is extremely stable, always remaining between -3.96 and -4 dB. As explained in section 2.1c, a bias of -3.9 dB had been added to σ_o(V6). Figure 7 essentially reveals this bias plus very small retracking effects that modify the σ_o values by less than 0.1 dB.

7-.IMPACT ON RADIOMETER WET TROPOSPHERIC CORRECTION

In V6, the revised calibration of CETP (Boukabara and Eymard, 1996) is used for ERS-1 and ERS-2. Figure 8 shows the comparison between ERS-1 and TOPEX (top) and ERS-2 and TOPEX (bottom) wet tropospheric corrections at crossovers with less than 1-hour time lag. The comparison was made using ERS data obtained during TOPEX cycles 101 to 105. The two ERS radiometers are now in very good relative agreement.

The means of the ERS-2 cycle 2 radiometer wet tropospheric correction for V5 and V6 are:

Mean (V5) = 15.93 cm
Mean (V6) = 15.88 cm

The difference is thus only 0.5 mm. For the ERS-1 radiometer, the slight change introduced in V6 relative to V5 (see the quality assessment reports) has no impact on the mean tropospheric correction. Consequently, the wet tropospheric correction change from V5 to V6 has no significant effect on the ERS-1/ERS-2 relative range bias (i.e. the effect is well below the millimetre level).

8 - CONCLUSIONS

This comparison study between V5 and V6 OPR has been carried out on a limited amount of data (one ERS-2 35-day cycle). The main results are:

- The altimeter range in V6 is (on average) 17.5 mm shorter than in V5. This combines with a -20.5 mm change of the centre of gravity offset to yield a net V6-V5 bias of -38 $\pm$ 12 mm.

- The 20-Hz range standard deviation in V6 is about 18% greater than in V5, due to the application of the anti-aliasing filter at the waveform level. Still, the 1-Hz standard deviation is virtually unchanged (about 3.4 cm) as the elementary range measurements are better decorrelated in V6.

- The difference σ_0(V6)-σ_0(V5) is nearly equal to -3.9 dB, the calibration bias that was added to σ_o(V6). Deviations from this mean difference are generally negative but very small (always between 0 and -0.1 dB)

- SWH is, by far, the most affected parameter. The number of zero wave heights is reduced from 1.1% in V5 to 0.2 % in V6. SWH values are generally larger in V6 (+19 cm in average) but the difference SWH(V6) -SWH(V5) is largely variable. It is minimum (12cm) for SWH = 1.4 m, reaches 25 cm at low wave heights, and goes up to 30 to 35 cm for SWH > 6 m. These variations largely explain why different SWH calibration relations had to be used for SWH values below and above 1.5 m. Our preliminary analysis indicates that the calibration relation between SWH(TOPEX) and SWH(V6) should no longer be discontinuous at (about) SWH = 1.5 m.

- The sea state bias appears to be well estimated by the same constant fraction of SWH (-5 to -6 % of SWH) in both V5 and V6. Still, as SWH is on average 19 cm larger in V6, the mean SSB should be 1cm larger (more negative) in V6.

- The ERS-1 and ERS-2 radiometer wet tropospheric correction in V6 have been compared to TOPEX data and are now in good relative agreement. The change from V5 to V6 has no impact on the ERS-1/ERS-2 relative bias.

Finally, it is worth mentioning that this work focused on ERS-2 V6 data only. No ERS-1 V6 data was available when this study was completed and, accordingly, no direct intercalibration between ERS-1 and ERS-2 V6 data was performed. Even if the V5 to V6 software modifications are the same for ERS-1 and ERS-2, different instrumental characteristics (like filter shape and point target response) of the two altimeters may induce slightly different reactions to these software changes. The impact of V6 on ERS-1 data shall thus be assessed separately.

REFERENCES

Barrick, D.E., and B.J. Lipa, 1985: Analysis and interpretation of altimeter sea echo. Adv. Geophys., **27**, 61-99.

Boukabara, S, and L. Eymard, 1996 : Calibration/Validation of the ATSR/M and MWR2 products. Update. July 1996.

Dorandeu, J. and J. Stum, 1996: CLS contribution to the ERS-2 radar altimeter range bias determination using OPR2. Study report for ESA Purchase Order N°143187.

Francis, O., and P. Mazzega, 1990: Global charts of ocean tides loading effects. J. Geophys. Res., **95**, 11411-11424.

Gaspar, P., and F. Ogor, 1994: Estimation and analysis of the sea state bias of the ERS-1 altimeter. CLS Technical Report for IFREMER contract N°94/2.426 016/C.

Le Provost, C., M.L. Genco, F. Lyard, P. Vincent and P. Canceil, 1994: Spectroscopy of the world ocean tides from a finite element hydrodynamic model. J. Geophys. Res., **99**, 24777-24797.

Queffeulou, P., 1996: Significant wave height and backscatter coefficient at ERS1/2 and TOPEX-POSEIDON ground-track crossing points-OPR. IFREMER final report for ESA contract N°143189

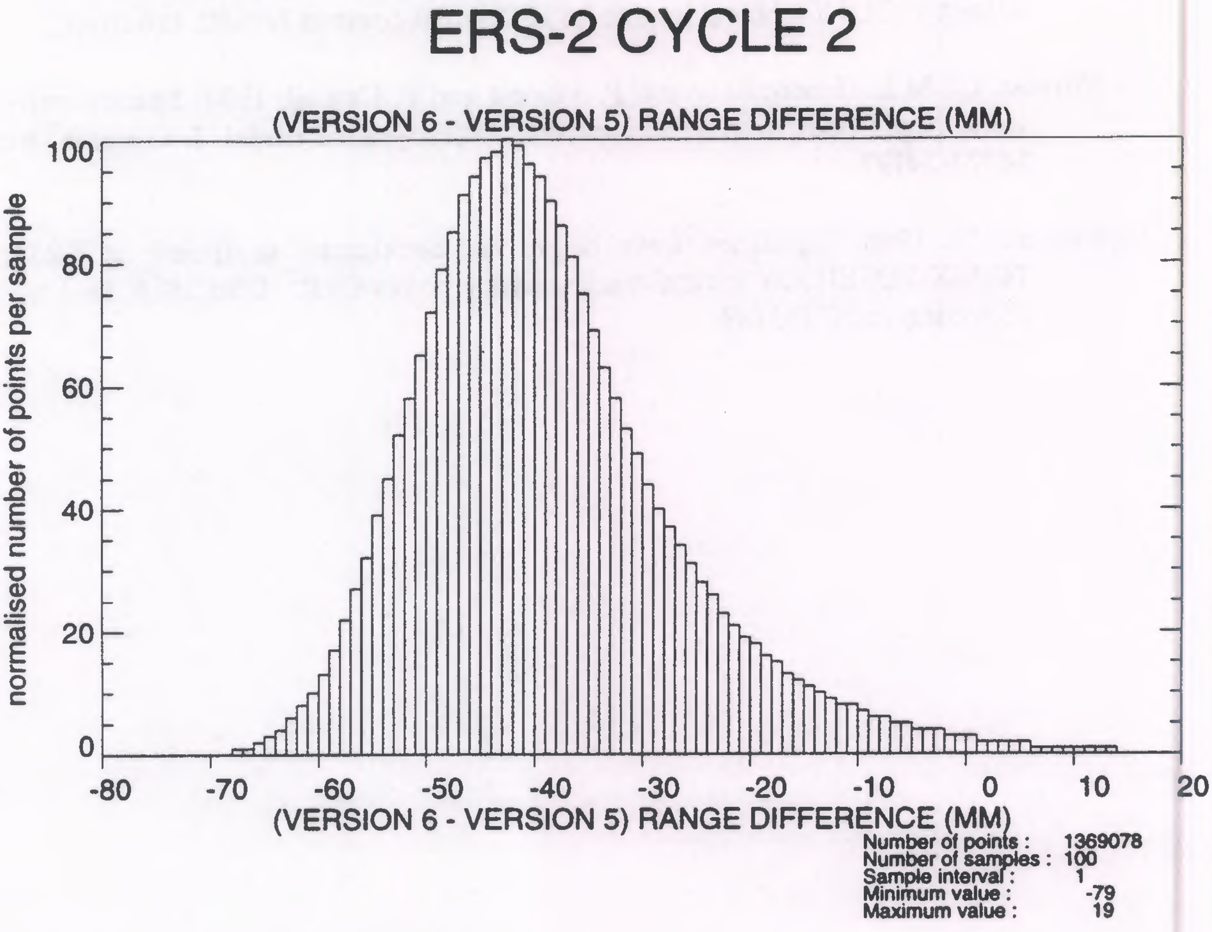

FIGURE 1 : Normalised histogram of the (V6-V5) range difference in mm. "Normalised" means that the number of data in each class is divided by the number of data found in the most populated class and is expressed in percent of that maximum number.

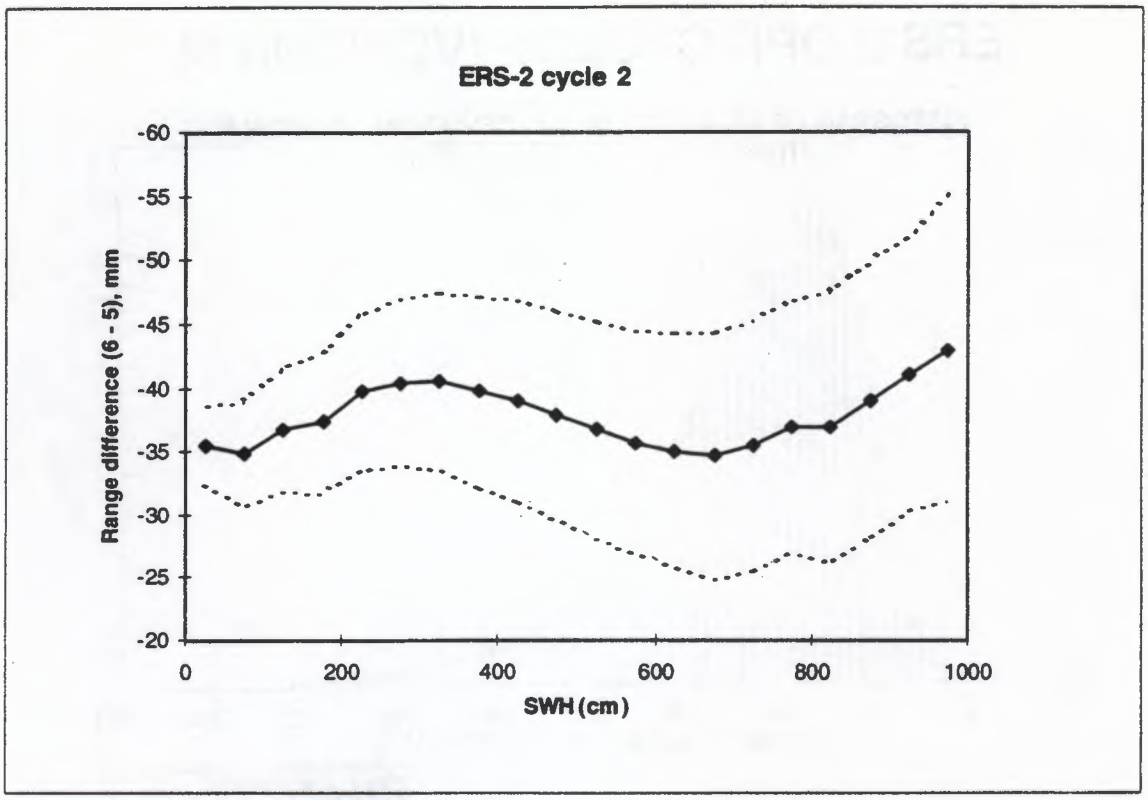

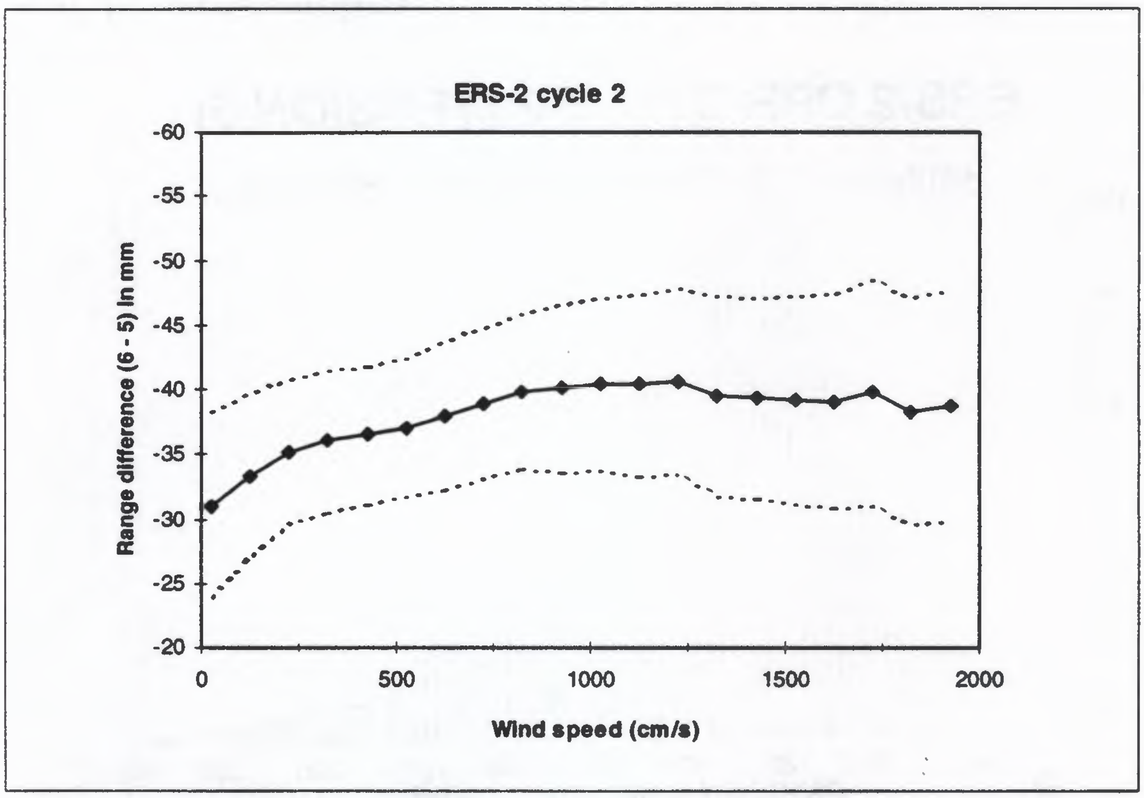

FIGURE 2 : (V6 - V5) range difference, versus SWH (top), and wind speed (bottom). The black diamonds show averages computed on SWH bins of width 0.5 m (top) and on wind speed bins of width 0.5 m/s (bottom). In each plot, the dotted upper and lower curves represent the mean difference± one standard deviation.

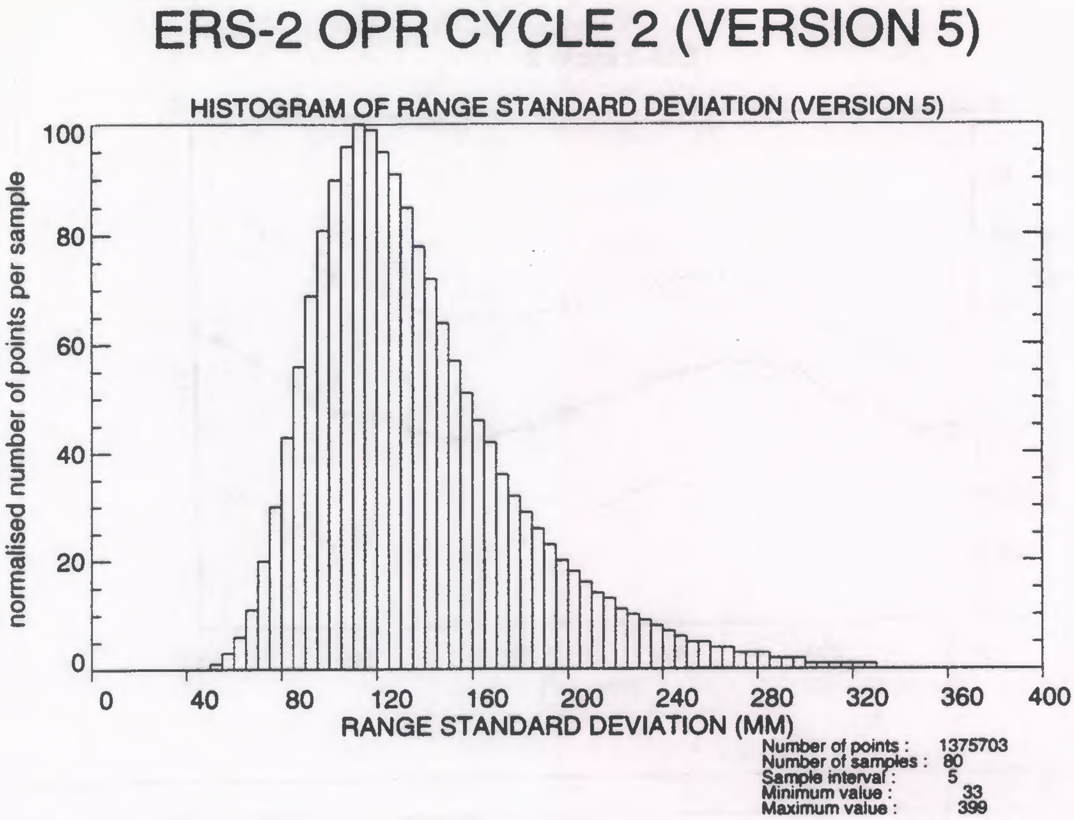

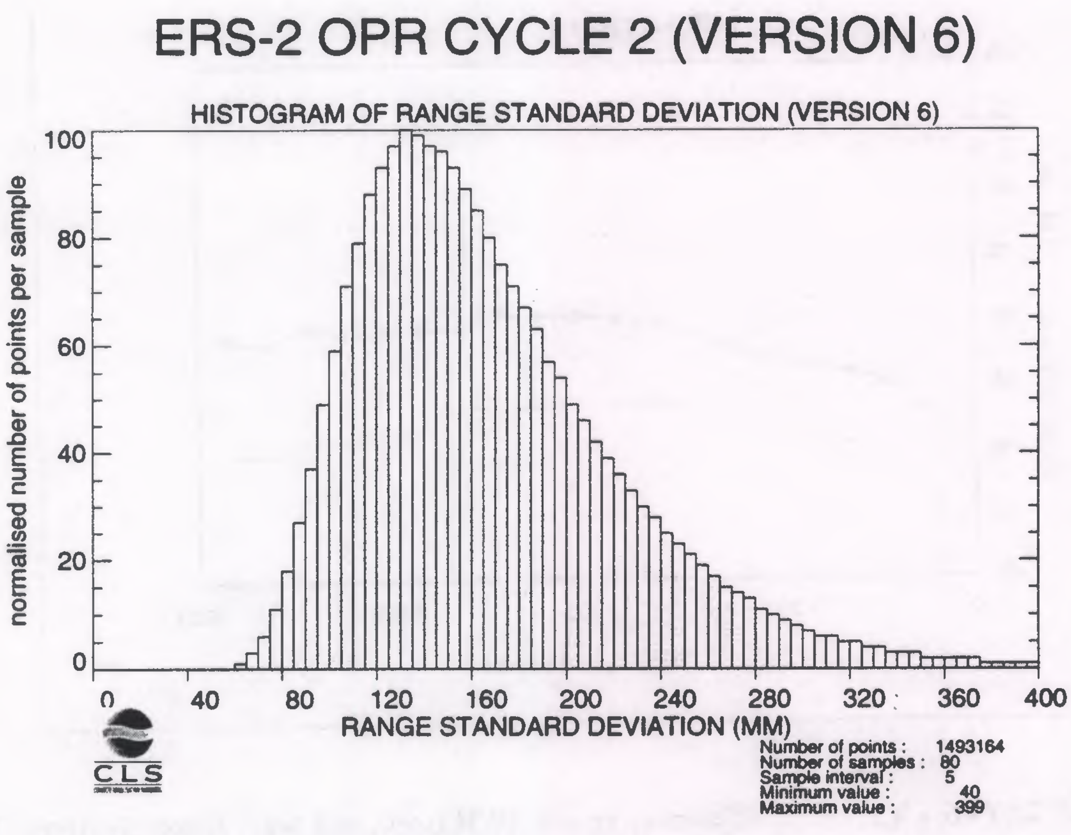

FIGURE 3 : Normalised histogram of range standard deviation (mm), for V5 (top), and V6 (bottom).

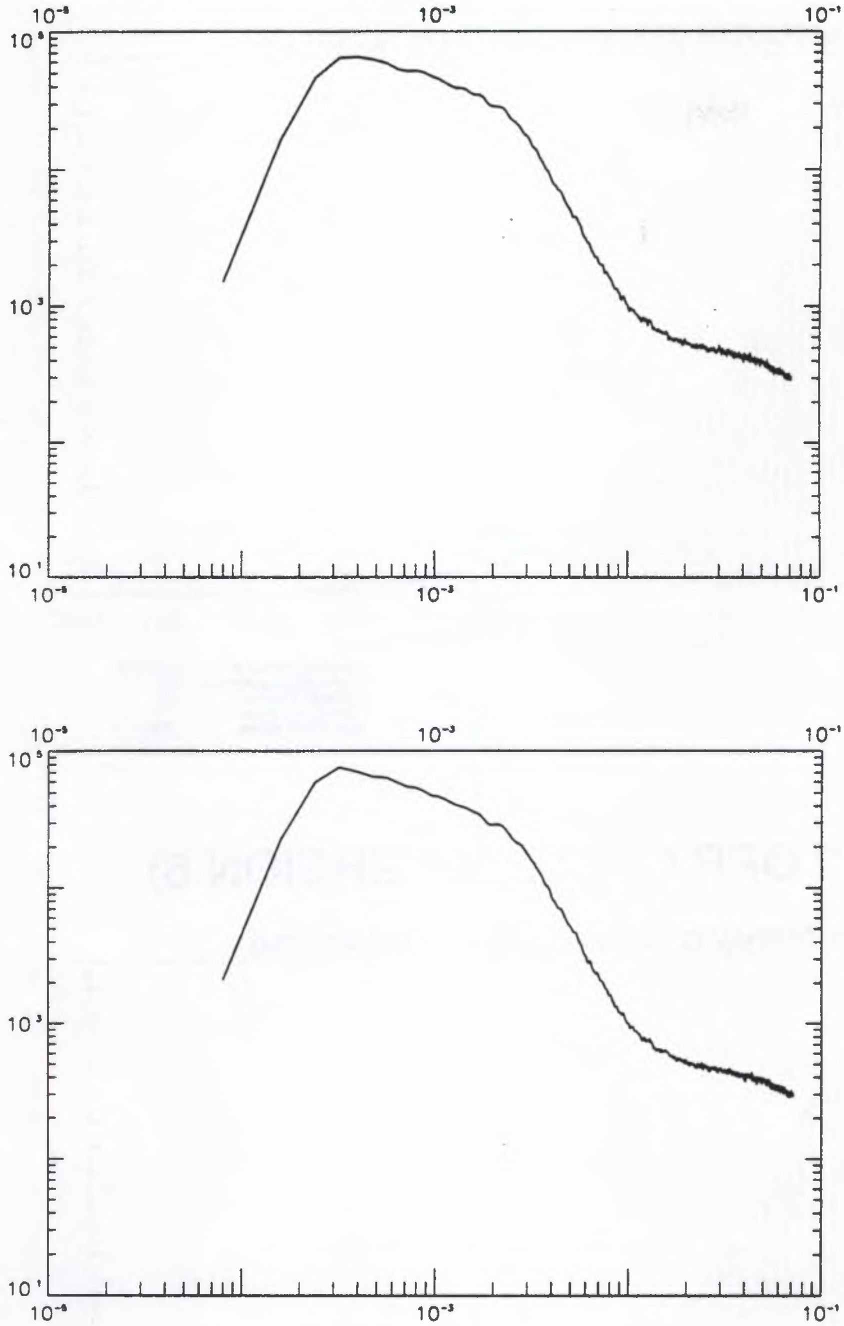

FIGURE 4 : Power spectral density (cm^2/cycle.km), versus wavenumber (km^{-1}), computed from (cycle 3 - cycle 2) collinear differences, for V5 (top), and V6 (bottom)

ERS-2 OPR CYCLE 2 (VERSION 5)

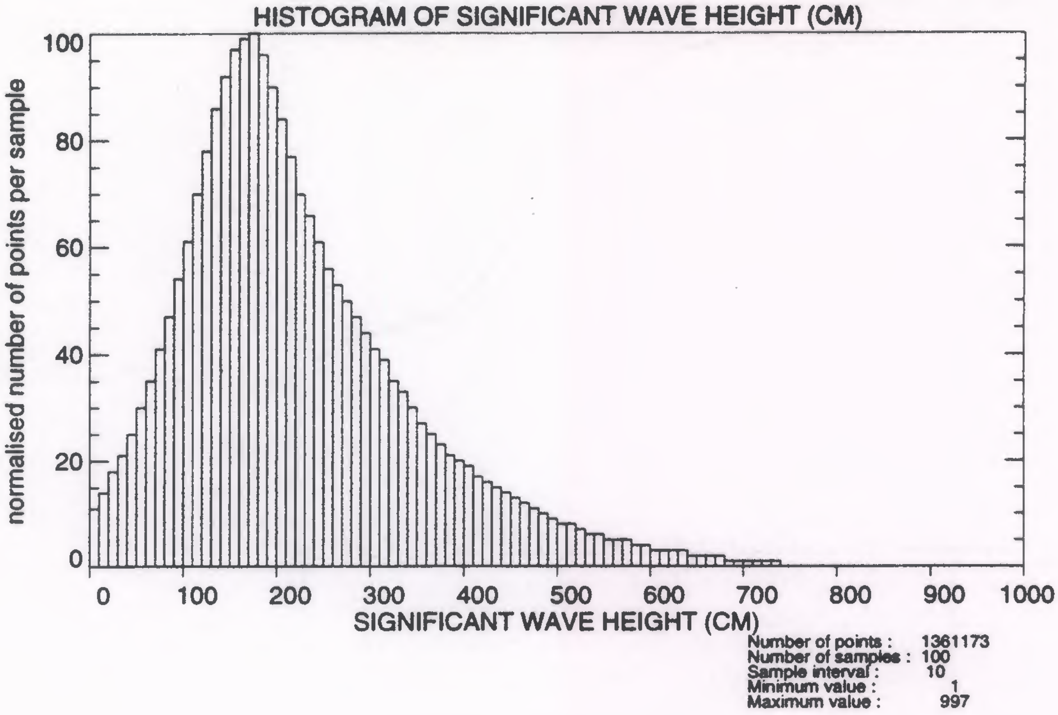

ERS-2 OPR CYCLE 2 (VERSION 6)

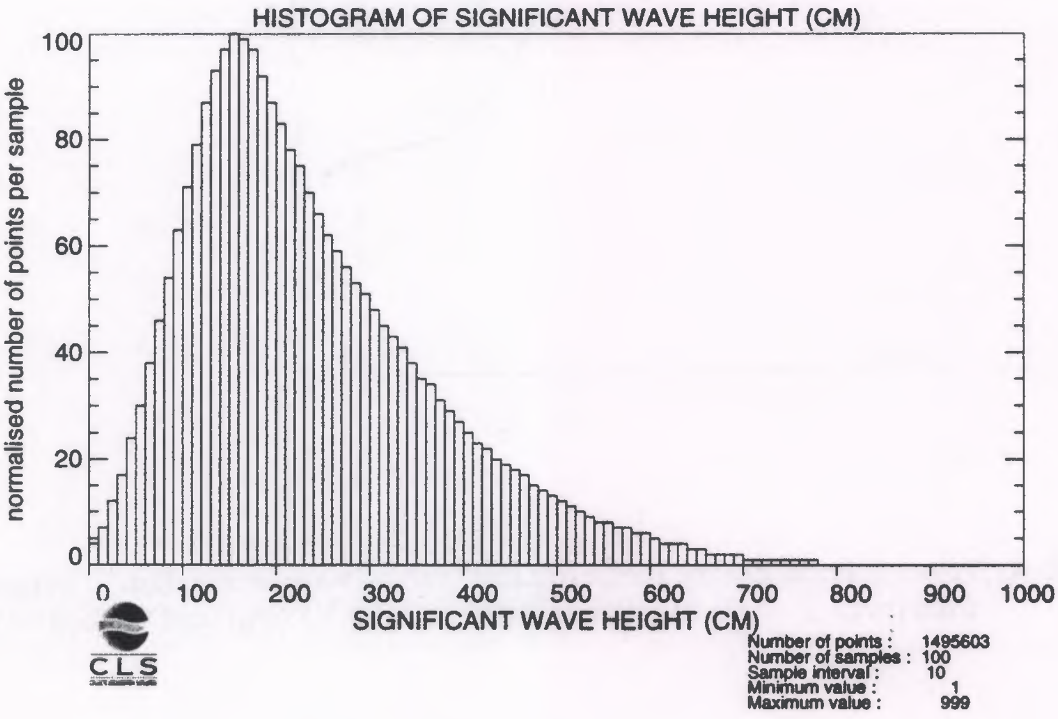

FIGURE 5 : Normalised histogram of SWH, for V5 (top), and V6 (bottom).

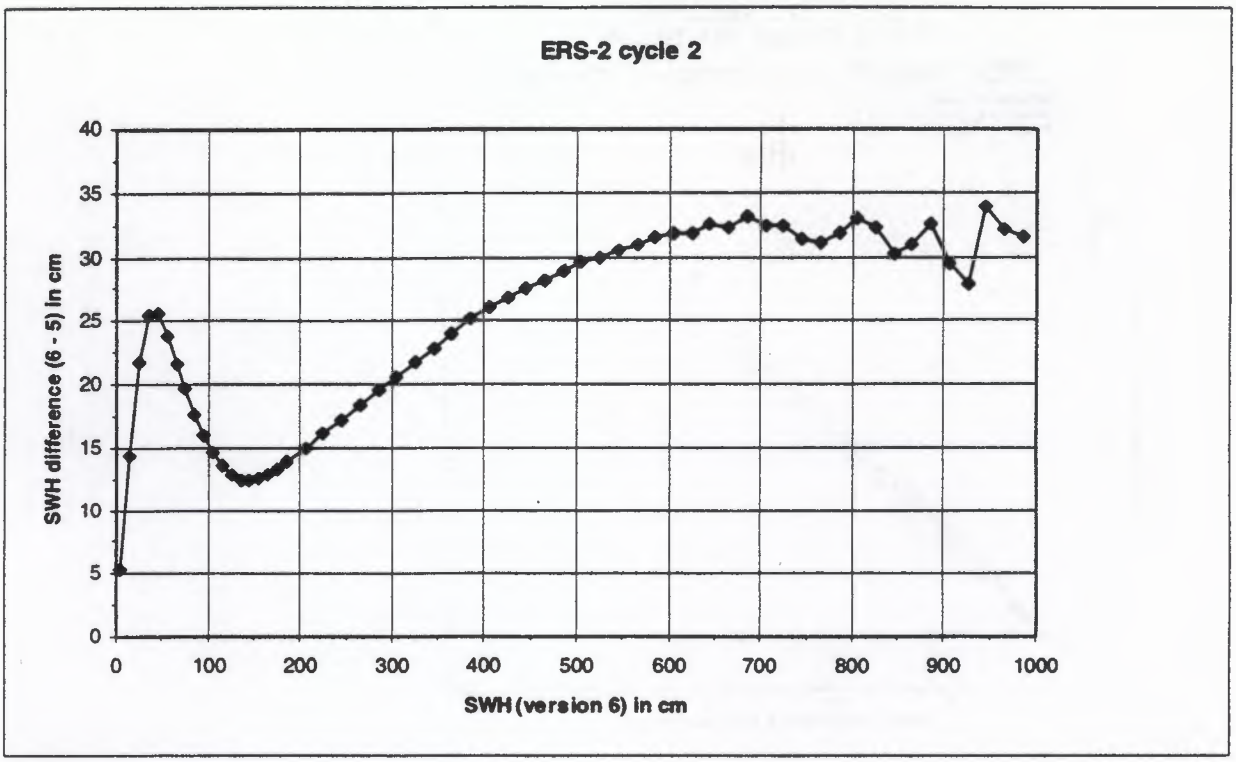

FIGURE 6 : SWH difference (V6 - V5), versus SWH (V6). . Differences are averaged over SWH bins of 0.1m width.

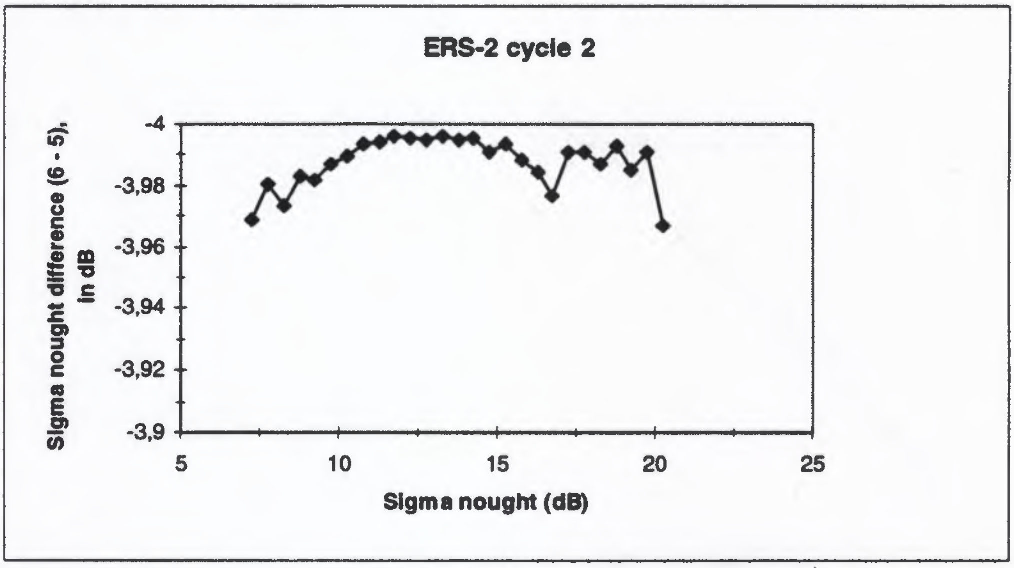

FIGURE 7 : σ_0 difference(V6 - V5) versus σ_0(V6). Differences are averaged over σ_o bins of 0.5 dB width.

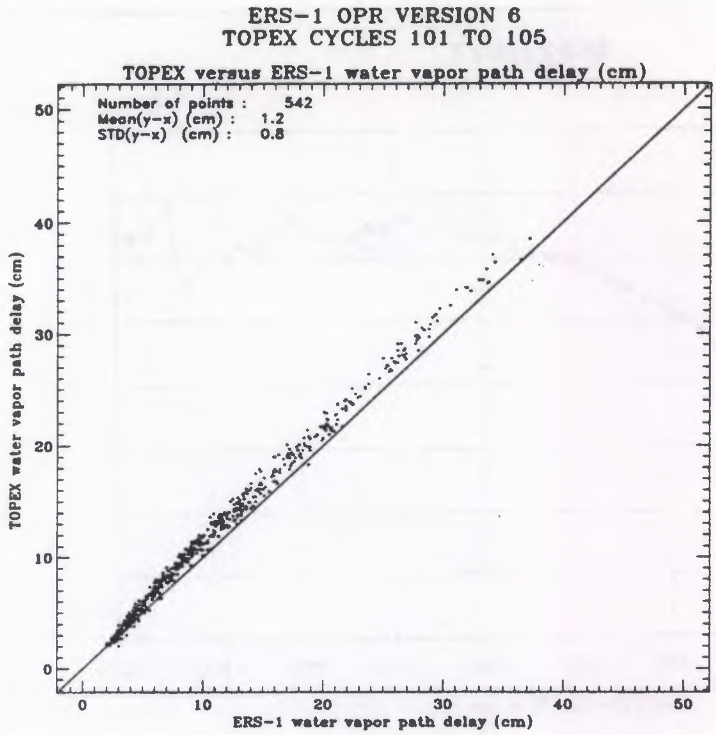

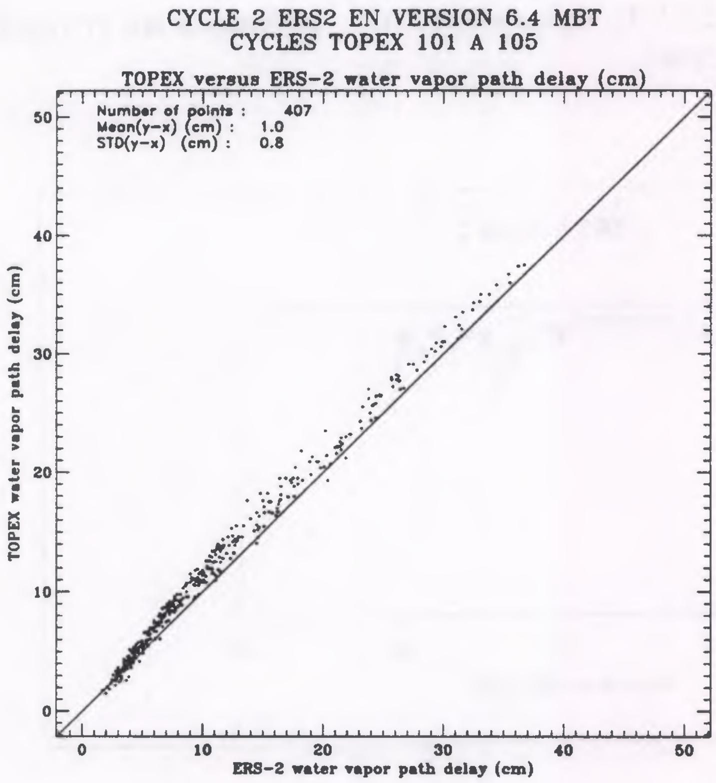

FIGURE 8 : TOPEX water vapour path delay (cm), versus ERS-1 (top) and ERS-2 (bottom) water vapour path delay. ERS data corresponding to concurrent TOPEX cycles 101 to 105. Each dot corresponds to a TOPEX/ERS crossover point having less than 1 hour time lag.

3.6 ERS-2 OPR version 6.3 validation: Comparison of ERS-2 and Topex SWH and Sigma0 measurements

P. Queffeulou

IFREMER

**ERS-2 OPR version 6.3 validation.
Comparison of ERS-2 and TOPEX
swh and sigma0 measurements.**

Pierre Queffeulou

Département d'Océanographie Spatiale
IFREMER
BP 70, 29280 Plouzané, France
tel (33) 98 22 42 94, e-mail pierre.queffeulou@ifremer.fr

31 October 1996

1 Introduction

The first validation of ERS-2 OPR *swh* and σ_0 was performed during the commissioning phase. The tested data set corresponded to the version 5 of the OPR processing. Results from the work of the ESA calibration validation group (ref. 1 and 2) indicate that the ERS σ_0 measurement was almost satisfying, while the *swh* measurement suffered from a significant underestimate, larger for ERS-1 than for ERS-2, and that two rates of underestimate appeared according to a *swh* threshold at low sea state (about 1.0 m to 1.5 m). Furthermore, significant increase of ERS measurement variability was found at low sea state.

A new version (6.0) of OPR ERS altimeter processing was then implemented. Main algorithm changes concerning *swh* and σ_0 altimeter estimates are given in ref. 3. Statistical study of this version, on *swh* and σ_0 (ref. 4), concluded in:

- no significant change in σ_0 estimates
- a significant increase of the standard deviation of the *swh* estimate, particularly at low sea state
- a drastic increase (by a factor about 3) of the number of valid data for which *swh* is set to zero (corresponding to negative *swh* estimate)
- this last effect occuring mainly at low wind and waves, the impact over some areas is very strong. For the Mediterranean Sea, for instance over 33 days, the percentage of such zero *swh* data increases from 17% in v.5 to 44% in v.6
- increase of *swh* estimates at medium to high sea state. This is an improvement relative to the previous version, that was shown to underestimate high *swh*.

Then modifications were done by CLS to the waveform retrieval algorithm, resulting in a a new OPR version: 6.3. Improvement of this new version, relative to the previous one, was shown on the statistics (ref 5):

- a decrease of the number of zero *swh* cases
- an increasae of *swh* estimates at both low and high values of *swh*
- a slight decrease of *swh* estimate standard deviation, for the lowest sea states
- but inversely (and this is not an improvement) an increase of *swh* estimate standard deviation at high sea states.

Hereunder the ERS-2 OPR data from the v6.3 version are compared to the TOPEX measurements in the same way as in the previous studies dedicated to v5, during the commissioning phase.

2 The collocation procedure

The collocation procedure is the same as in ref. 2 and is briefly described. First, data from ERS-2 and TOPEX are collocated in selecting altimeter ground track crossing points within 1 hour. Average values of *swh* and σ_0 are then constructed taking along track data within 50 km each side of the crossing point. Cases are selected when all the data within this limit are valid:

- considered as valid (bit 0 of MCD)
- quality flag of *swh* estimate set to 0 (bit 7)
- quality flag of σ_0 estimate set to 0 (bit 8)
- $Nval \geq 17$. $Nval$ is the number of 20 Hz elementary measurements used for computing the 1 Hz estimate. Nominal value is 20, and Nval is equal to 17 for internal calibration sequences.

This results in averaging, for each selected crossover, 15 and 17 1s measurements for ERS-2 and TOPEX respectively. Considering only the cases for which all the data within 100 km are valid significantly reduces the scatter in the data.

According to the status of ERS processing in CERSAT at the present time of this report, the following periods were selected:

- a first one gathering data from 19/06/95 to 21/07/95 and from 11/12/95 to 04/04/96, corresponding to TOPEX cycles 101 to 104, and 119 to 130 for OPR version v6.3
- a second one, from 21/07/95 to 06/11/95, corresponding to TOPEX cycles 105 to 115, and relative to OPR version v6.0.

3 Results for SWH

The v6.3 data set consists of 1375 crossovers. Improvement of the version v6.3 processing appears in figure 1, comparing v6.0 and v6.3 results relative to TOPEX. The main improvement is observed at low *swh*. Statistical results are given in table 1.

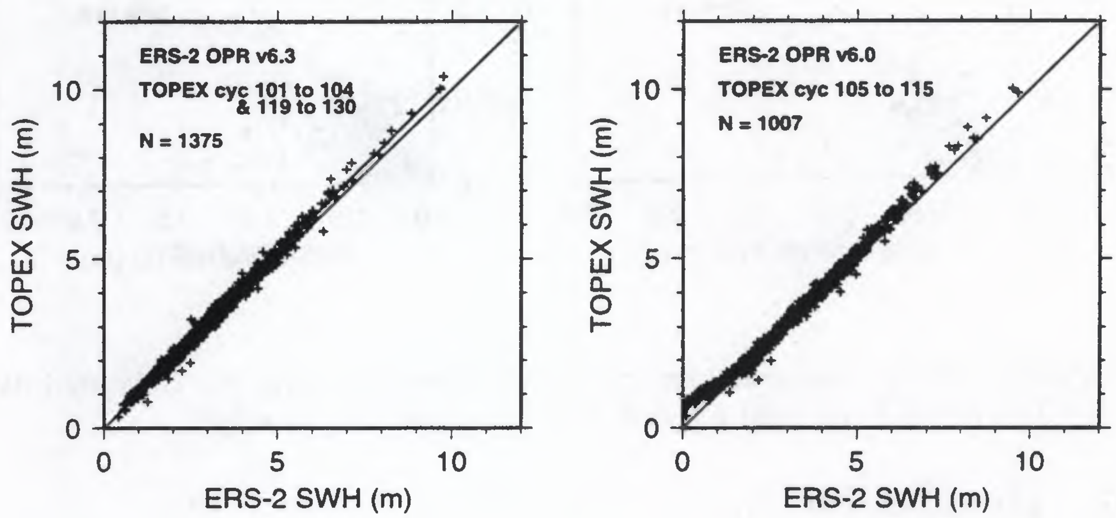

Figure 1: Scatterplot of ERS-2 and TOPEX *swh* collocated measurements (100 km averages). Left OPR v6.3 and right OPR v6.0.

The linear regression line (1), in left graph of figure 1, is obtained with an rms fit of 0.12 m, a slope coefficient of 1.032 and an intercept of 0.025 m:

$$swh_{TOPEX} = 1.03 swh_{ERS-2} + 0.03 \tag{1}$$

swh	ERS-2	TOPEX	Δ
n	1375	1375	1375
mean (m)	2.84	2.95	-0.12
st.dev. (m)	1.22	1.27	0.13

Table 1: statistical characteristics of ERS-2 (v6.3), TOPEX and ERS - TOPEX (Δ) *swh* data sets at crossing points.

Figure 2 compares the standard deviations over the 100 km of the *swh* measurements for the collocated data sets. As in the previous versions, the level of variability as measured by TOPEX is less than for ERS-2. Nevertheless a slight decrease of the ERS variability level is observed in v6.3.

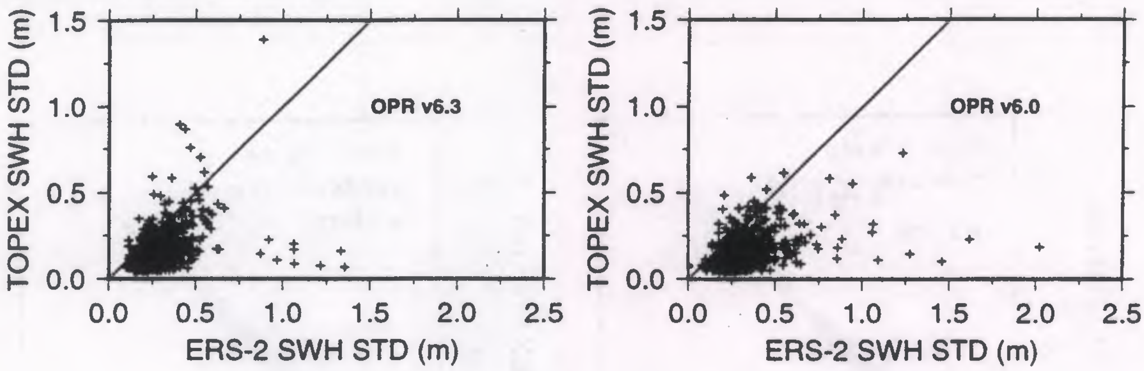

Figure 2: 100 km *swh* measurement standard deviation over the collocated data sets. Left for v6.3 and right for v6.0. Full line is perfect $y = x$ line.

4 Results for σ_0

Collocated σ_0 measurements are compared in figure 3. As already observed (ref. 5), the new version has no significant impact on σ_0. Some scatter is present in the v6.0 data set, but at high σ_0.

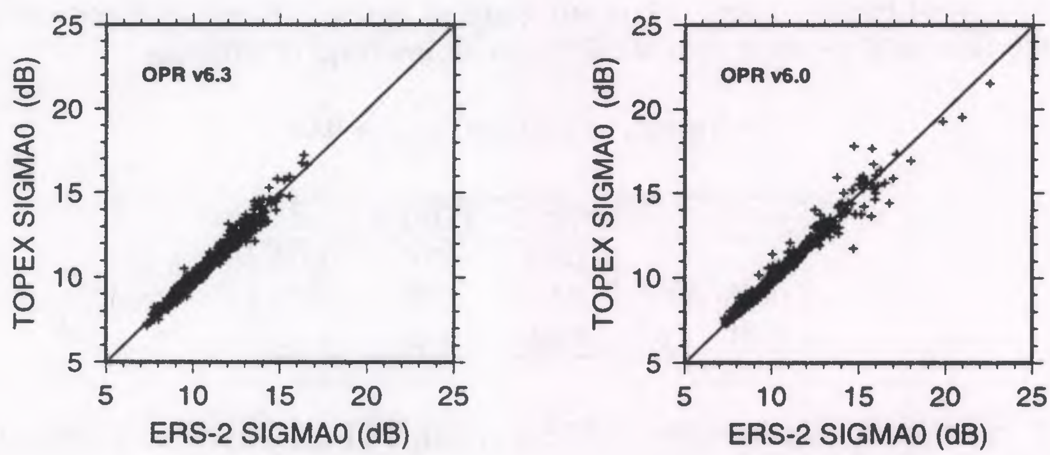

Figure 3: scatterplots of ERS-2 - TOPEX collocated σ_0 measurements. Left for v6.3 and right for v6.0. 100 km averaged data.

5 Summary and recommendations

From the present investigation it can be observed that implementation of the last OPR version, 6.3, results in :

- no significant change in σ_0 estimates, which can be considered as satisfying
- a significant improvement of *swh* estimate, particularly at low sea state where the non-linearities observed in previous versions disappear

At this time, we can suggest to complete investigation on the v6.3 *swh* estimates, as the data will become available from CERSAT. Test of the new version on ERS-1 has also to be done, in the view of reprocessing the whole data set, if needed.

REFERENCES

(1) Cotton, P.D. and P.G. Challenor, 1996, ERS-2 OPR wind and wave calibration and validation, report prepared for ESA *ERS-2 Radar Altimeter and Microwave Radiometer Commissioning Group*, Southampton Oceanography Center, james Rennell Division, European way, Southampton SO143ZH, UK.
(2) Queffeulou P., 1996-b, Significant wave height and backscatter coefficient at ERS-1/2 and Topex Poseidon ground track crossing points-**OPR**, amendment to ESA contract 143189, final report, 24 p., May 1996, IFREMER, BP 70, 29280 Plouzané, France.
(3) The New OPR software version 06, CLS.OC/NT.96.012, issue 1, 26-02-1996, CLS 18 Av. E. Belin, 31055 Toulouse cedex, France.
(4) Queffeulou P., A note on ERS-2 OPR new version 6 processing. Test of Sigma_0 and Significant Wave Height estimates, 18 June 1996, Département d'Océanographie Spatiale, IFREMER, Département d'Océanographie Spatiale, BP 70, 29280 Plouzané, France.
(5) Queffeulou P., Test du traitement OPR version 6.03 de *SWH* et σ_0, 12 août 1996, IFREMER, Département d'Océanographie Spatiale, BP 70, 29280 Plouzané, France.

4. Summary Conclusion

The validation exercise was aimed at the evaluation of the quality of the processing and occasionally the modification of the processing after analysis. It has been carried out in various steps, of which the work dealt with in this document is the last step.

In the first instances, following rigorously a Software Verification and Validation Plan obeying severe standards, the processing software was successfully tested. Then the products themselves generated by the processor were scrutinised in view of its validation.

The objective of this validation step was to obtain an appreciation on the product quality from the point of view of users totally disconnected from the development and operation framework, and thus totally independent.

This approach had the two additional advantages of performing an extensive hands-on review of the user documentation and also of evaluating the product suitability for science applications.

Calibration was out of scope of the work related herewithin and therefore calibration coefficients were not determined as this was done in another framework, namely the ERS-2 RA & MWR Commissioning Working Group. Nevertheless, calibration was considered as far it influenced data plausibility and in some cases, wind and waves, a first estimate was produced. Obviously the validation task was performed prior to the application of the data for the calibration activity of the above mentioned Working Group.

The lessons learned from ERS-1 influenced the study, and all the areas found critical for ERS-1 were checked with great care.

The time-scale for this exercise was determined by the availability of ERS-1 and ERS-2 data, and started in November '95 and ended in February '96, using four cycles of data in version 5. Subsequently, the product was upgraded to incorporate the latest models and algorithms, and a version 6 was produced. The last two sections in this report covered the validation of the version 6 changes with respect to the deltas with version 5 and a verification against Topex wind and wave data.

At the end of the exercise the product was recognised as valid, and so the distribution to the users started immediately, without performing other changes. The OPR product has now reached a high level of maturity, is widely used and no major change is expected during the lifetime of ERS-2.

A systematic quality assessment report is produced cycle per cycle and is shipped with the data. These reports are the vectors of any information the user needs to make full and accurate use of the OPR product.